NASA Technical Memorandum 81787

DO NOT DESTROY
RETURN TO LIBRARY

A Study of Panel Loads and Centers of Pressure of Three Different Cruciform Aft-Tail Control Surfaces of a Wingless Missile From Mach 1.60 to 3.70

Milton Lamb and Charles D. Trescot, Jr.

MAY 1980

11 JUN 1980
MCDONNELL DOUGLAS
RESEARCH & ENGINEERING LIBRARY
ST. LOUIS

NASA

LM168116E

M80-13590

NASA Technical Memorandum 81787

A Study of Panel Loads and Centers of Pressure of Three Different Cruciform Aft-Tail Control Surfaces of a Wingless Missile From Mach 1.60 to 3.70

Milton Lamb and Charles D. Trescot, Jr.
Langley Research Center
Hampton, Virginia

National Aeronautics
and Space Administration

Scientific and Technical
Information Office

1980

SUMMARY

An investigation was made of the forces and moments on the cruciform aft-tail control surfaces of a wingless missile model to determine the variation of panel load and center of pressure with angle of attack, tail deflection, model roll angle, and Mach number. Also, a limited force-moment and surface-pressure investigation was made on a noncircular aft end to determine the effects of fin unporting. These investigations were made in the Langley Unitary Plan Wind Tunnel at Mach numbers of 1.60, 2.36, and 3.70 and at a Reynolds number per meter of 6.6×10^6.

The results indicated very little variation in center of pressure for the highly loaded windward tail. Equally good results can be obtained with force or pressure measurements. The normal-force slope can be predicted quite well using linear theory, but the location of the center of pressure cannot be. The centers of pressure for all three sets of tails tend to be at the spanwise location of the mean aerodynamic chord and at 36 percent of the mean aerodynamic chord. The results of the noncircular aft-end tests indicate no significant effect of fin unporting on fin loads.

INTRODUCTION

The estimation of hinge moments for all-movable control surfaces is a difficult task because of frequent nonlinear variations of hinge-moment coefficients with control deflection and angle of attack (refs. 1 and 2). It was postulated (refs. 3 and 4) that these nonlinearities are due to the influence of vortices generated by the body or forward surfaces and/or the unporting of the control surfaces at large deflections.

An investigation of control-surface nonlinearities has been undertaken to provide a data base for missile panel loads from both pressure measurements and panel force- and moment-balance measurements on several tail planforms. The results of the pressure measurements are presented in reference 5, and the current paper presents a comparison of the panel force and moment measurements with integrated pressure loads, as well as with existing theoretical analysis. A limited investigation is also made to evaluate panel loads with a missile body that is shaped such that the panels do not unport when deflected.

The experimental investigation to determine panel loads and center of pressure was conducted in the Langley Unitary Plan Wind Tunnel at Mach numbers from 1.60 to 3.70 and over an angle-of-attack range of -4° to 20° and a roll-angle range of 0° to 90°.

SYMBOLS

The aerodynamic coefficient data are referred to the body axis system, except for lift and drag, which are referred to the stability axis system. Both body axis and stability axis systems are fixed in the vertical-horizontal planes regardless of the model roll angle. The moment reference was located at 62.15 percent of the body length measured from the nose.

A maximum cross-sectional area, m^2

b exposed semispan of control surface, cm

C_A axial-force coefficient, $\frac{\text{Axial force}}{q_\infty A}$

C_{BM} control-surface root bending-moment coefficient, $\frac{\text{Bending moment}}{q_\infty A b}$

C_D drag coefficient, $\frac{\text{Drag}}{q_\infty A}$

C_{HM} control-surface hinge-moment coefficient, $\frac{\text{Hinge moment}}{q_\infty A c_r}$

C_L lift coefficient, $\frac{\text{Lift}}{q_\infty A}$

C_m pitching-moment coefficient, $\frac{\text{Pitching moment}}{q_\infty A l}$

C_N normal-force coefficient, $\frac{\text{Normal force}}{q_\infty A}$

C_{NF} control-surface normal-force coefficient, $\frac{\text{Panel normal force}}{q_\infty A}$

$C_{NF\alpha}$ control-surface normal-force slope near $\alpha = 0^\circ$, per deg

C_p pressure coefficient, $\frac{p_l - p_\infty}{q_\infty}$

c_r exposed root chord of control surface, cm

$\bar{c}$	mean aerodynamic chord, cm
l	body length, cm
M	free-stream Mach number
p_l	local pressure, Pa
p_∞	free-stream static pressure, Pa
q_∞	free-stream dynamic pressure, Pa
T_A, T_B, T_C	tail planforms (see fig. 1)
x/c	fraction of local tail chord (see fig. B2)
$\frac{x_{cp}}{c_r}$	chordwise center-of-pressure location of tail in exposed root-chord lengths
$\frac{x_{HL}}{c_r}$	hinge-line location of tail in exposed root-chord lengths
$x_{LE,\bar{c}}$	leading edge of mean aerodynamic chord measured from root-chord leading edge, cm
$\frac{y_{cp}}{b}$	spanwise center-of-pressure location of tail in exposed span lengths
$y_{\bar{c}}$	spanwise location of mean aerodynamic chord
α	angle of attack, deg
δ	pitch-control deflection (negative with leading edge down; two tails deflected for $\phi = 0^\circ$ and 90°; four tails deflected for $\phi = 45^\circ$), deg
ΔC_p	$= C_{p,L.S.} - C_{p,U.S.}$
ϕ	model roll angle (positive clockwise when viewed from rear; $\phi = 0^\circ$ when tail 1 is at upper vertical position (see fig. 1)), deg
ϕ_f	roll altitude of specific tail panel (positive clockwise when viewed from rear; tail 1 for $\phi_f < 90^\circ$; tail 2 for $\phi_f \geqq 90^\circ$), deg

Abbreviations:

L.S.	lower surface (see fig. B1)
U.S.	upper surface (see fig. B1)

APPARATUS AND TESTS

Tunnel

The tests were conducted in both the low and high Mach number test sections of the Langley Unitary Plan Wind Tunnel, which is a variable-pressure, continuous-flow facility. Asymmetric sliding-block nozzles permit a continuous variation in Mach number from about 1.5 to 2.9 in the low Mach number test section and from about 2.3 to 4.7 in the high Mach number test section.

Model

The configuration consisted of a wingless aft-tail cruciform control missile model with three sets of interchangeable tail surfaces having identical root chords and span lengths. Details of the model are given in figure 1 and table I. The missile model was sting-mounted from the rear on the main model support system of the tunnel.

Test Conditions

The model was tested at the following conditions:

Mach number	Stagnation temperature, K	Stagnation pressure, Pa	Reynolds number, m^{-1}
1.60	339	54.6	6.6×10^6
2.36	339	75.7	6.6
3.70	339	152.7	6.6

The dewpoint temperature measured at stagnation pressure was maintained below 239 K to assure negligible condensation effects. In order to insure turbulent boundary layer, all tests were conducted with boundary-layer transition strips on the body 3.05 cm aft of the nose and 1.02 cm (measured streamwise) aft of the leading edges of the tails. At a Mach number of 1.60, the 0.16-cm-wide transition strips were composed of No. 60 sand sprinkled lightly; for the other two Mach numbers, the strips were composed of single-spaced No. 40 sand.

Measurements and Corrections

Aerodynamic forces and moments on the model were measured by means of a six-component strain-gage balance which was housed within the model. Forces and moments on two adjacent tails (tails 1 and 2) were measured by means of three-component strain-gage balances in the tails. The model was rolled in order to provide ϕ_f variation for tail loads. Balance-chamber pressure was measured by means of a static-pressure orifice located within the balance cavity.

The angles of attack have been corrected for sting and balance deflection due to aerodynamic loads and for tunnel airflow misalinement. The axial-force coefficients have been adjusted to free-stream conditions acting over the model base.

PRESENTATION OF RESULTS

For the convenience of the reader, tabulated values of the aerodynamic characteristics α, C_N, C_A, C_m, C_L, and C_D for the configuration with the three sets of interchangeable tail surfaces are given in tables A1 to A9 of appendix A. The longitudinal aerodynamic characteristics and control-panel data for the configuration with tail B employing a circular aft end or a flattened aft end are given in appendix B for $M = 1.60$. The control-panel loads and the resulting center-of-pressure locations for the circular aft-end configurations are presented in figures 2 to 20 as follows:

DISCUSSION

The experimental tail loads for the three sets of tails are given in figures 2 to 7. The loads for all of the tails are based on the same geometric characteristics. The effects of roll orientation on the tail loads are as might be expected. The lift on the windward tail tends to be quite linear with angle of attack, and the increment due to tail deflection is generally constant. The lift on the leeward tail is nonlinear, especially at the low Mach number, but becomes more linear with increasing Mach number (fig. 2). The data for $\phi_f = 0^\circ$ and $\phi_f = 180^\circ$ do not coincide exactly and are especially noticeable at $M = 1.60$ for tails T_A and T_B.

Comparison of the balance-measured loads and center of pressure of the present test and the pressure-integrated loads and center of pressure of reference 5 is shown in figures 8 to 19. The comparisons are quite good; in fact, the areas of disagreement are limited to conditions of very small panel loads. In general, the center-of-pressure variation with angle of attack and deflection is constant for the highly loaded windward tail.

Comparisons of experimental and theoretical control-surface normal-force slope and center of pressure of the horizontal panel are shown in figure 20. The theoretical values were obtained from the method of reference 6. The experimental values for y_{cp}/b and x_{cp}/c_r are averages over the angle-of attack range. For all cases, $C_{NF\alpha}$ is predicted quite well, but the comparison of center of pressure is not so good. However, if a correlation based on $y_{\bar{c}}$ is used as the spanwise location and $0.36\bar{c}$ is used as the longitudinal location, good agreement can be obtained.

CONCLUDING REMARKS

A study of the forces and moments on the cruciform aft-tail control surfaces of a wingless missile model was made to determine the variation of panel loads and center of pressure with angle of attack, tail deflection, model roll, and Mach number. The results indicate very little variation in center of pressure for the highly loaded windward tail. Also equally good results can be obtained with force or pressure measurements as shown by the comparisons. The normal-force slope can be predicted quite well using linear-theory methods, but the location of center of pressure cannot be. However, if the spanwise location of the mean aerodynamic chord is used as the spanwise center-of-pressure location and if 36 percent of the mean aerodynamic chord is used as the longitudinal center-of-pressure location, good estimates of the center-of-pressure location can be made. The results of the noncircular aft-end test indicate no significant effect of fin unporting on fin loads.

Langley Research Center
National Aeronautics and Space Administration
Hampton, VA 23665
March 27, 1980

APPENDIX A

LONGITUDINAL AERODYNAMIC CHARACTERISTICS

The longitudinal aerodynamic characteristics for the configuration with the three sets of interchangeable control surfaces are given in tables A1 to A9. The characteristics are referred to the body axis system, except for lift and drag, which are referred to the stability axis system. Both body axis and stability axis systems are fixed in the vertical-horizontal plane regardless of the model roll angle.

APPENDIX A

TABLE A1.- LONGITUDINAL AERODYNAMIC CHARACTERISTICS FOR CONFIGURATION WITH TAIL A FOR M = 1.60

$\Phi=0^\circ, \delta=0^\circ$					
α, deg	C_N	C_A	C_m	C_L	C_D
-3.80	-1.4674	1.1534	.1645	-1.3875	1.2483
-1.83	-.7291	1.1606	.0849	-.6916	1.1833
.19	.0869	1.1721	-.0108	.0830	1.1724
2.17	.8469	1.1661	-.1004	.8021	1.1974
4.27	1.6513	1.1658	-.1873	1.5599	1.2856
6.28	2.4270	1.1641	-.2569	2.2850	1.4227
8.25	3.1496	1.1514	-.3097	2.9517	1.5915
10.21	3.9088	1.1377	-.3498	3.6449	1.8131
12.25	4.7041	1.1197	-.3709	4.3594	2.0924
16.22	6.3716	1.1010	-.3006	5.8102	2.8374
20.24	8.0843	1.0621	-.1494	7.2176	3.7934

$\Phi=22.5^\circ, \delta=0^\circ$					
α, deg	C_N	C_A	C_m	C_L	C_D
-3.64	-1.4156	1.1405	.1607	-1.3402	1.2282
-1.61	-.6525	1.1583	.0786	-.6196	1.1763
.41	.1682	1.1697	-.0202	.1596	1.1709
2.39	.9616	1.1687	-.1130	.9119	1.2079
4.35	1.7144	1.1612	-.1961	1.6211	1.2882
6.44	2.5239	1.1527	-.2725	2.3787	1.4286
8.34	3.2627	1.1392	-.3304	3.0629	1.6005
10.39	4.0570	1.1154	-.3752	3.7892	1.8292
12.35	4.8490	1.0933	-.4014	4.5029	2.1054
16.36	6.4623	1.0414	-.3178	5.9071	2.8199
20.31	8.0917	.9897	-.1732	7.2448	3.7374

$\Phi=45.0^\circ, \delta=0^\circ$					
α, deg	C_N	C_A	C_m	C_L	C_D
-3.63	-1.4389	1.1289	.1636	-1.3645	1.2178
-1.59	-.6586	1.1579	.0786	-.6262	1.1758
.34	.1353	1.1720	-.0155	.1282	1.1728
2.47	.9842	1.1657	-.1162	.9330	1.2071
4.42	1.7454	1.1539	-.2010	1.6511	1.2852
6.38	2.5196	1.1454	-.2752	2.3765	1.4187
8.43	3.2947	1.1271	-.3344	3.0937	1.5982
10.40	4.0542	1.1051	-.3745	3.7880	1.8189
12.37	4.8322	1.0806	-.3973	4.4884	2.0908
16.40	6.4302	1.0284	-.3037	5.8780	2.8026
20.42	8.1294	.9979	-.1385	7.2703	3.7717

$\Phi=67.5^\circ, \delta=0^\circ$					
α, deg	C_N	C_A	C_m	C_L	C_D
-3.61	-1.4372	1.1386	.1620	-1.3625	1.2271
-1.65	-.6508	1.1604	.0780	-.6171	1.1787
.33	.1179	1.1676	-.0143	.1110	1.1683
2.46	.9555	1.1670	-.1122	.9044	1.2071
4.40	1.7057	1.1585	-.1956	1.6117	1.2861
6.37	2.4775	1.1541	-.2689	2.3340	1.4220
8.39	3.2465	1.1371	-.3285	3.0458	1.5987
10.42	4.0018	1.1109	-.3688	3.7348	1.8166
12.39	4.7912	1.0904	-.3928	4.4456	2.0930
16.49	6.4706	1.0450	-.3124	5.9073	2.8397
20.47	8.1719	.9971	-.1465	7.3071	3.7921

$\Phi=90.0^\circ, \delta=0^\circ$					
α, deg	C_N	C_A	C_m	C_L	C_D
-3.66	-1.4192	1.1533	.1588	-1.3424	1.2417
-1.69	-.6663	1.1610	.0780	-.6315	1.1803
.32	.1422	1.1697	-.0176	.1356	1.1705
2.28	.8990	1.1713	-.1059	.8516	1.2062
4.28	1.6507	1.1691	-.1868	1.5588	1.2892
6.27	2.4073	1.1726	-.2560	2.2648	1.4286
8.36	3.1926	1.1648	-.3127	2.9890	1.6170
10.34	3.9368	1.1506	-.3511	3.6663	1.8388
12.22	4.6717	1.1371	-.3749	4.3250	2.1004
16.23	6.3306	1.1131	-.3023	5.7669	2.8387
20.28	8.0725	1.0682	-.1358	7.2015	3.8006

$\Phi=0^\circ, \delta=-15^\circ$					
α, deg	C_N	C_A	C_m	C_L	C_D
-3.78	-4.5647	2.0325	.8018	-4.4205	2.3294
-1.80	-3.8985	1.9079	.7385	-3.8364	2.0299
-.79	-3.5434	1.8490	.6995	-3.5174	1.8980
.23	-3.2002	1.7943	.6604	-3.2074	1.7814
2.21	-2.5214	1.6921	.5861	-2.5850	1.5932
4.21	-1.8440	1.6081	.5175	-1.9572	1.4683
6.22	-1.1584	1.5226	.4611	-1.3166	1.3880
8.20	-.4449	1.4237	.4131	-.6436	1.3456
10.22	.3810	1.3028	.3648	.1436	1.3498
12.22	1.2394	1.1623	.3245	.9651	1.3985
16.20	3.1873	.9002	.3428	2.8095	1.7537

$\Phi=45.0^\circ, \delta=-15^\circ$					
α, deg	C_N	C_A	C_m	C_L	C_D
-3.59	-5.7373	2.6347	1.0464	-5.5607	2.9894
-1.60	-5.1382	2.5226	.9918	-5.0656	2.6654
.42	-4.3840	2.3584	.9030	-4.4013	2.3260
2.41	-3.6456	2.2003	.8139	-3.7349	2.0451
4.40	-2.9122	2.0438	.7325	-3.0605	1.8141
6.40	-2.2528	1.9135	.6816	-2.4522	1.6502
8.39	-1.6024	1.7969	.6462	-1.8475	1.5438
10.41	-.8700	1.6606	.6123	-1.1557	1.4760
12.40	-.0953	1.5127	.5930	-.4181	1.4569
16.40	1.5859	1.2401	.6680	1.1712	1.6375
20.39	3.6032	.9251	.7655	3.0549	2.1229

APPENDIX A

TABLE A2.- LONGITUDINAL AERODYNAMIC CHARACTERISTICS FOR CONFIGURATION WITH TAIL A FOR M = 2.36

$\Phi=0^\circ, \delta=0^\circ$					
α, deg	C_N	C_A	C_m	C_L	C_D
-4.27	-1.1215	.7632	.1359	-1.0615	.8447
-2.22	-.5680	.7502	.0695	-.5385	.7716
-.17	-.0450	.7463	.0054	-.0427	.7464
1.87	.4831	.7485	-.0595	.4584	.7638
3.92	1.0428	.7576	-.1263	.9886	.8271
5.98	1.6301	.7682	-.1886	1.5411	.9341
8.06	2.3133	.7785	-.2459	2.1813	1.0952
10.15	3.0842	.7881	-.2858	2.8970	1.3194
12.27	3.9264	.7965	-.3097	3.6672	1.6132
16.54	5.6251	.7808	-.3188	5.1699	2.3502
20.82	7.5288	.7838	-.3493	6.7583	3.4092

$\Phi=22.5^\circ, \delta=0^\circ$					
α, deg	C_N	C_A	C_m	C_L	C_D
-4.43	-1.1650	.7641	.1422	-1.1023	.8519
-2.38	-.6198	.7561	.0755	-.5878	.7812
-.33	-.1000	.7545	.0121	-.0955	.7551
1.71	.4161	.7562	-.0508	.3933	.7682
3.76	.9852	.7615	-.1182	.9331	.8245
5.82	1.5818	.7715	-.1822	1.4954	.9280
7.89	2.2380	.7737	-.2372	2.1104	1.0739
9.99	3.0005	.7755	-.2781	2.8203	1.2846
12.12	3.8390	.7787	-.3002	3.5899	1.5675
16.39	5.6114	.7774	-.3251	5.1639	2.3294
20.68	7.4832	.7908	-.3484	6.7214	3.3833

$\Phi=45.0^\circ, \delta=0^\circ$					
α, deg	C_N	C_A	C_m	C_L	C_D
-4.52	-1.1952	.7589	.1440	-1.1315	.8509
-2.47	-.6442	.7576	.0769	-.6109	.7847
-.43	-.1127	.7557	.0128	-.1070	.7565
1.62	.4116	.7591	-.0497	.3899	.7704
3.67	.9590	.7621	-.1148	.9081	.8220
5.72	1.5549	.7697	-.1780	1.4703	.9211
7.81	2.2273	.7748	-.2357	2.1014	1.0704
9.91	2.9624	.7785	-.2706	2.7842	1.2767
12.03	3.7937	.7827	-.2861	3.5471	1.5567
16.32	5.5977	.7868	-.3255	5.1509	2.3283
20.62	7.5721	.8244	-.3717	6.7964	3.4387

$\Phi=67.5^\circ, \delta=0^\circ$					
α, deg	C_N	C_A	C_m	C_L	C_D
-4.43	-1.1673	.7625	.1395	-1.1048	.8505
-2.38	-.6216	.7588	.0743	-.5895	.7841
-.33	-.1044	.7566	.0123	-.0999	.7572
1.71	.4231	.7610	-.0508	.4001	.7733
3.76	.9704	.7694	-.1159	.9177	.8315
5.83	1.5655	.7778	-.1784	1.4783	.9331
5.84	1.5791	.7773	-.1797	1.4918	.9339
7.89	2.2184	.7808	-.2340	2.0901	1.0782
10.00	2.9846	.7827	-.2723	2.8031	1.2895
12.13	3.7935	.7870	-.2941	3.5432	1.5671
16.42	5.5735	.7841	-.3173	5.1243	2.3281

$\Phi=90.0^\circ, \delta=0^\circ$					
α, deg	C_N	C_A	C_m	C_L	C_D
-4.42	-1.1544	.7674	.1354	-1.0917	.8542
-2.38	-.5979	.7594	.0714	-.5659	.7836
-.33	-.0696	.7581	.0082	-.0652	.7585
1.71	.4468	.7630	-.0536	.4237	.7761
3.76	.9915	.7741	-.1190	.9385	.8376
5.83	1.5956	.7881	-.1837	1.5072	.9462
7.90	2.2517	.7983	-.2393	2.1205	1.1005
10.01	3.0311	.8109	-.2817	2.8438	1.3258
12.14	3.8590	.8199	-.3048	3.6000	1.6136
16.44	5.5877	.8041	-.3138	5.1315	2.3529
20.75	7.4737	.8065	-.3448	6.7027	3.4030

$\Phi=0^\circ, \delta=-15^\circ$					
α, deg	C_N	C_A	C_m	C_L	C_D
-4.30	-3.3887	1.5467	.7534	-3.2630	1.7966
-2.25	-2.8851	1.4627	.6992	-2.8253	1.5752
-.21	-2.3988	1.3730	.6432	-2.3936	1.3819
1.83	-1.8704	1.2708	.5788	-1.9102	1.2102
3.88	-1.2957	1.1570	.5081	-1.3712	1.0664
5.95	-.6835	1.0521	.4427	-.7889	.9755
8.03	-.0235	.9493	.3904	-.1559	.9367
10.12	.7113	.8504	.3592	.5507	.9622
12.24	1.5465	.7530	.3421	1.3516	1.0639
16.52	3.3712	.5748	.3098	3.0684	1.5100
20.82	5.2351	.4674	.2943	4.7270	2.2978

$\Phi=45.0^\circ, \delta=-15^\circ$					
α, deg	C_N	C_A	C_m	C_L	C_D
-4.52	-4.4854	2.2310	1.0613	-4.2954	2.5780
-2.46	-3.9504	2.1192	.9973	-3.8556	2.2872
-.41	-3.4368	2.0004	.9342	-3.4221	2.0254
1.62	-2.9033	1.8600	.8655	-2.9549	1.7769
3.67	-2.2850	1.6807	.7825	-2.3880	1.5308
5.73	-1.6209	1.4975	.7041	-1.7625	1.3279
7.81	-.9385	1.3354	.6439	-1.1114	1.1954
9.91	-.1998	1.1864	.6088	-.4012	1.1342
12.04	.5991	1.0596	.5992	.3649	1.1613
16.32	2.3180	.8699	.5845	1.9800	1.4864
20.63	4.0951	.7494	.5890	3.5683	2.1443

APPENDIX A

TABLE A3.- LONGITUDINAL AERODYNAMIC CHARACTERISTICS FOR CONFIGURATION WITH TAIL A FOR M = 3.70

Φ=0°, δ=0°					
α, deg	C_N	C_A	C_m	C_L	C_D
-4.07	-.8053	.5354	.0403	-.7652	.5913
-2.04	-.3893	.5246	.0188	-.3704	.5381
.01	.0065	.5203	-.0003	.0065	.5203
2.04	.3840	.5213	-.0183	.3652	.5346
4.07	.7978	.5257	-.0365	.7585	.5811
6.12	1.2889	.5357	-.0544	1.2244	.6701
8.18	1.8731	.5446	-.0683	1.7766	.8055
10.24	2.4863	.5545	-.0783	2.3481	.9877
12.30	3.1357	.5761	-.0888	2.9409	1.2311
16.44	4.5490	.6377	-.1203	4.1824	1.8992
20.61	6.2392	.7154	-.1828	5.5882	2.8657

Φ=22.5°, δ=0°					
α, deg	C_N	C_A	C_m	C_L	C_D
-4.06	-.7994	.5418	.0389	-.7590	.5971
-2.03	-.3798	.5338	.0179	-.3607	.5469
0.00	.0077	.5309	-.0008	.0077	.5309
2.04	.3955	.5290	-.0182	.3764	.5428
4.07	.8141	.5284	-.0383	.7745	.5849
6.12	1.2908	.5345	-.0544	1.2264	.6691
8.19	1.8646	.5374	-.0656	1.7690	.7975
10.24	2.4736	.5455	-.0758	2.3373	.9764
12.31	3.1089	.5663	-.0845	2.9167	1.2161
16.45	4.5255	.6243	-.1174	4.1635	1.8804
20.62	6.2198	.7135	-.1821	5.5703	2.8579

Φ=45.0°, δ=0°					
α, deg	C_N	C_A	C_m	C_L	C_D
-4.06	-.7859	.5312	.0375	-.7463	.5856
-2.04	-.3654	.5281	.0159	-.3464	.5408
.01	.0254	.5232	-.0020	.0254	.5232
2.04	.3996	.5212	-.0183	.3808	.5351
4.08	.8184	.5200	-.0372	.7794	.5768
6.12	1.2978	.5239	-.0550	1.2345	.6594
8.18	1.8667	.5345	-.0652	1.7716	.7947
10.25	2.4699	.5512	-.0720	2.3324	.9818
12.32	3.1076	.5740	-.0815	2.9137	1.2236
16.47	4.5212	.6388	-.1120	4.1548	1.8941
20.64	6.1857	.7207	-.1734	5.5348	2.8545

Φ=67.5°, δ=0°					
α, deg	C_N	C_A	C_m	C_L	C_D
-4.10	-.7801	.5294	.0353	-.7403	.5839
-2.07	-.3643	.5271	.0154	-.3450	.5399
-.03	.0172	.5233	-.0012	.0174	.5233
2.01	.3924	.5247	-.0172	.3737	.5381
4.05	.8060	.5274	-.0357	.7667	.5830
6.10	1.2832	.5342	-.0519	1.2191	.6675
8.15	1.8476	.5382	-.0627	1.7526	.7948
10.22	2.4633	.5487	-.0721	2.3268	.9772
12.29	3.0973	.5709	-.0823	2.9047	1.2173
16.45	4.5181	.6311	-.1137	4.1544	1.8849
20.62	6.1937	.7200	-.1768	5.5433	2.8553

Φ=90.0°, δ=0°					
α, deg	C_N	C_A	C_m	C_L	C_D
-4.26	-.8229	.5490	.0365	-.7799	.6086
-2.22	-.4043	.5420	.0177	-.3830	.5572
-.18	-.0151	.5382	-.0004	-.0134	.5382
1.86	.3603	.5398	-.0164	.3426	.5512
3.90	.7773	.5467	-.0351	.7384	.5983
5.95	1.2600	.5579	-.0525	1.1953	.6856
8.00	1.8303	.5679	-.0669	1.7334	.8172
10.07	2.4400	.5787	-.0762	2.3011	.9966
12.15	3.0854	.6009	-.0857	2.8899	1.2367
16.30	4.4938	.6633	-.1159	4.1270	1.8980
20.48	6.1689	.7424	-.1765	5.5191	2.8540

Φ=0°, δ=-15°					
α, deg	C_N	C_A	C_m	C_L	C_D
-4.09	-2.5045	1.1748	.5012	-2.4144	1.3504
-2.05	-2.0141	1.0750	.4607	-1.9743	1.1464
-.02	-1.5436	.9802	.4198	-1.5434	.9806
2.02	-1.1089	.8912	.3839	-1.1396	.8515
4.07	-.6355	.8114	.3516	-.6915	.7643
6.11	-.1206	.7308	.3244	-.1977	.7138
8.16	.5055	.6516	.3001	.4078	.7167
10.23	1.1016	.6049	.2967	.9767	.7909
12.29	1.6413	.5877	.3135	1.4786	.9236
16.43	2.7707	.5812	.3623	2.4932	1.3411
20.59	4.0756	.5736	.4052	3.6135	1.9703

Φ=45.0°, δ=-15°					
α, deg	C_N	C_A	C_m	C_L	C_D
-4.07	-3.1356	1.6631	.6731	-3.0095	1.8817
-2.04	-2.6595	1.5441	.6343	-2.6029	1.6377
0.00	-2.2067	1.4162	.5955	-2.2066	1.4163
2.04	-1.7530	1.2885	.5571	-1.7977	1.2254
4.07	-1.2674	1.1557	.5172	-1.3462	1.0629
6.12	-.7306	1.0337	.4818	-.8366	.9500
8.18	-.1798	.9531	.4712	-.3136	.9179
10.24	.3823	.8958	.4735	.2169	.9495
12.31	.9375	.8644	.4854	.7316	1.0444
16.46	2.0963	.8257	.5233	1.7765	1.3858
20.62	3.4040	.7939	.5623	2.9062	1.9420

APPENDIX A

TABLE A4.- LONGITUDINAL AERODYNAMIC CHARACTERISTICS FOR CONFIGURATION WITH TAIL B FOR M = 1.60

$\Phi=0^\circ, \delta=0^\circ$					
α, deg	C_N	C_A	C_m	C_L	C_D
-3.85	-1.3130	1.0670	.1310	-1.2382	1.1530
-1.84	-.6285	1.0800	.0644	-.5934	1.0997
.15	.0464	1.0882	-.0058	.0435	1.0883
2.14	.6941	1.0862	-.0727	.6529	1.1114
4.15	1.3858	1.0751	-.1409	1.3042	1.1727
6.14	2.0774	1.0646	-.2011	1.9515	1.2808
8.16	2.7958	1.0506	-.2519	2.6183	1.4369
10.14	3.5133	1.0290	-.2889	3.2771	1.6318
12.15	4.2999	1.0129	-.3096	3.9901	1.8958
16.16	5.9681	.9908	-.2400	5.4565	2.6127
20.13	7.6372	.9598	-.0830	6.8400	3.5302

$\Phi=22.5^\circ, \delta=0^\circ$					
α, deg	C_N	C_A	C_m	C_L	C_D
-3.74	-1.2552	1.0618	.1247	-1.1833	1.1414
-1.72	-.5755	1.0808	.0589	-.5427	1.0977
.26	.0834	1.0902	-.0095	.0783	1.0906
2.26	.7377	1.0868	-.0773	.6942	1.1151
4.24	1.4062	1.0700	-.1446	1.3231	1.1712
6.26	2.1198	1.0485	-.2093	1.9928	1.2734
8.27	2.8738	1.0234	-.2647	2.6966	1.4262
10.24	3.6090	.9930	-.3031	3.3747	1.6194
12.25	4.3909	.9619	-.3275	4.0867	1.8721
16.26	6.0284	.9230	-.2447	5.5287	2.5743
20.24	7.6518	.8827	-.0716	6.8738	3.4757

$\Phi=45.0^\circ, \delta=0^\circ$					
α, deg	C_N	C_A	C_m	C_L	C_D
-3.74	-1.2197	1.0460	.1201	-1.1487	1.1234
-1.73	-.5683	1.0738	.0590	-.5356	1.0905
.25	.0864	1.0856	-.0092	.0816	1.0860
2.25	.7393	1.0807	-.0772	.6962	1.1089
4.25	1.4272	1.0592	-.1473	1.3447	1.1621
6.25	2.1609	1.0341	-.2128	2.0353	1.2635
8.25	2.8779	1.0081	-.2649	2.7034	1.4107
10.24	3.6159	.9785	-.3036	3.3841	1.6063
12.26	4.4072	.9466	-.3272	4.1056	1.8610
16.25	6.0445	.9114	-.2446	5.5478	2.5667
20.27	7.6930	.8839	-.0717	6.9103	3.4946

$\Phi=67.5^\circ, \delta=0^\circ$					
α, deg	C_N	C_A	C_m	C_L	C_D
-3.73	-1.2290	1.0552	.1214	-1.1576	1.1330
-1.73	-.5613	1.0751	.0579	-.5284	1.0916
.25	.0741	1.0836	-.0080	.0692	1.0839
2.26	.7426	1.0814	-.0780	.6994	1.1098
4.25	1.4273	1.0634	-.1468	1.3444	1.1665
6.26	2.1471	1.0431	-.2098	2.0205	1.2710
8.25	2.8550	1.0197	-.2615	2.6790	1.4191
10.26	3.5993	.9881	-.2979	3.3657	1.6135
12.26	4.3890	.9583	-.3214	4.0852	1.8688
16.26	6.0380	.9219	-.2459	5.5380	2.5765
20.27	7.7054	.8863	-.0726	6.9211	3.5011

$\Phi=90.0^\circ, \delta=0^\circ$					
α, deg	C_N	C_A	C_m	C_L	C_D
-3.80	-1.2586	1.0644	.1251	-1.1853	1.1456
-1.78	-.5889	1.0767	.0609	-.5550	1.0946
.21	.0691	1.0836	-.0074	.0651	1.0839
2.21	.7229	1.0814	-.0756	.6806	1.1086
4.21	1.4126	1.0736	-.1436	1.3299	1.1745
6.22	2.1050	1.0621	-.2040	1.9775	1.2839
8.21	2.8365	1.0515	-.2557	2.6571	1.4461
10.20	3.5539	1.0345	-.2901	3.3143	1.6481
12.21	4.3234	1.0177	-.3104	4.0101	1.9096
16.22	6.0029	.9976	-.2375	5.4852	2.6348
20.21	7.7025	.9703	-.0745	6.8926	3.5724

$\Phi=0^\circ, \delta=-15^\circ$					
α, deg	C_N	C_A	C_m	C_L	C_D
-3.90	-4.2476	1.7982	.7351	-4.1152	2.0834
-1.85	-3.6052	1.6950	.6772	-3.5486	1.8105
.20	-2.9295	1.6062	.6064	-2.9352	1.5958
2.17	-2.2697	1.5247	.5384	-2.3259	1.4375
4.15	-1.6745	1.4574	.4838	-1.7757	1.3322
6.14	-1.0087	1.3812	.4282	-1.1508	1.2652
8.17	-.2771	1.2887	.3778	-.4576	1.2362
10.16	.4684	1.1892	.3385	.2513	1.2532
12.14	1.2586	1.0739	.3120	1.0045	1.3147
16.15	3.0134	.8516	.3706	2.6575	1.6563
20.15	4.8782	.6332	.5074	4.3615	2.2749

$\Phi=45.0^\circ, \delta=-15^\circ$					
α, deg	C_N	C_A	C_m	C_L	C_D
-3.74	-5.4598	2.4370	.9982	-5.2891	2.7882
-1.76	-4.8968	2.3254	.9528	-4.8229	2.4750
.27	-4.1924	2.1731	.8738	-4.2026	2.1533
2.25	-3.4720	2.0191	.7873	-3.5488	1.8809
4.25	-2.7572	1.8697	.7078	-2.8885	1.6597
6.28	-2.1012	1.7401	.6570	-2.2791	1.4996
8.27	-1.4426	1.6232	.6157	-1.6611	1.3988
10.27	-.7231	1.4906	.5820	-.9775	1.3376
12.27	.0338	1.3626	.5653	-.2565	1.3387
16.26	1.5867	1.1307	.6667	1.2064	1.5299
20.23	3.3777	.8826	.8050	2.8638	1.9966

APPENDIX A

TABLE A5.- LONGITUDINAL AERODYNAMIC CHARACTERISTICS FOR CONFIGURATION WITH TAIL B FOR M = 2.36

$\Phi=0^\circ, \delta=0^\circ$					
α, deg	C_N	C_A	C_m	C_L	C_D
-4.02	-1.0131	.7608	.0470	-.9572	.8300
-2.06	-.4963	.7494	.0244	-.4690	.7668
-.11	-.0189	.7401	.0009	-.0174	.7401
1.78	.4528	.7393	-.0213	.4296	.7530
3.61	.8968	.7434	-.0405	.8482	.7985
5.42	1.3937	.7504	-.0566	1.3165	.8788
7.25	1.9276	.7601	-.0613	1.8163	.9973
8.89	2.4486	.7633	-.0481	2.3011	1.1329
10.51	3.0128	.7626	-.0181	2.8231	1.2995
13.57	4.1510	.7574	.0702	3.8572	1.7106
16.55	5.3448	.7419	.1553	4.9120	2.2338

$\Phi=22.5^\circ, \delta=0^\circ$					
α, deg	C_N	C_A	C_m	C_L	C_D
-3.94	-.9925	.7561	.0473	-.9382	.8225
-2.01	-.4854	.7453	.0242	-.4589	.7619
-.15	-.0293	.7372	.0013	-.0273	.7372
1.83	.4587	.7362	-.0220	.4348	.7505
3.66	.9129	.7379	-.0413	.8638	.7948
5.48	1.4078	.7439	-.0593	1.3302	.8751
7.28	1.9354	.7480	-.0661	1.8250	.9872
9.14	2.5268	.7503	-.0557	2.3754	1.1425
10.75	3.1083	.7466	-.0212	2.9143	1.3136
13.93	4.3200	.7369	.0679	4.0152	1.7558
17.00	5.5483	.7362	.1568	5.0902	2.3271

$\Phi=45.0^\circ, \delta=0^\circ$					
α, deg	C_N	C_A	C_m	C_L	C_D
-3.91	-1.0006	.7523	.0469	-.9468	.8189
-2.07	-.5219	.7450	.0249	-.4946	.7634
-.13	-.0335	.7375	.0011	-.0319	.7376
1.84	.4427	.7370	-.0216	.4187	.7509
3.71	.9229	.7385	-.0430	.8731	.7968
5.77	1.4901	.7438	-.0620	1.4076	.8900
7.58	2.0134	.7471	-.0652	1.8972	1.0062
9.45	2.6242	.7496	-.0508	2.4654	1.1704
11.12	3.2312	.7531	-.0152	3.0251	1.3626
14.60	4.5650	.7504	.0815	4.2282	1.8773
18.10	6.0422	.7614	.1720	5.5065	2.6012

$\Phi=67.5^\circ, \delta=0^\circ$					
α, deg	C_N	C_A	C_m	C_L	C_D
-4.09	-1.0228	.7546	.0467	-.9663	.8257
-1.98	-.4779	.7425	.0229	-.4518	.7586
-.13	-.0271	.7369	.0013	-.0254	.7369
1.85	.4650	.7372	-.0220	.4408	.7519
3.88	.9781	.7435	-.0448	.9255	.8081
5.81	1.5129	.7512	-.0613	1.4290	.9006
7.80	2.1028	.7567	-.0626	1.9805	1.0353
9.76	2.7412	.7569	-.0399	2.5730	1.2111
11.67	3.4212	.7539	.0066	3.1979	1.4306
15.38	4.8883	.7458	.1123	4.5153	2.0158
19.40	6.5778	.7557	.2205	5.9531	2.8979

$\Phi=90.0^\circ, \delta=0^\circ$					
α, deg	C_N	C_A	C_m	C_L	C_D
-4.07	-1.0332	.7530	.0470	-.9771	.8245
-2.04	-.4977	.7414	.0248	-.4710	.7586
-.09	-.0318	.7356	.0028	-.0307	.7357
1.94	.4640	.7394	-.0204	.4386	.7548
3.96	.9858	.7483	-.0433	.9316	.8147
5.98	1.5468	.7603	-.0593	1.4591	.9173
8.02	2.1507	.7722	-.0585	2.0219	1.0648
9.96	2.7929	.7753	-.0318	2.6166	1.2470
11.94	3.5067	.7750	.0194	3.2704	1.4839
15.97	5.0654	.7578	.1406	4.6614	2.1223
19.97	6.8120	.7582	.2422	6.1435	3.0392

$\Phi=0^\circ, \delta=-15^\circ$					
α, deg	C_N	C_A	C_m	C_L	C_D
-4.75	-3.0512	1.3919	.4325	-2.9254	1.6399
-3.00	-2.6194	1.3242	.4221	-2.5464	1.4597
-1.10	-2.1774	1.2550	.4071	-2.1528	1.2967
.84	-1.7480	1.1809	.3892	-1.7652	1.1552
2.63	-1.3124	1.1115	.3733	-1.3621	1.0500
4.53	-.8400	1.0315	.3558	-.9190	.9618
6.35	-.3188	.9497	.3429	-.4220	.9086
8.00	.1880	.8774	.3444	.0640	.8950
9.72	.7681	.8036	.3605	.6213	.9218
12.79	1.9744	.6922	.4372	1.7721	1.1123
15.82	3.2601	.5803	.5096	2.9782	1.4474

$\Phi=45.0^\circ, \delta=-15^\circ$					
α, deg	C_N	C_A	C_m	C_L	C_D
-4.64	-3.8815	5.9749	.6125	-3.3844	6.2699
-2.79	-3.4576	5.9171	.6025	-3.1644	6.0789
-.80	-3.0028	5.8313	.5847	-2.9201	5.8731
1.13	-2.5725	5.7407	.5673	-2.6858	5.6886
3.05	-2.1073	5.6282	.5472	-2.4044	5.5078
4.99	-1.5833	5.4934	.5241	-2.0558	5.3346
6.95	-1.0100	5.3495	.5104	-1.6504	5.1878
8.83	-.4277	5.2155	.5158	-1.2241	5.0879
10.50	.1546	5.1104	.5458	-.7795	5.0530
14.08	1.5258	4.9299	.6477	.2804	5.1530
17.41	2.8905	4.8019	.7438	1.3210	5.4469

APPENDIX A

TABLE A6.- LONGITUDINAL AERODYNAMIC CHARACTERISTICS FOR CONFIGURATION WITH TAIL B FOR M = 3.70

$\phi=0^\circ, \delta=0^\circ$					
α, deg	C_N	C_A	C_m	C_L	C_D
-3.87	-.7124	.5182	-.0220	-.6758	.5651
-2.04	-.3628	.5108	-.0115	-.3443	.5234
-.15	-.0313	.5087	-.0010	-.0300	.5088
1.66	.2874	.5082	.0096	.2725	.5164
3.52	.6495	.5139	.0208	.6167	.5529
5.35	1.0549	.5241	.0385	1.0014	.6203
7.13	1.5229	.5310	.0626	1.4451	.7160
8.85	2.0265	.5413	.0917	1.9191	.8467
10.56	2.5456	.5564	.1231	2.4004	1.0138
14.02	3.6344	.6092	.1866	3.3784	1.4720
17.42	4.8297	.6675	.2510	4.4080	2.0833

$\phi=22.5^\circ, \delta=0^\circ$					
α, deg	C_N	C_A	C_m	C_L	C_D
-3.93	-.7254	.5118	-.0200	-.6886	.5603
-2.01	-.3545	.5073	-.0094	-.3365	.5194
-.24	-.0312	.5042	-.0012	-.0291	.5043
1.67	.3104	.5039	.0089	.2955	.5127
3.50	.6609	.5075	.0209	.6286	.5469
5.36	1.0747	.5121	.0376	1.0221	.6104
7.17	1.5570	.5173	.0620	1.4802	.7078
8.95	2.0730	.5299	.0924	1.9652	.8463
10.69	2.5918	.5446	.1237	2.4458	1.0161
14.17	3.7001	.5939	.1866	3.4420	1.4821
17.66	4.9732	.6610	.2440	4.5380	2.1392

$\phi=45.0^\circ, \delta=0^\circ$					
α, deg	C_N	C_A	C_m	C_L	C_D
-4.10	-.7530	.5128	-.0210	-.7143	.5654
-2.24	-.3892	.5072	-.0101	-.3691	.5221
-.33	-.0425	.5042	-.0011	-.0396	.5044
1.64	.3063	.5064	.0097	.2917	.5149
3.52	.6787	.5070	.0213	.6462	.5478
5.45	1.1133	.5117	.0391	1.0596	.6153
7.32	1.6117	.5215	.0656	1.5321	.7226
9.19	2.1380	.5367	.1012	2.0247	.8715
11.04	2.6896	.5557	.1354	2.5334	1.0605
14.70	3.8827	.6175	.1995	3.5988	1.5829
18.41	5.2791	.6941	.2596	4.7895	2.3263

$\phi=67.5^\circ, \delta=0^\circ$					
α, deg	C_N	C_A	C_m	C_L	C_D
-4.23	-.7846	.5145	-.0229	-.7445	.5710
-2.25	-.3995	.5081	-.0111	-.3792	.5234
-.27	-.0421	.5050	-.0012	-.0397	.5052
1.73	.3192	.5069	.0094	.3037	.5164
3.69	.6993	.5113	.0222	.6650	.5552
5.66	1.1472	.5180	.0407	1.0905	.6287
7.63	1.6802	.5260	.0708	1.5955	.7445
9.58	2.2408	.5408	.1063	2.1194	.9066
11.54	2.8397	.5621	.1426	2.6697	1.1192
15.47	4.1501	.6276	.2111	3.8322	1.7121
19.37	5.6553	.7112	.2742	5.0990	2.5471

$\phi=90.0^\circ, \delta=0^\circ$					
α, deg	C_N	C_A	C_m	C_L	C_D
-4.24	-.8007	.5182	-.0269	-.7601	.5760
-2.25	-.4207	.5100	-.0137	-.4002	.5262
-1.19	-.2254	.5087	-.0078	-.2147	.5133
-.19	-.0532	.5077	-.0022	-.0515	.5079
1.78	.2979	.5101	.0098	.2819	.5192
3.84	.7072	.5190	.0247	.6708	.5653
5.77	1.1384	.5329	.0441	1.0790	.6447
7.77	1.6950	.5426	.0730	1.6060	.7669
9.81	2.2965	.5587	.1108	2.1677	.9421
11.78	2.8958	.5845	.1476	2.7154	1.1636
15.83	4.2542	.6535	.2217	3.9143	1.7897

$\phi=0^\circ, \delta=-15^\circ$					
α, deg	C_N	C_A	C_m	C_L	C_D
-4.36	-2.2381	1.0643	.2714	-2.1506	1.2315
-2.44	-1.8211	.9842	.2754	-1.7775	1.0608
-.61	-1.4380	.9030	.2720	-1.4281	.9185
1.25	-1.0518	.8279	.2702	-1.0697	.8047
3.15	-.6564	.7606	.2735	-.6973	.7233
4.98	-.2333	.7005	.2830	-.2932	.6776
6.76	.2505	.6403	.2991	.1734	.6654
8.49	.7795	.5858	.3211	.6844	.6945
10.21	1.2503	.5652	.3605	1.1302	.7780
13.62	2.1588	.5617	.4575	1.9658	1.0543
16.96	3.1130	.5682	.5659	2.8116	1.4520

$\phi=45.0^\circ, \delta=-15^\circ$					
α, deg	C_N	C_A	C_m	C_L	C_D
-4.54	-2.8424	7.5060	.3921	-2.2387	7.7076
-2.59	-2.4179	7.3997	.3943	-2.0803	7.5015
-.61	-2.0001	7.2812	.3912	-1.9215	7.3024
1.30	-1.6076	7.1817	.3879	-1.7712	7.1431
3.23	-1.1757	7.0723	.3860	-1.5729	6.9947
5.14	-.6921	6.9718	.3887	-1.3146	6.8817
7.02	-.2134	6.8941	.4119	-1.0546	6.8163
8.91	.2865	6.8430	.4519	-.7768	6.8048
10.73	.7680	6.8090	.4955	-.5131	6.8329
14.42	1.7679	6.7741	.5969	.0251	7.0010
18.05	2.8507	6.7707	.7123	.6115	7.3208

APPENDIX A

TABLE A7.- LONGITUDINAL AERODYNAMIC CHARACTERISTICS FOR CONFIGURATION WITH TAIL C FOR M = 1.60

$\phi = 0^\circ, \delta = 0^\circ$					
α, deg	C_N	C_A	C_m	C_L	C_D
-4.28	-1.2264	1.0197	.1008	-1.1467	1.1085
-2.16	-.6328	1.0272	.0556	-.5934	1.0504
-.09	-.0231	1.0369	.0030	-.0214	1.0370
1.98	.5676	1.0328	-.0478	.5315	1.0518
4.07	1.1968	1.0224	-.0990	1.1211	1.1050
6.18	1.8404	1.0113	-.1411	1.7207	1.2038
8.30	2.4873	.9959	-.1702	2.3175	1.3445
10.44	3.1641	.9824	-.1791	2.9336	1.5397
12.61	3.8614	.9696	-.1597	3.5564	1.7896
17.05	5.4848	.9440	.0010	4.9669	2.5108
-.08	.0041	1.0392	.0029	.0056	1.0392

$\phi = 22.5^\circ, \delta = 0^\circ$					
α, deg	C_N	C_A	C_m	C_L	C_D
-3.87	-1.1260	1.0103	.0931	-1.0551	1.0840
-1.76	-.5195	1.0277	.0469	-.4875	1.0433
.29	.0722	1.0369	-.0051	.0669	1.0373
2.39	.6741	1.0325	-.0581	.6302	1.0598
4.48	1.2969	1.0174	-.1079	1.2134	1.1157
6.58	1.9367	1.0008	-.1519	1.8091	1.2163
8.71	2.6090	.9828	-.1822	2.4300	1.3667
10.84	3.2648	.9556	-.1942	3.0266	1.5529
13.00	4.0180	.9281	-.1868	3.7059	1.8088
17.48	5.6379	.8981	-.0103	5.1076	2.5503
22.01	7.5378	.8492	.2053	6.6701	3.6123

$\phi = 45.0^\circ, \delta = 0^\circ$					
α, deg	C_N	C_A	C_m	C_L	C_D
-3.62	-1.0387	1.0063	.0837	-.9730	1.0699
-1.58	-.4614	1.0282	.0419	-.4328	1.0406
.51	.1406	1.0378	-.0109	.1313	1.0391
2.62	.7452	1.0321	-.0639	.6972	1.0651
4.69	1.3578	1.0130	-.1135	1.2703	1.1207
4.69	1.3550	1.0132	-.1138	1.2675	1.1207
6.78	2.0011	.9976	-.1584	1.8691	1.2271
8.90	2.6369	.9821	-.1847	2.4532	1.3783
11.03	3.3134	.9579	-.1959	3.0689	1.5742
13.20	4.0943	.9450	-.1942	3.7702	1.8552
17.68	5.6583	.9216	-.0025	5.1111	2.5967

$\phi = 67.5^\circ, \delta = 0^\circ$					
α, deg	C_N	C_A	C_m	C_L	C_D
-3.50	-1.0150	1.0104	.0823	-.9513	1.0706
-1.41	-.4298	1.0279	.0390	-.4042	1.0382
.66	.1686	1.0353	-.0140	.1566	1.0372
2.74	.7612	1.0321	-.0660	.7108	1.0674
4.84	1.3856	1.0196	-.1171	1.2944	1.1331
6.94	2.0145	1.0069	-.1580	1.8781	1.2430
9.05	2.6575	.9911	-.1854	2.4684	1.3971
11.20	3.3258	.9686	-.1942	3.0742	1.5963
13.35	4.0489	.9453	-.1844	3.7212	1.8547
17.82	5.6590	.9205	-.0009	5.1057	2.6084
22.36	7.5451	.8797	.2196	6.6425	3.6850

$\phi = 90.0^\circ, \delta = 0^\circ$					
α, deg	C_N	C_A	C_m	C_L	C_D
-3.56	-1.0304	1.0167	.0833	-.9651	1.0788
-1.46	-.4192	1.0261	.0376	-.3928	1.0365
.61	.1560	1.0353	-.0133	.1449	1.0369
2.70	.7775	1.0309	-.0681	.7280	1.0664
4.78	1.3730	1.0285	-.1158	1.2824	1.1395
4.79	1.3920	1.0285	-.1172	1.3012	1.1412
6.91	2.0226	1.0252	-.1575	1.8846	1.2612
9.00	2.6682	1.0166	-.1823	2.4762	1.4217
11.14	3.3379	1.0085	-.1914	3.0800	1.6346
13.30	3.9979	1.0033	-.1707	3.6598	1.8962
.61	.1667	1.0355	-.0138	.1557	1.0372

$\phi = 0^\circ, \delta = -15^\circ$					
α, deg	C_N	C_A	C_m	C_L	C_D
-4.05	-3.3913	1.5907	.5553	-3.2704	1.8265
-4.05	-3.3804	1.5847	.5543	-3.2600	1.8196
-2.03	-2.8952	1.5288	.5314	-2.8391	1.6307
-.04	-2.3976	1.4675	.4954	-2.3965	1.4693
1.95	-1.8841	1.4109	.4581	-1.9312	1.3457
3.97	-1.3416	1.3590	.4219	-1.4325	1.2628
5.94	-.7637	1.2964	.3874	-.8939	1.2103
7.96	-.1306	1.2183	.3546	-.2981	1.1884
9.95	.5381	1.1328	.3316	.3341	1.2088
11.95	1.2498	1.0409	.3252	1.0069	1.2773
15.98	2.8490	.8543	.4158	2.5037	1.6056

$\phi = 45.0^\circ, \delta = -15^\circ$					
α, deg	C_N	C_A	C_m	C_L	C_D
-3.43	-4.3660	2.0411	.7684	-4.2358	2.2990
-1.42	-3.9081	1.9618	.7509	-3.8581	2.0584
.55	-3.3839	1.8696	.7096	-3.4019	1.8368
2.54	-2.8238	1.7692	.6616	-2.8997	1.6418
4.56	-2.2689	1.6755	.6201	-2.3951	1.4896
6.54	-1.7107	1.5931	.5945	-1.8812	1.3877
8.55	-1.1294	1.5021	.5714	-1.3403	1.3173
10.55	-.4940	1.3924	.5533	-.7407	1.2784
12.56	.1939	1.2779	.5529	-.0886	1.2895
14.56	.8969	1.1739	.5825	.5730	1.3617
16.53	1.5698	1.0963	.6677	1.1928	1.4977

APPENDIX A

TABLE A8.- LONGITUDINAL AERODYNAMIC CHARACTERISTICS FOR CONFIGURATION WITH TAIL C AT M = 2.36

$\Phi=0^\circ, \delta=0^\circ$					
α, deg	C_N	C_A	C_m	C_L	C_D
-4.32	-.9573	.7455	.0879	-.8983	.8156
-2.27	-.4714	.7408	.0430	-.4416	.7590
-.22	-.0533	.7368	.0045	-.0504	.7370
1.81	.3891	.7391	-.0359	.3654	.7511
3.87	.8612	.7443	-.0770	.8089	.8008
5.92	1.3582	.7557	-.1119	1.2729	.8920
8.00	1.9193	.7632	-.1343	1.7942	1.0232
10.10	2.5463	.7639	-.1364	2.3728	1.1987
12.23	3.2499	.7582	-.1177	3.0155	1.4296
16.49	4.7702	.7474	-.0736	4.3616	2.0711
20.78	6.5007	.7538	-.0550	5.8104	3.0111

$\Phi=22.5^\circ, \delta=0^\circ$					
α, deg	C_N	C_A	C_m	C_L	C_D
-4.47	-.9701	.7497	.0867	-.9086	.8231
-2.42	-.5107	.7454	.0464	-.4787	.7664
-.38	-.0708	.7412	.0061	-.0658	.7416
1.66	.3590	.7422	-.0327	.3372	.7524
3.71	.8207	.7443	-.0723	.7707	.7960
5.78	1.3385	.7497	-.1077	1.2562	.8807
7.85	1.8761	.7486	-.1296	1.7561	.9981
9.96	2.5303	.7498	-.1326	2.3625	1.1762
12.07	3.2221	.7448	-.1202	2.9949	1.4026
16.34	4.7459	.7385	-.0751	4.3461	2.0445
20.64	6.4485	.7506	-.0465	5.7698	2.9759

$\Phi=45.0^\circ, \delta=0^\circ$					
α, deg	C_N	C_A	C_m	C_L	C_D
-4.47	-.9848	.7469	.0884	-.9236	.8214
-2.41	-.5144	.7448	.0457	-.4824	.7659
-.36	-.0918	.7419	.0073	-.0870	.7425
1.67	.3424	.7419	-.0303	.3205	.7516
3.73	.7891	.7440	-.0677	.7390	.7938
5.79	1.3002	.7474	-.1010	1.2181	.8748
7.86	1.8388	.7469	-.1254	1.7192	.9916
9.97	2.4731	.7466	-.1261	2.3063	1.1637
12.10	3.1652	.7464	-.1094	2.9383	1.3934
16.38	4.7367	.7475	-.0760	4.3334	2.0534
20.68	6.4429	.7645	-.0529	5.7576	2.9909

$\Phi=67.5^\circ, \delta=0^\circ$					
α, deg	C_N	C_A	C_m	C_L	C_D
-4.58	-1.0074	.7495	.0915	-.9443	.8275
-2.53	-.5384	.7464	.0480	-.5049	.7695
-.47	-.0987	.7437	.0086	-.0925	.7445
1.56	.3211	.7460	-.0286	.3006	.7545
3.62	.8051	.7504	-.0682	.7561	.7998
5.69	1.2873	.7550	-.1012	1.2061	.8790
7.77	1.8447	.7576	-.1251	1.7253	1.0000
9.87	2.4585	.7537	-.1272	2.2928	1.1641
12.00	3.1421	.7473	-.1101	2.9181	1.3843
16.29	4.6856	.7373	-.0664	4.2904	2.0226
20.61	6.3884	.7482	-.0364	5.7158	2.9497

$\Phi=90.0^\circ, \delta=0^\circ$					
α, deg	C_N	C_A	C_m	C_L	C_D
-4.43	-.9880	.7566	.0879	-.9266	.8307
-2.38	-.5214	.7507	.0464	-.4897	.7717
-.32	-.0849	.7485	.0071	-.0806	.7490
1.72	.3465	.7491	-.0311	.3239	.7592
3.77	.8281	.7588	-.0732	.7763	.8117
5.83	1.3242	.7684	-.1079	1.2392	.8991
7.92	1.8731	.7753	-.1321	1.7483	1.0261
10.02	2.4897	.7767	-.1337	2.3164	1.1983
12.16	3.1941	.7691	-.1182	2.9603	1.4248
16.46	4.7118	.7574	-.0689	4.3039	2.0617
20.78	6.4424	.7622	-.0505	5.7525	2.9990

$\Phi=0^\circ, \delta=-15^\circ$					
α, deg	C_N	C_A	C_m	C_L	C_D
-4.34	-2.5377	1.2724	.5163	-2.4339	1.4611
-2.29	-2.1382	1.2129	.4940	-2.0878	1.2977
-.24	-1.7388	1.1473	.4645	-1.7338	1.1549
1.79	-1.3330	1.0847	.4339	-1.3664	1.0423
3.85	-.8919	1.0153	.3993	-.9581	.9531
5.91	-.3959	.9403	.3633	-.4906	.8946
7.98	.1817	.8594	.3344	.0606	.8763
10.08	.8556	.7761	.3238	.7065	.9139
12.19	1.5726	.6973	.3248	1.3898	1.0138
16.46	3.2621	.5684	.3350	2.9672	1.4698
20.74	4.9646	.4917	.3611	4.4685	2.2185

$\Phi=45.0^\circ, \delta=-15^\circ$					
α, deg	C_N	C_A	C_m	C_L	C_D
-4.47	-3.2687	1.7442	.7168	-3.1227	1.9939
-2.41	-2.8687	1.6752	.6916	-2.7955	1.7947
-.37	-2.4801	1.5945	.6624	-2.4697	1.6106
1.68	-2.0628	1.5041	.6295	-2.1060	1.4429
3.72	-1.6203	1.3976	.5907	-1.7078	1.2892
5.79	-1.0894	1.2720	.5490	-1.2123	1.1556
7.86	-.5511	1.1616	.5233	-.7049	1.0753
9.97	.0981	1.0535	.5242	-.0857	1.0546
12.10	.7918	.9392	.5372	.5773	1.0844
16.38	2.3150	.8017	.5742	1.9949	1.4221
20.68	3.9774	.7219	.6185	3.4661	2.0800

APPENDIX A

TABLE A9.- LONGITUDINAL AERODYNAMIC CHARACTERISTICS FOR CONFIGURATION WITH TAIL C AT M = 3.70

$\Phi=0^\circ, \delta=0^\circ$					
α, deg	C_N	C_A	C_m	C_L	C_D
-4.40	-.7388	.5478	.0101	-.6945	.6029
-2.36	-.3629	.5366	.0036	-.3405	.5511
-.33	-.0443	.5330	.0001	-.0412	.5332
1.70	.2919	.5303	-.0050	.2760	.5388
3.74	.6557	.5377	-.0095	.6192	.5794
5.78	1.0794	.5468	-.0104	1.0188	.6529
7.84	1.5963	.5545	-.0080	1.5057	.7670
9.90	2.1587	.5652	-.0028	2.0292	.9282
11.97	2.7512	.5874	.0054	2.5695	1.1455
16.11	3.9971	.6425	.0145	3.6618	1.7265
20.27	5.4963	.7081	.0114	4.9104	2.5688

$\Phi=22.5^\circ, \delta=0^\circ$					
α, deg	C_N	C_A	C_m	C_L	C_D
-4.24	-.7185	.5455	.0109	-.6761	.5972
-2.21	-.3647	.5380	.0053	-.3436	.5517
-.17	-.0293	.5348	.0001	-.0276	.5349
1.85	.3134	.5331	-.0046	.2959	.5430
3.89	.6701	.5345	-.0080	.6323	.5787
5.93	1.0850	.5380	-.0087	1.0235	.6473
7.99	1.5954	.5428	-.0041	1.5044	.7595
10.06	2.1424	.5528	.0038	2.0128	.9186
12.13	2.7274	.5716	.0097	2.5463	1.1320
16.26	4.0101	.6267	.0154	3.6739	1.7251
20.43	5.5133	.7060	.0059	4.9200	2.5862

$\Phi=45.0^\circ, \delta=0^\circ$					
α, deg	C_N	C_A	C_m	C_L	C_D
-4.29	-.7375	.5484	.0108	-.6944	.6020
-2.25	-.3670	.5429	.0037	-.3453	.5569
-.22	-.0446	.5385	-.0000	-.0426	.5386
1.81	.2891	.5355	-.0029	.2720	.5444
3.85	.6501	.5349	-.0072	.6127	.5774
5.90	1.0707	.5396	-.0088	1.0095	.6469
7.96	1.5803	.5459	-.0038	1.4894	.7595
10.02	2.1139	.5596	.0069	1.9842	.9191
12.10	2.6977	.5800	.0150	2.5161	1.1327
16.24	3.9898	.6380	.0193	3.6519	1.7289
20.41	5.5073	.7148	.0033	4.9120	2.5910

$\Phi=67.5^\circ, \delta=0^\circ$					
α, deg	C_N	C_A	C_m	C_L	C_D
-4.50	-.7718	.5515	.0124	-.7261	.6104
-2.46	-.3943	.5417	.0048	-.3706	.5582
-.42	-.0663	.5384	.0013	-.0623	.5389
1.60	.2652	.5381	-.0020	.2500	.5453
3.64	.6285	.5403	-.0063	.5929	.5793
5.69	1.0480	.5475	-.0070	.9885	.6487
7.76	1.5535	.5533	-.0025	1.4645	.7580
9.82	2.1065	.5613	.0041	1.9798	.9126
11.89	2.6886	.5793	.0111	2.5114	1.1212
16.05	3.9673	.6335	.0186	3.6373	1.7061
20.22	5.4669	.7136	.0090	4.8830	2.5598

$\Phi=90.0^\circ, \delta=0^\circ$					
α, deg	C_N	C_A	C_m	C_L	C_D
-4.50	-.7865	.5525	.0113	-.7407	.6126
-2.46	-.4128	.5426	.0059	-.3890	.5599
-.42	-.0780	.5394	.0016	-.0739	.5400
1.60	.2601	.5376	-.0029	.2449	.5447
3.65	.6193	.5456	-.0073	.5833	.5839
5.70	1.0387	.5547	-.0087	.9785	.6552
7.75	1.5477	.5632	-.0068	1.4576	.7669
9.82	2.1183	.5724	-.0019	1.9895	.9256
11.89	2.6923	.5963	.0068	2.5115	1.1386
16.05	3.9566	.6544	.0173	3.6212	1.7233
20.24	5.4334	.7212	.0138	4.8484	2.5564

$\Phi=0^\circ, \delta=-15^\circ$					
α, deg	C_N	C_A	C_m	C_L	C_D
-4.40	-1.9698	1.0159	.3438	-1.8859	1.1643
-2.37	-1.5870	.9370	.3324	-1.5468	1.0019
-.33	-1.2091	.8647	.3169	-1.2040	.8718
1.69	-.8495	.7958	.3019	-.8727	.7704
3.72	-.4608	.7320	.2901	-.5074	.7005
5.78	-.0038	.6701	.2810	-.0713	.6663
7.83	.5632	.6035	.2721	.4757	.6747
9.90	1.1246	.5650	.2760	1.0107	.7500
11.95	1.6399	.5547	.3008	1.4894	.8824
16.10	2.7187	.5576	.3619	2.4574	1.2898
20.25	3.9748	.5609	.4208	3.5349	1.9020

$\Phi=45.0^\circ, \delta=-15^\circ$					
α, deg	C_N	C_A	C_m	C_L	C_D
-4.28	-2.4079	1.3879	.4756	-2.2973	1.5641
-2.25	-2.0202	1.3019	.4627	-1.9674	1.3804
-.21	-1.6473	1.2049	.4453	-1.6427	1.2111
1.81	-1.2728	1.1028	.4283	-1.3072	1.0619
3.85	-.8708	.9979	.4095	-.9359	.9371
5.90	-.4017	.9031	.3943	-.4925	.8570
7.96	.0940	.8403	.4006	-.0232	.8453
10.02	.6041	.7971	.4179	.4561	.8901
12.09	1.1258	.7712	.4387	.9392	.9900
16.23	2.2024	.7563	.4972	1.9030	1.3420
20.40	3.4576	.7481	.5534	2.9796	1.9069

APPENDIX B

EFFECT OF A FLATTENED AFT END

It was thought that if the deflected control surface could remain in contact with the body, then the high-pressure air below the surface would not bleed over onto the upper surface, and thus the characteristics of the tail surface could be improved. Simple fairing pieces were added to the aft end of the circular configuration to obtain the flattened aft end. The details of the fairing pieces and the resulting aft end, which allowed tail B to be in contact with the body up to 15° tail deflection, are shown in figure B1.

Figure B2 shows a typical comparison at $M = 1.60$ of ΔC_p for the tails on the circular and flattened aft ends. There appear to be no real differences in the ΔC_p for the two configurations. The basic aerodynamic data for the flattened aft-end configuration are given in table B1. Figure B3 shows the panel loads for the two configurations, and there only seem to be slight variations in the two configurations, with the largest differences occurring at the higher angles of attack. Figure B4 shows the resulting center-of-pressure locations, and the only difference seems to be an outboard shift in the center of pressure for $\phi_f = 90^{\circ}$. The scatter of data in figure B4 at the higher angles of attack results from dividing the panel moments by panel forces that approach zero. The overall conclusion is that the flattened aft end does not greatly improve the characteristics of tail B.

APPENDIX B

TABLE B1.- LONGITUDINAL AERODYNAMIC CHARACTERISTICS FOR CONFIGURATION WITH FLATTENED AFT END AND TAIL B

M = 1.60

$\Phi=0^\circ, \delta=-15^\circ$					
α, deg	C_N	C_A	C_m	C_L	C_D
-3.84	-4.2183	1.8985	.7343	-4.0815	2.1771
-1.84	-3.5663	1.7919	.6724	-3.5066	1.9060
.16	-2.9146	1.7024	.6033	-2.9195	1.6939
2.15	-2.2928	1.6230	.5402	-2.3522	1.5356
4.16	-1.6520	1.5573	.4834	-1.7606	1.4333
6.15	-1.0082	1.4889	.4309	-1.1621	1.3722
8.13	-.2930	1.3991	.3816	-.4879	1.3436
10.15	.4720	1.2915	.3398	.2369	1.3545
12.15	1.2653	1.1765	.3140	.9892	1.4165
16.16	3.0504	.9382	.3645	2.6687	1.7502
20.15	4.8869	.7168	.4866	4.3407	2.3565

M = 1.60

$\Phi=45.0^\circ, \delta=-15^\circ$					
α, deg	C_N	C_A	C_m	C_L	C_D
-3.74	-5.4925	2.5213	1.0054	-5.3162	2.8745
-1.74	-4.9114	2.4033	.9555	-4.8360	2.5518
.25	-4.2293	2.2467	.8776	-4.2391	2.2282
2.25	-3.4965	2.0963	.7911	-3.5764	1.9568
4.24	-2.7728	1.9511	.7118	-2.9097	1.7404
6.24	-2.1244	1.8263	.6614	-2.3106	1.5842
8.25	-1.4517	1.7099	.6189	-1.6823	1.4836
10.25	-.7436	1.5878	.5879	-1.0144	1.4301
12.26	-.0105	1.4608	.5699	-.3205	1.4253
16.24	1.5279	1.2524	.6802	1.1164	1.6299
20.26	3.3534	1.0085	.8133	2.7964	2.1076

M = 2.36

$\Phi=0^\circ, \delta=-15^\circ$					
α, deg	C_N	C_A	C_m	C_L	C_D
-4.74	-3.0872	1.4637	.4404	-2.9554	1.7142
-3.02	-2.6544	1.3993	.4281	-2.5768	1.5375
-1.08	-2.1858	1.3233	.4097	-2.1604	1.3644
.76	-1.7839	1.2538	.3945	-1.8005	1.2299
2.72	-1.3176	1.1744	.3778	-1.3720	1.1104
4.52	-.8591	1.0990	.3622	-.9431	1.0277
6.36	-.3270	1.0162	.3484	-.4377	.9737
8.13	.2252	.9322	.3447	.0909	.9547
9.69	.7883	.8612	.3592	.6320	.9816
12.75	1.9958	.7466	.4271	1.7817	1.1688
15.90	3.3809	.6256	.4981	3.0801	1.5281

M = 3.70

$\Phi=0^\circ, \delta=-15^\circ$					
α, deg	C_N	C_A	C_m	C_L	C_D
-4.37	-2.2782	1.1054	.2804	-2.1872	1.2760
-2.52	-1.8691	1.0282	.2834	-1.8220	1.1095
-.61	-1.4538	.9431	.2773	-1.4435	.9586
1.27	-1.0631	.8650	.2744	-1.0821	.8411
3.16	-.6538	.7928	.2765	-.6966	.7554
4.95	-.2156	.7286	.2806	-.2778	.7072
6.77	.2959	.6617	.2939	.2157	.6920
8.52	.8441	.6081	.3131	.7446	.7265
10.22	1.3263	.5895	.3512	1.2006	.8157
13.64	2.2541	.5842	.4458	2.0527	1.0995
17.00	3.2332	.5908	.5501	2.9192	1.5104

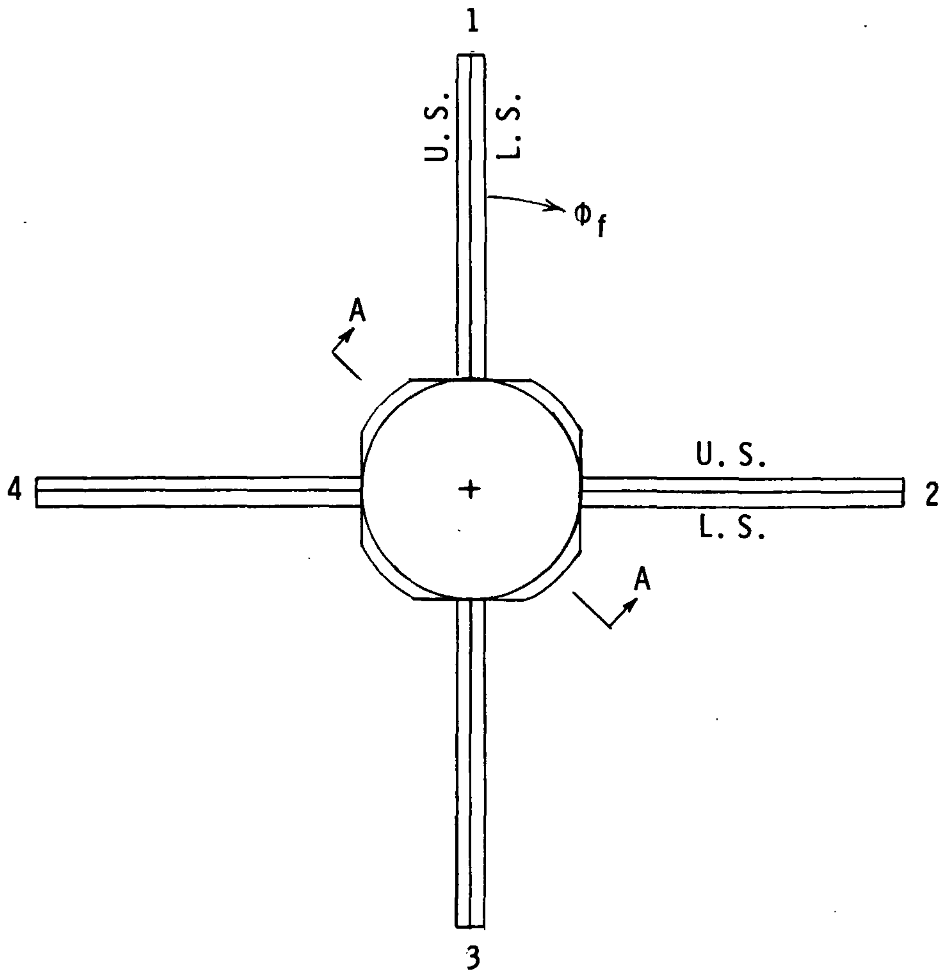

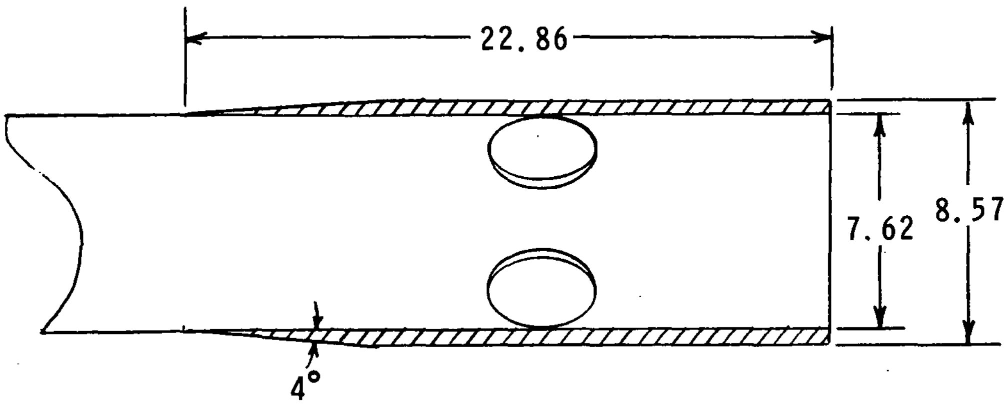

Section A-A rotated 45° clockwise

Figure B1.- Flattened aft end. All dimensions in centimeters.

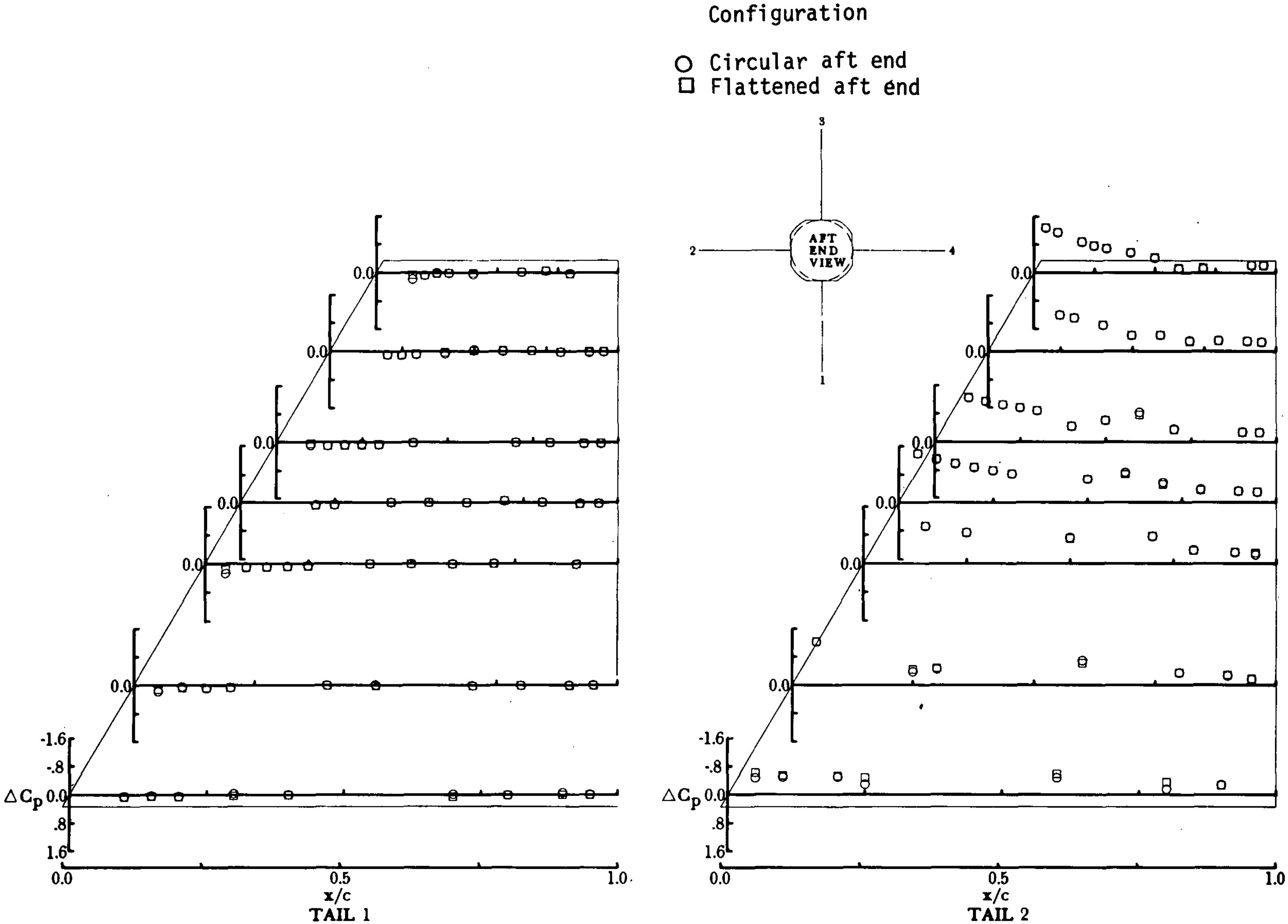

(a) $\alpha \approx 0^{o}$; $\delta = -15^{o}$; $\phi = 0^{o}$.

Figure B2.- Comparison of ΔC_p for circular and flattened aft end at $M = 1.60$.

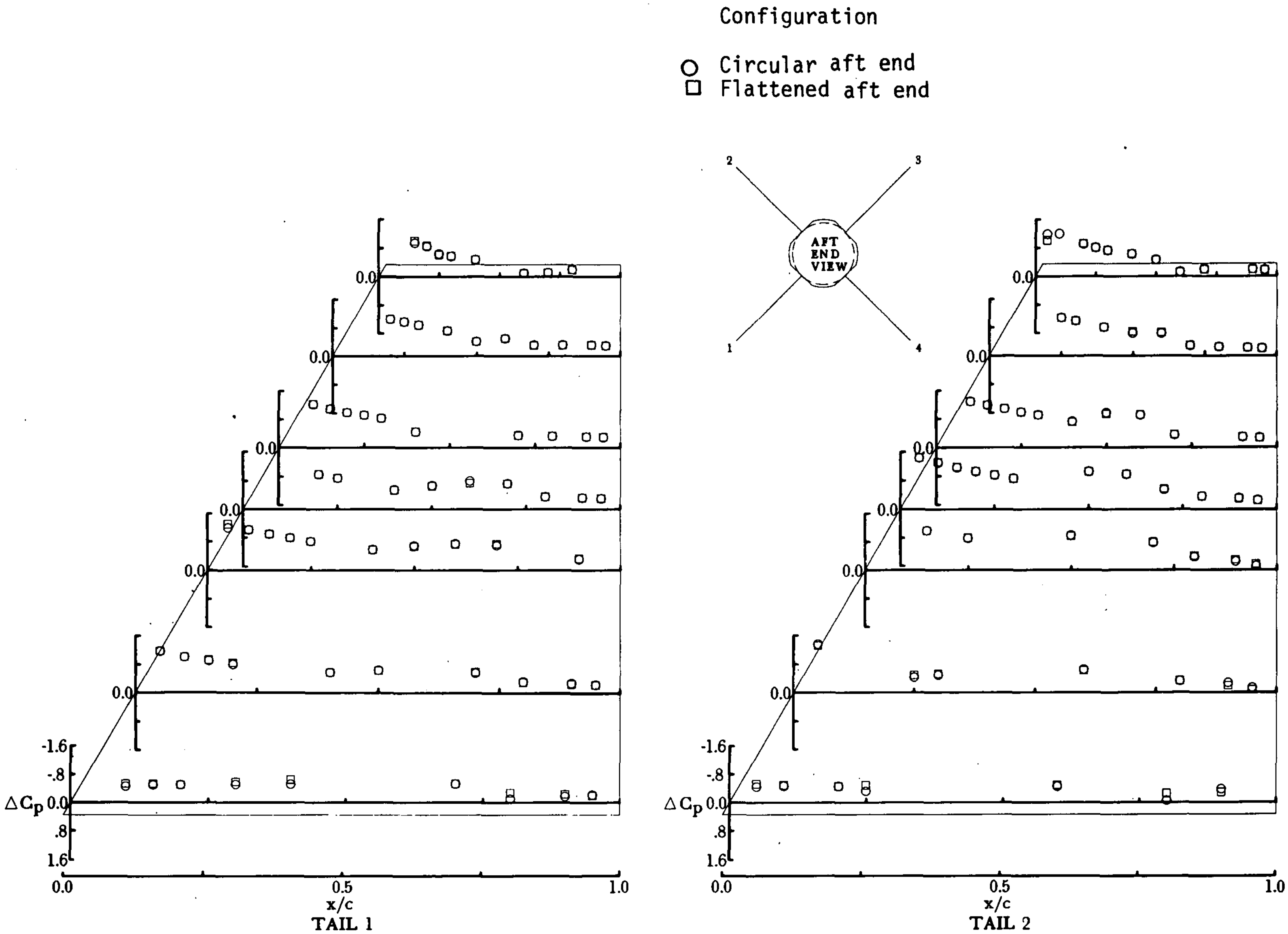

(b) $\alpha \approx 0^{\circ}$; $\delta = -15^{\circ}$; $\phi = 45^{\circ}$.

Figure B2.- Concluded.

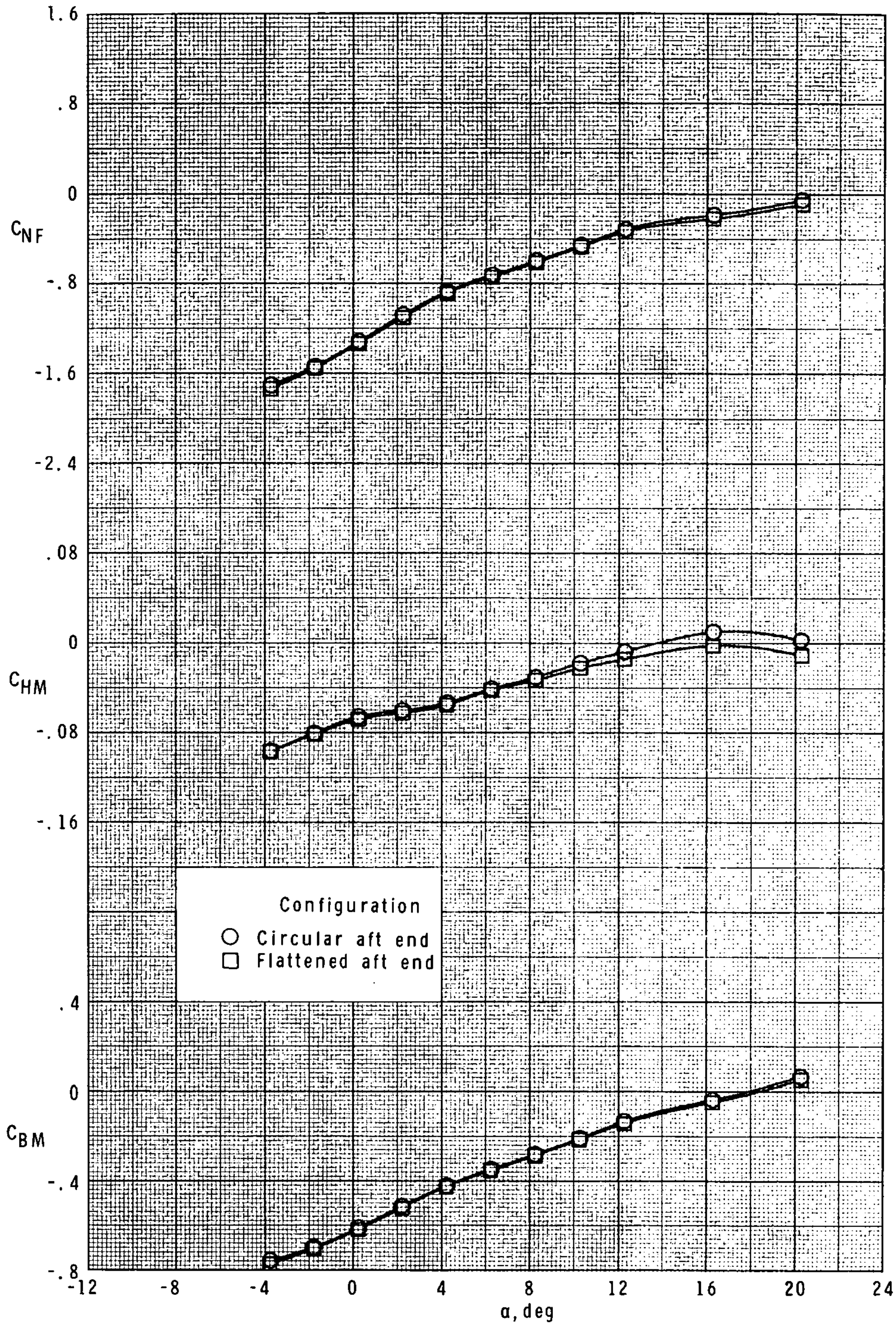

(a) $\phi_f = 45^{\circ}$; $\phi = 45^{\circ}$.

Figure B3.- Comparison of panel loads for circular and flattened aft-end configurations at M = 1.60.

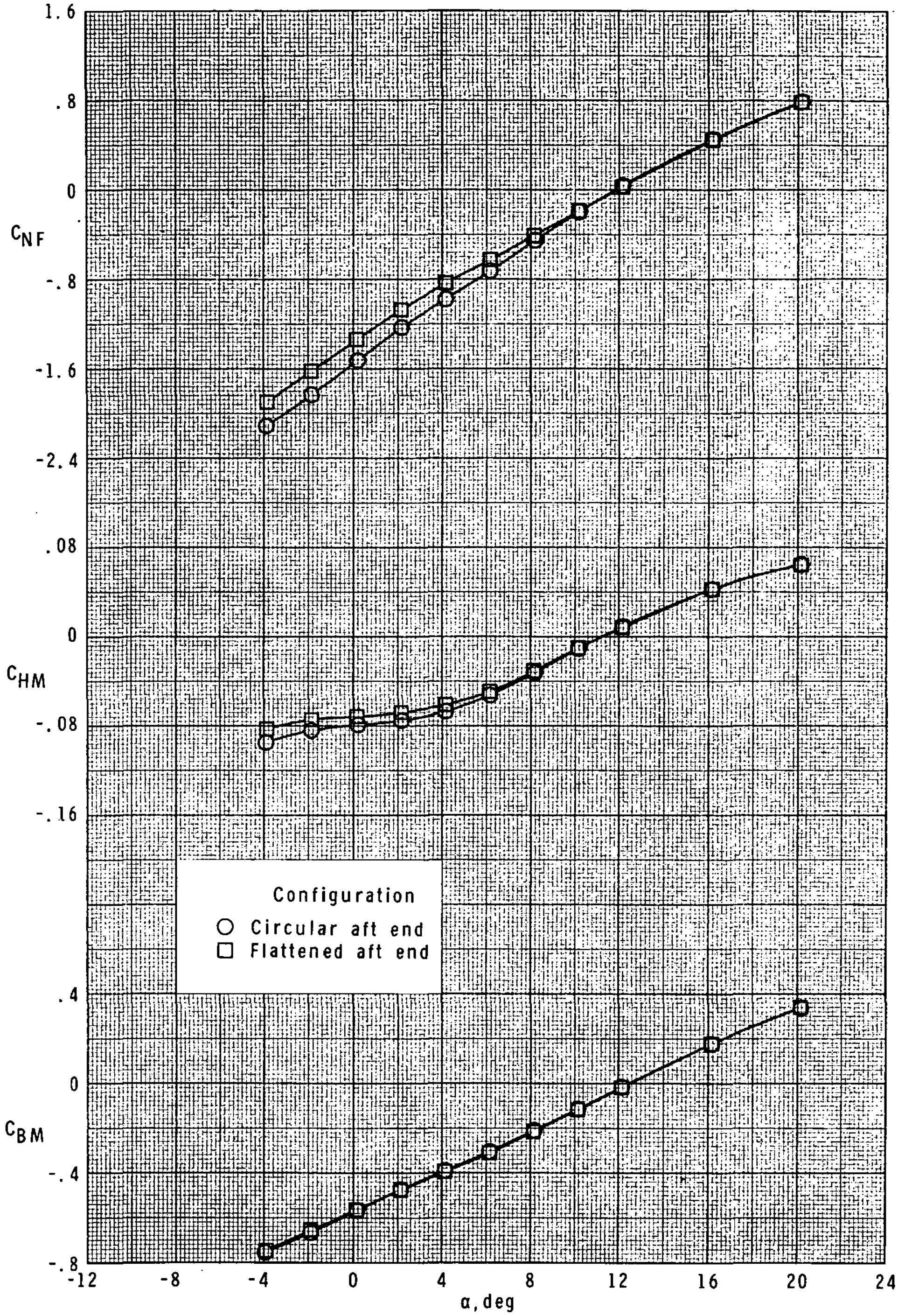

(b) $\phi_f = 90^\circ$; $\phi = 0^\circ$.

Figure B3.- Continued.

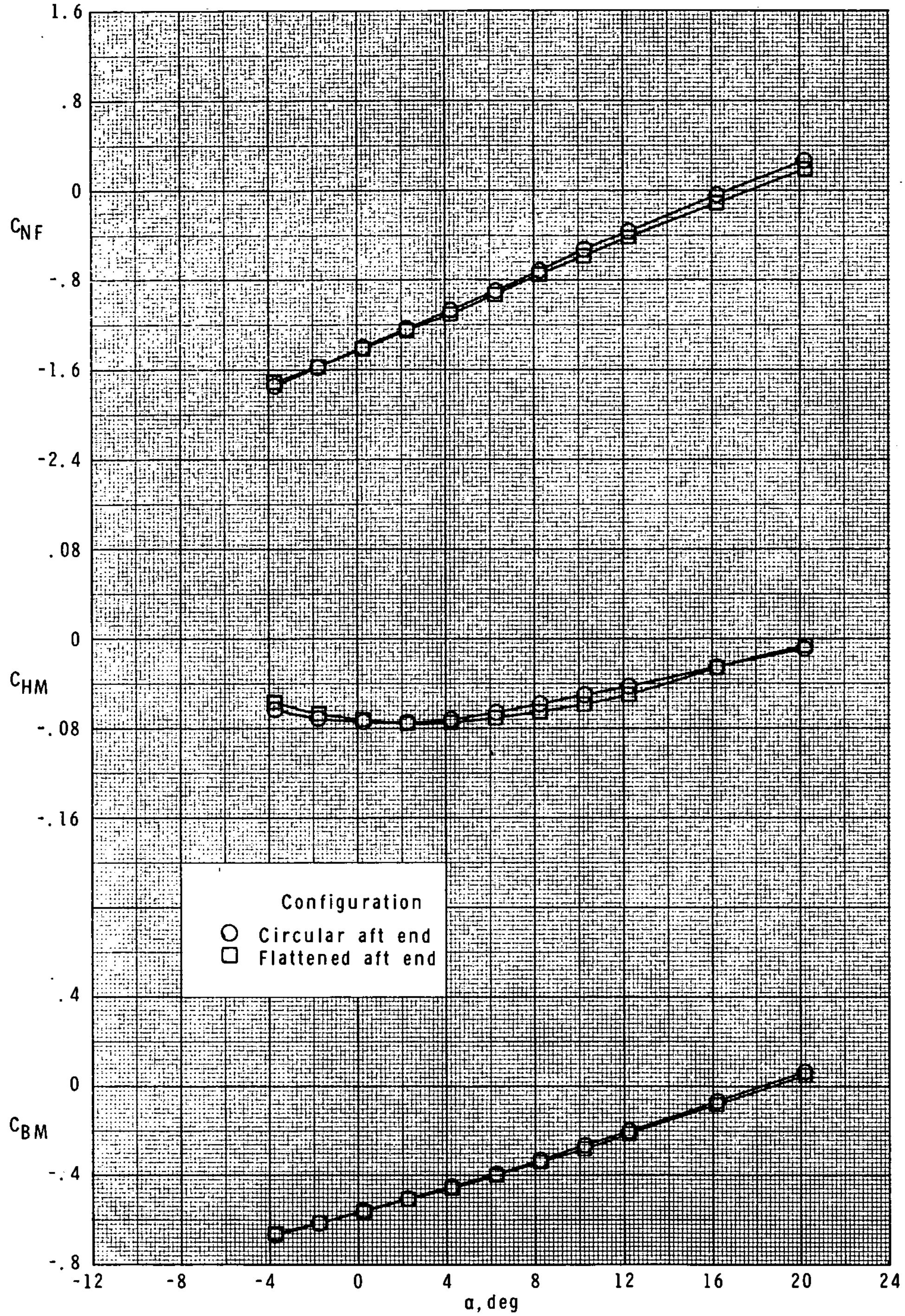

(c) $\phi_f = 135^\circ$; $\phi = 45^\circ$.

Figure B3.- Concluded.

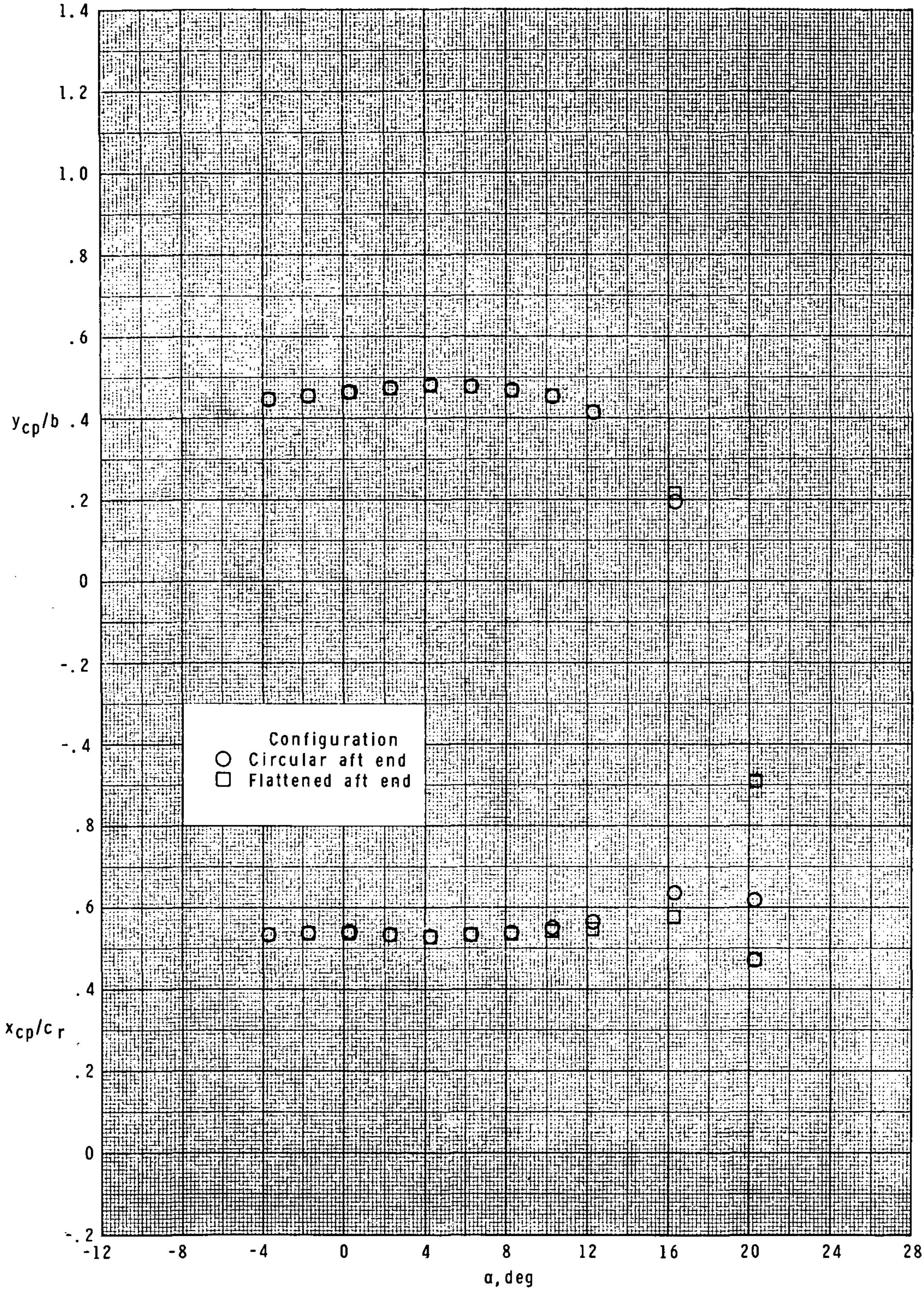

(a) $\phi_f = 45^o$; $\phi = 45^o$.

Figure B4.- Comparison of center of pressure for circular and flattened aft-end configurations at M = 1.60.

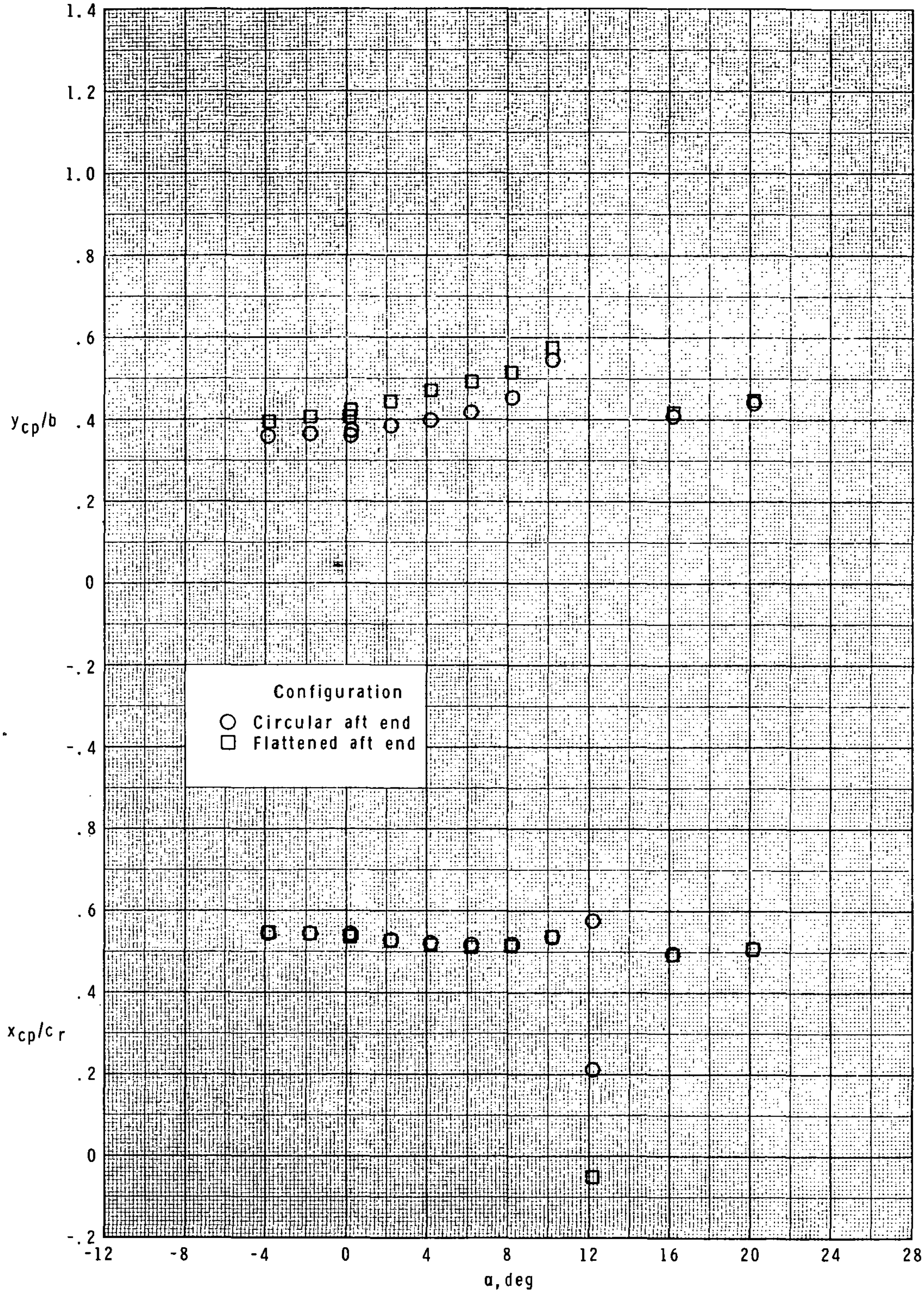

(b) $\phi_f = 90^\circ$; $\phi = 0^\circ$.

Figure B4.- Continued.

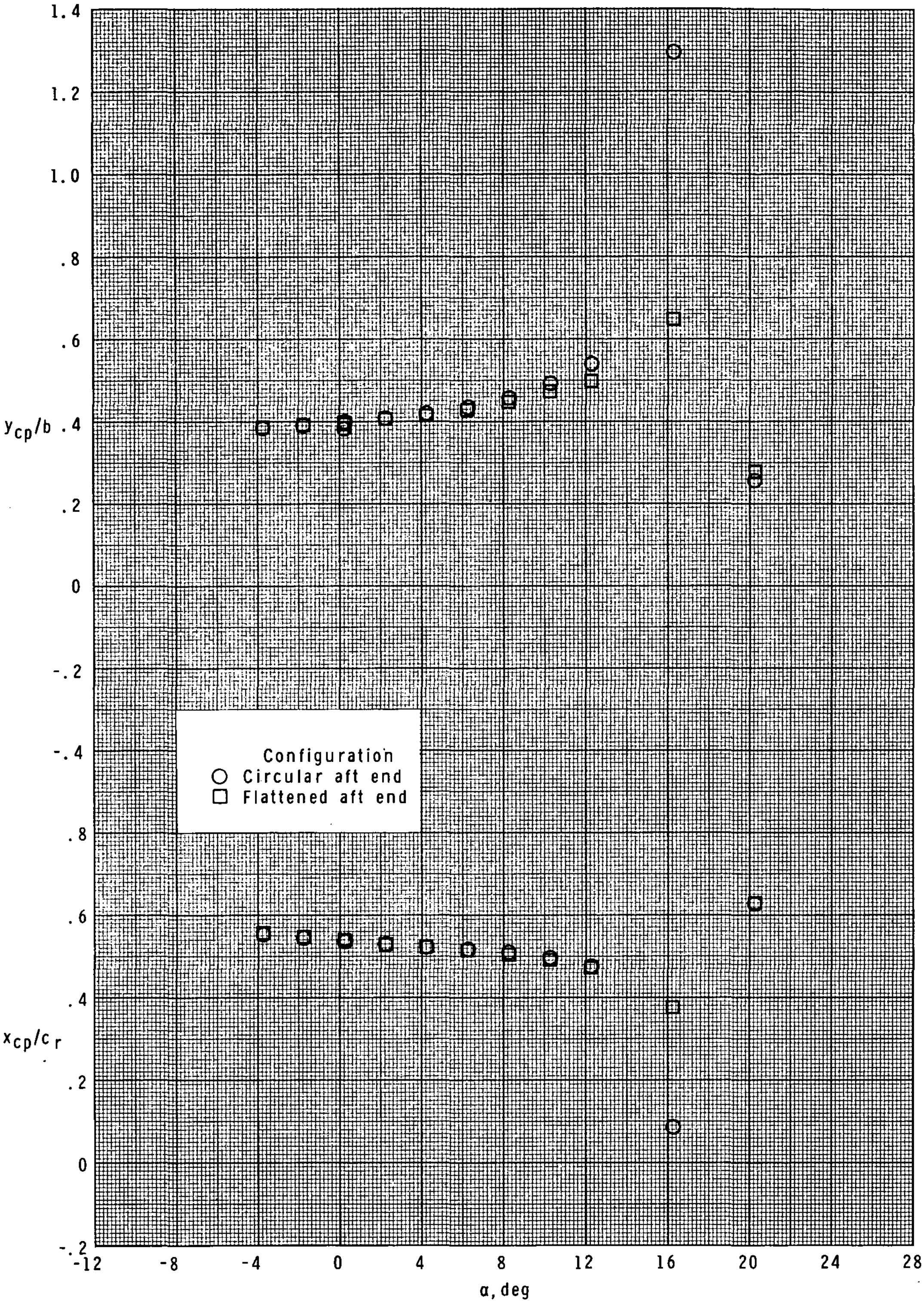

(c) $\phi_f = 135^{\circ}$; $\phi = 45^{\circ}$.

Figure B4.- Concluded.

REFERENCES

1. Corlett, William A.: Aerodynamic Characteristics at Mach Numbers From 0.40 to 2.86 of a Maneuverable Missile With Cruciform Trapezoidal Wings and Aft Tail Controls. NASA TM X-2681, 1972.

2. Corlett, William A.; and Howell, Dorothy T.: Aerodynamic Characteristics at Mach 0.60 to 4.63 of Two Cruciform Missile Models, One Having Trapezoidal Wings With Canard Controls and the Other Having Delta Wings With Tail Controls. NASA TM X-2780, 1973.

3. Nielsen, Jack N.: Missile Aerodynamics. McGraw-Hill Book Co., Inc., 1960.

4. Kaattari, George E.; Hill, William A., Jr.; and Nielsen, Jack N.: Control for Supersonic Missiles. NACA Conference on Automatic Stability and Control of Aircraft - A Compilation of Papers Presented, NACA, Mar. 1955, pp. 251-263.

5. Lamb, Milton; Sawyer, Wallace C.; Wassum, Donald L.; and Babb, C. Donald: Pressure Distributions on Three Different Cruciform Aft-Tail Control Surfaces of a Wingless Missile at Mach 1.60, 2.36, and 3.70. Volumes I to III. NASA TM-80097, 1979.

6. Jackson, Charlie M., Jr.; and Sawyer, Wallace C.: A Method for Calculating the Aerodynamic Loading on Wing-Body Combinations at Small Angles of Attack in Supersonic Flow. NASA TN D-6441, 1971.

TABLE I.- FIN CHARACTERISTICS

	T_A	T_B	T_C
Exposed area per panel, cm^2	101.613	92.926	75.000
Exposed semispan (reference span), cm	11.430	11.430	11.430
Exposed root chord (reference chord), cm . . .	11.430	11.430	11.430
Maximum thickness, cm	1.110	1.110	1.110
Exposed aspect ratio	1.286	1.406	1.742
Exposed taper ratio	0.556	0.423	0.333
Leading-edge sweep, deg	12.53	30.000	45.000 inboard 14.040 outboard
x_{HL}/c_r	0.467	0.589	0.680

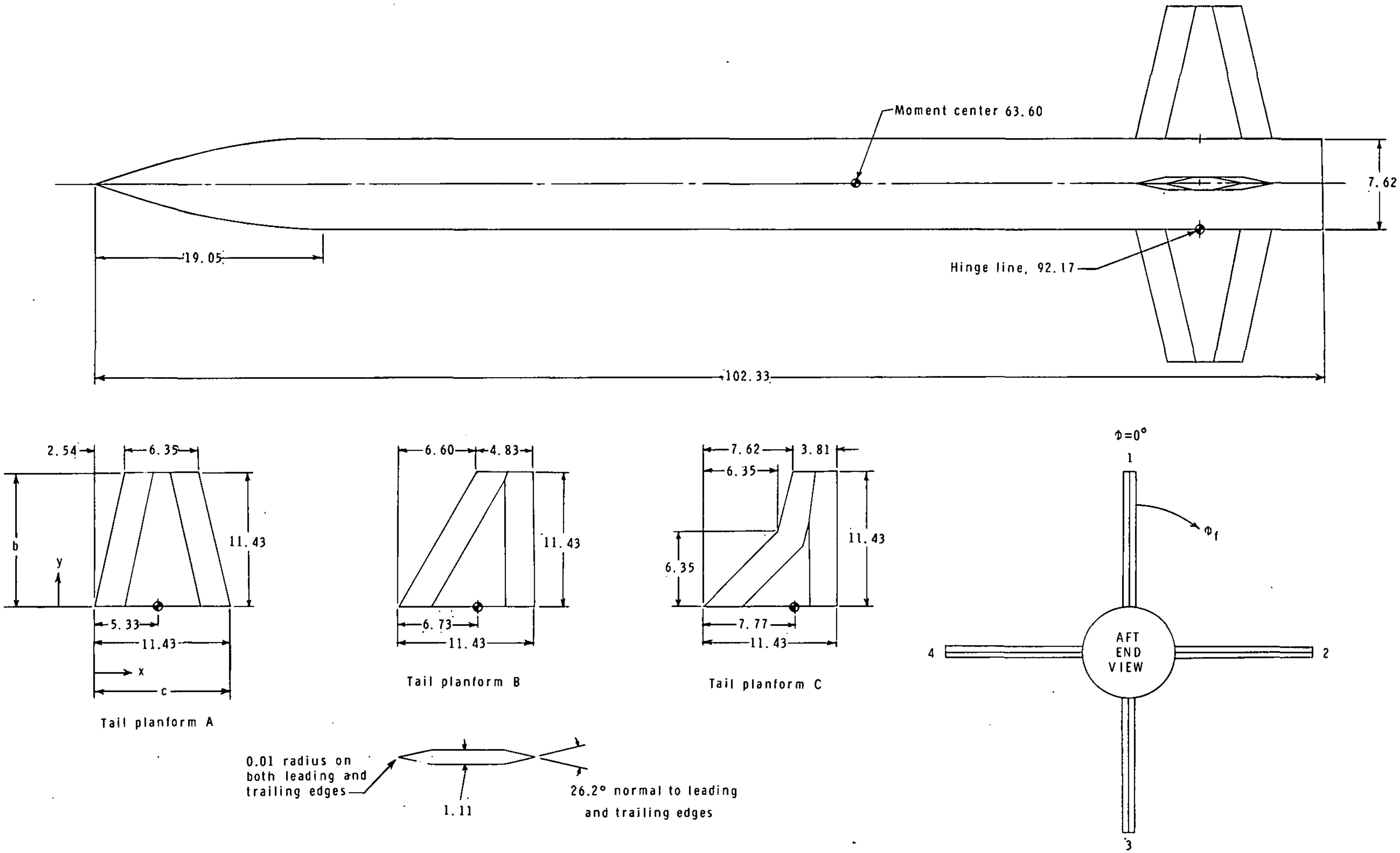

Figure 1.- Details of model. All dimensions are in centimeters.

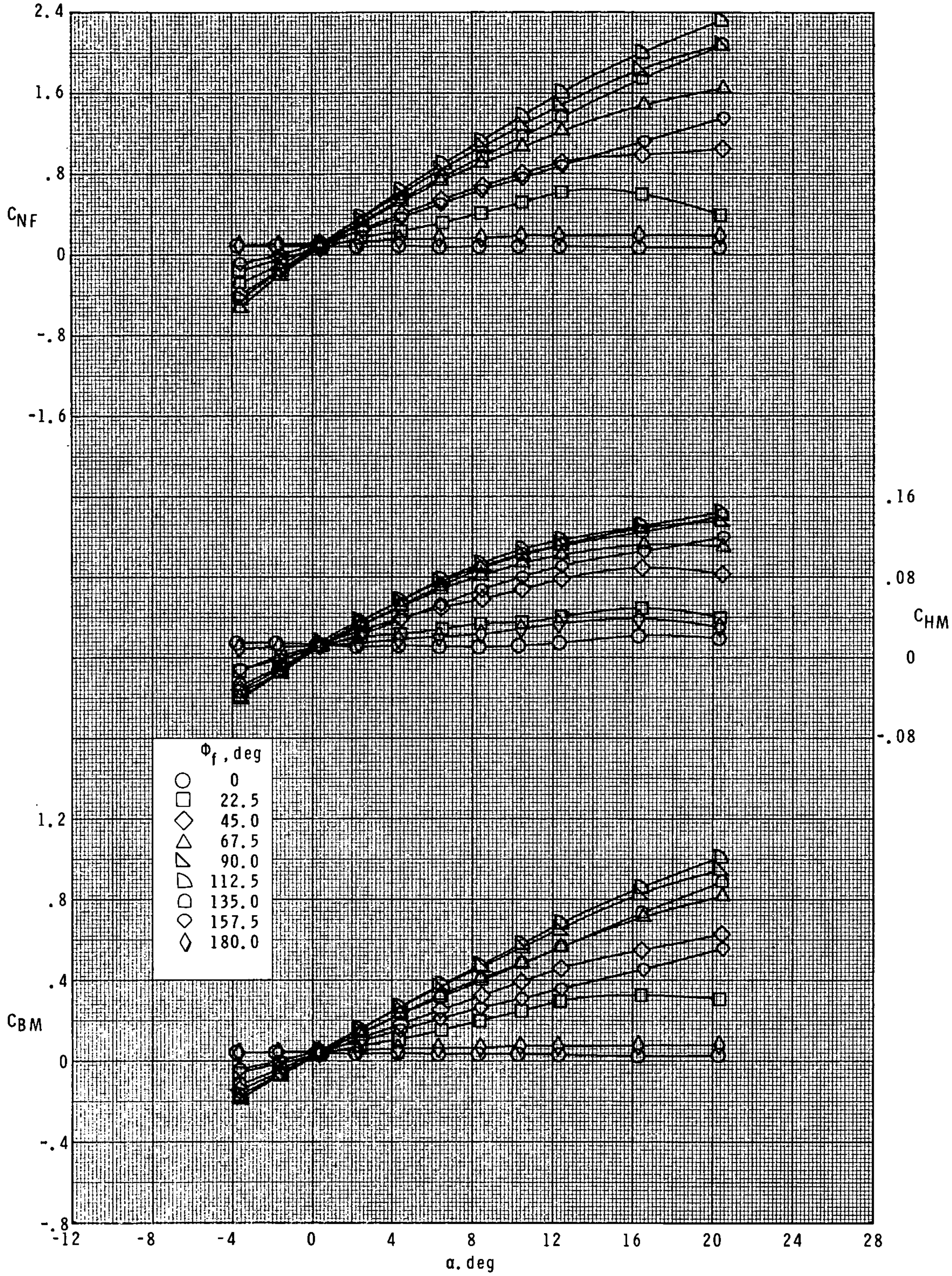

(a) M = 1.60.

Figure 2.- Effect of tail roll orientation on tail loads for T_A at $\delta = 0^{\circ}$.

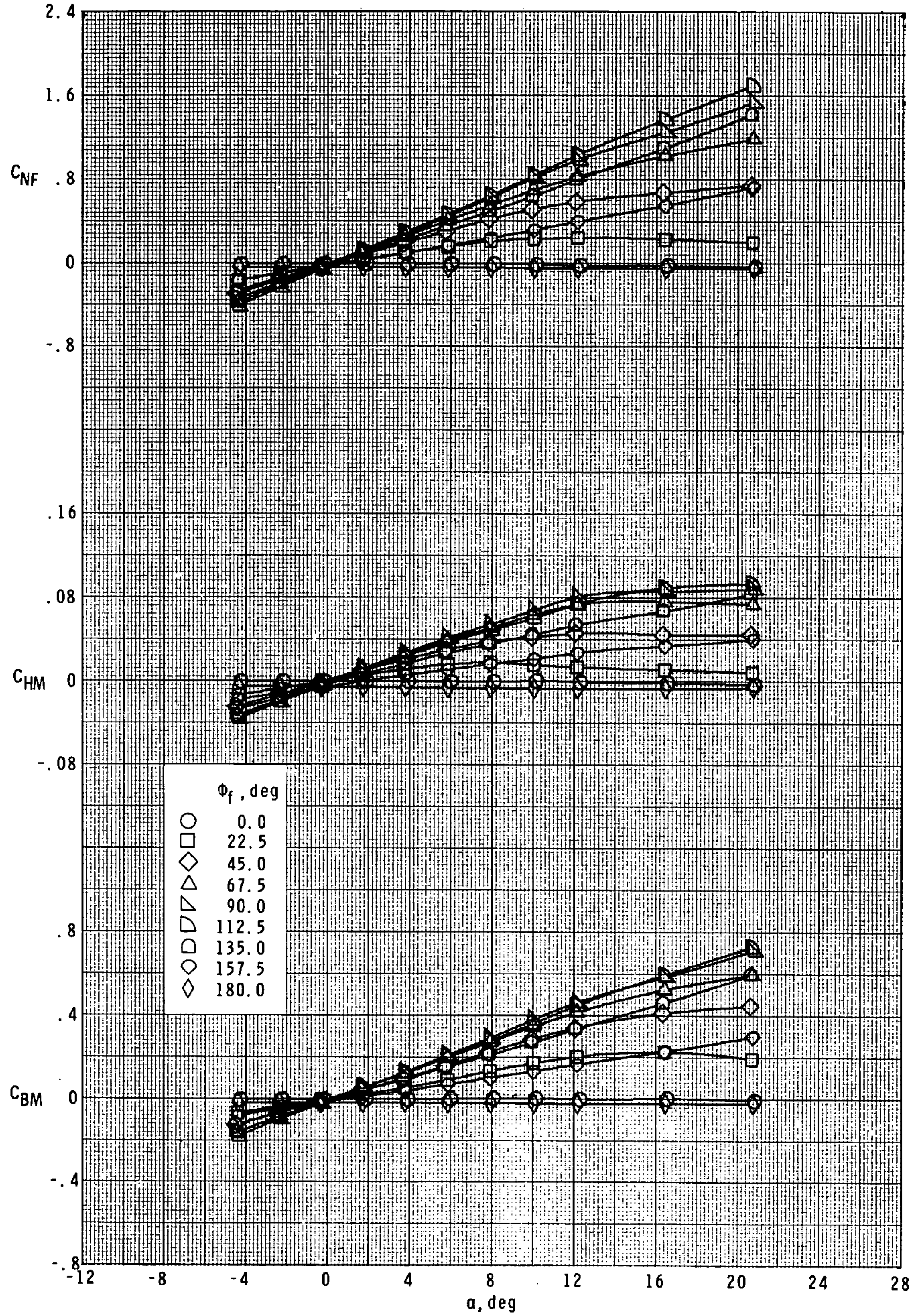

(b) M = 2.36.

Figure 2.- Continued.

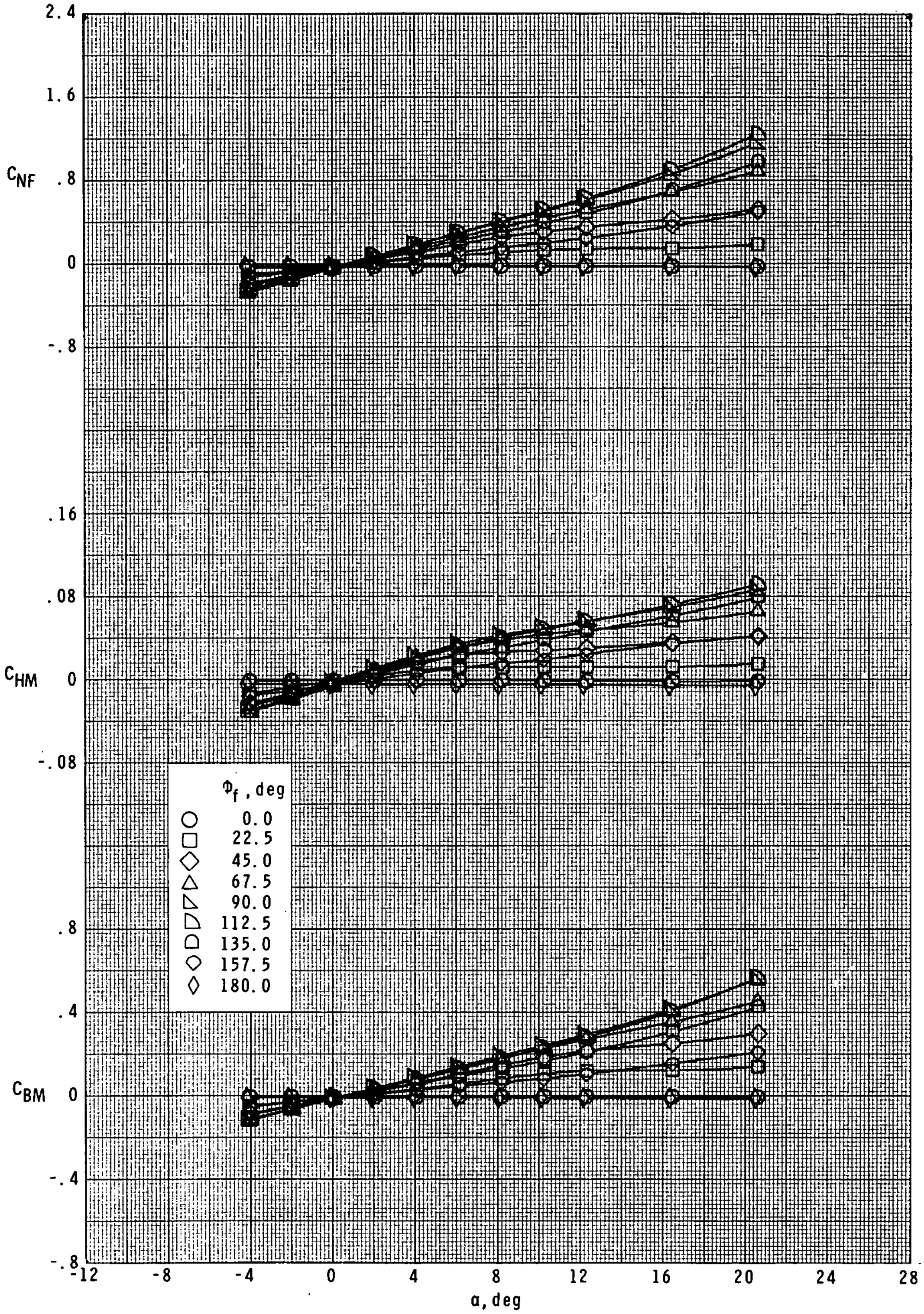

(c) M = 3.70.

Figure 2.- Concluded.

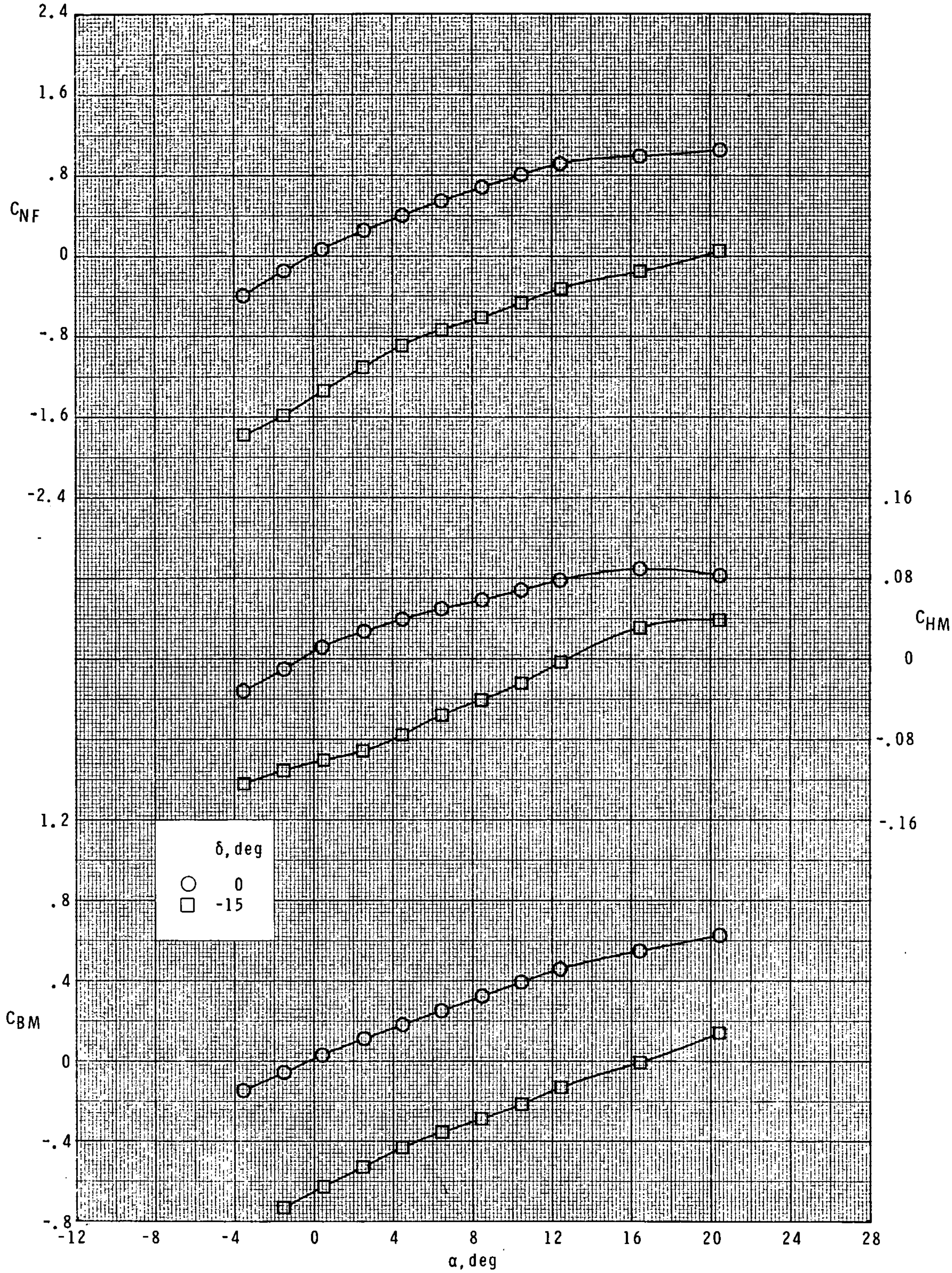

(a) M = 1.60; $\phi_f = 45^\circ$; $\phi = 45^\circ$.

Figure 3.- Effect of tail deflection on tail loads for T_A.

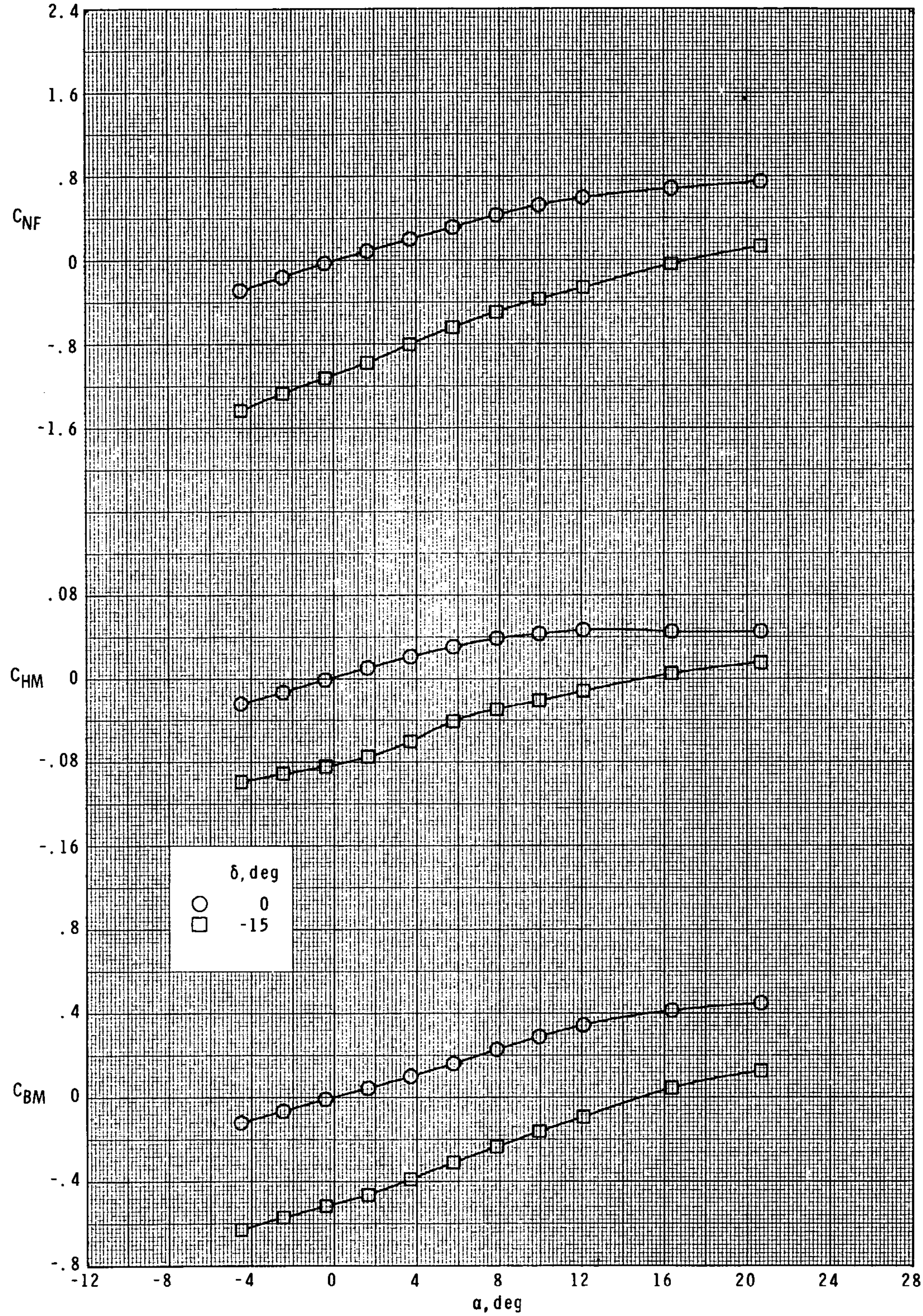

(b) $M = 2.36$; $\phi_f = 45^\circ$; $\phi = 45^\circ$.

Figure 3.- Continued.

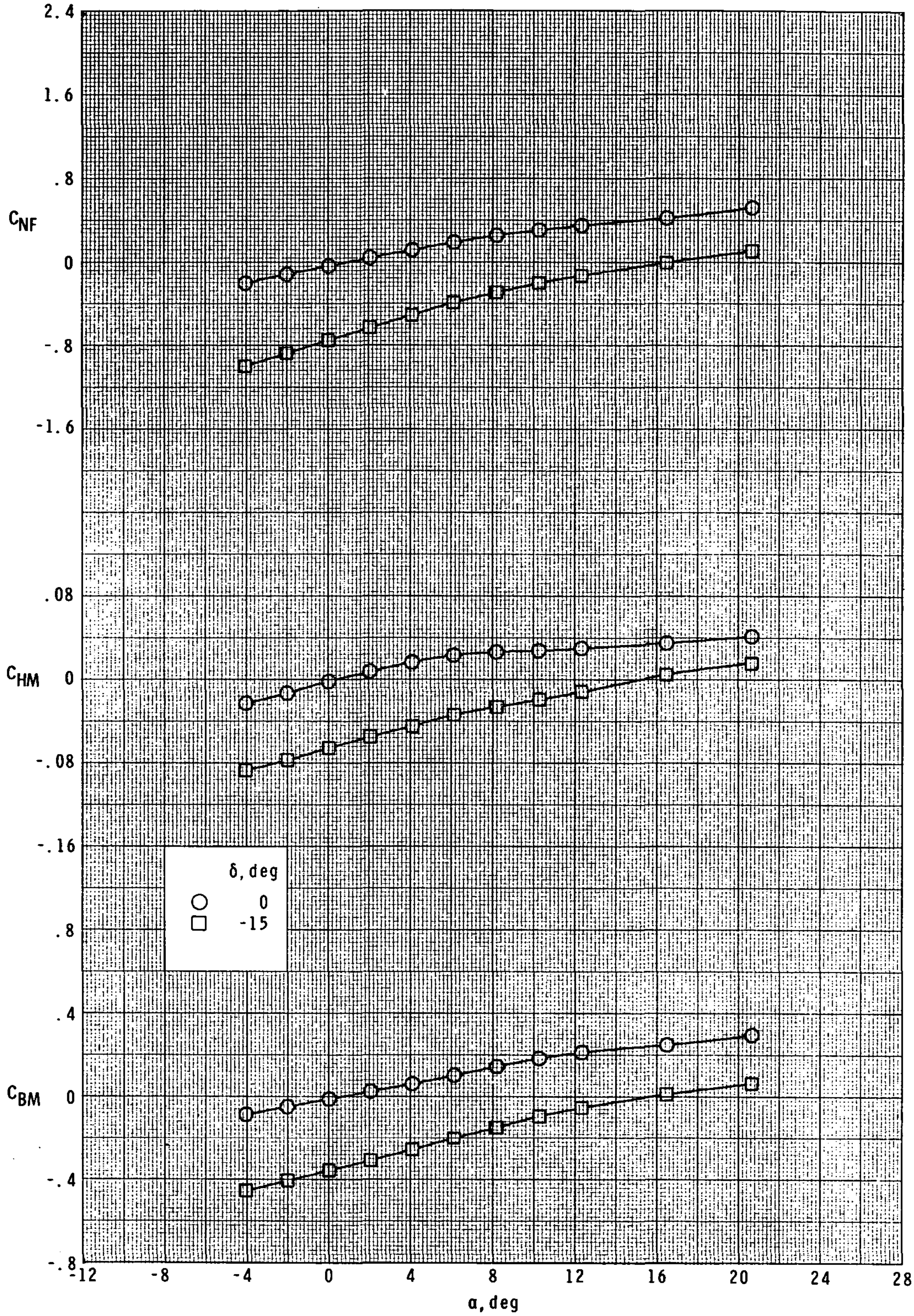

(c) $M = 3.70$; $\phi_f = 45^{\circ}$; $\phi = 45^{\circ}$.

Figure 3.- Continued.

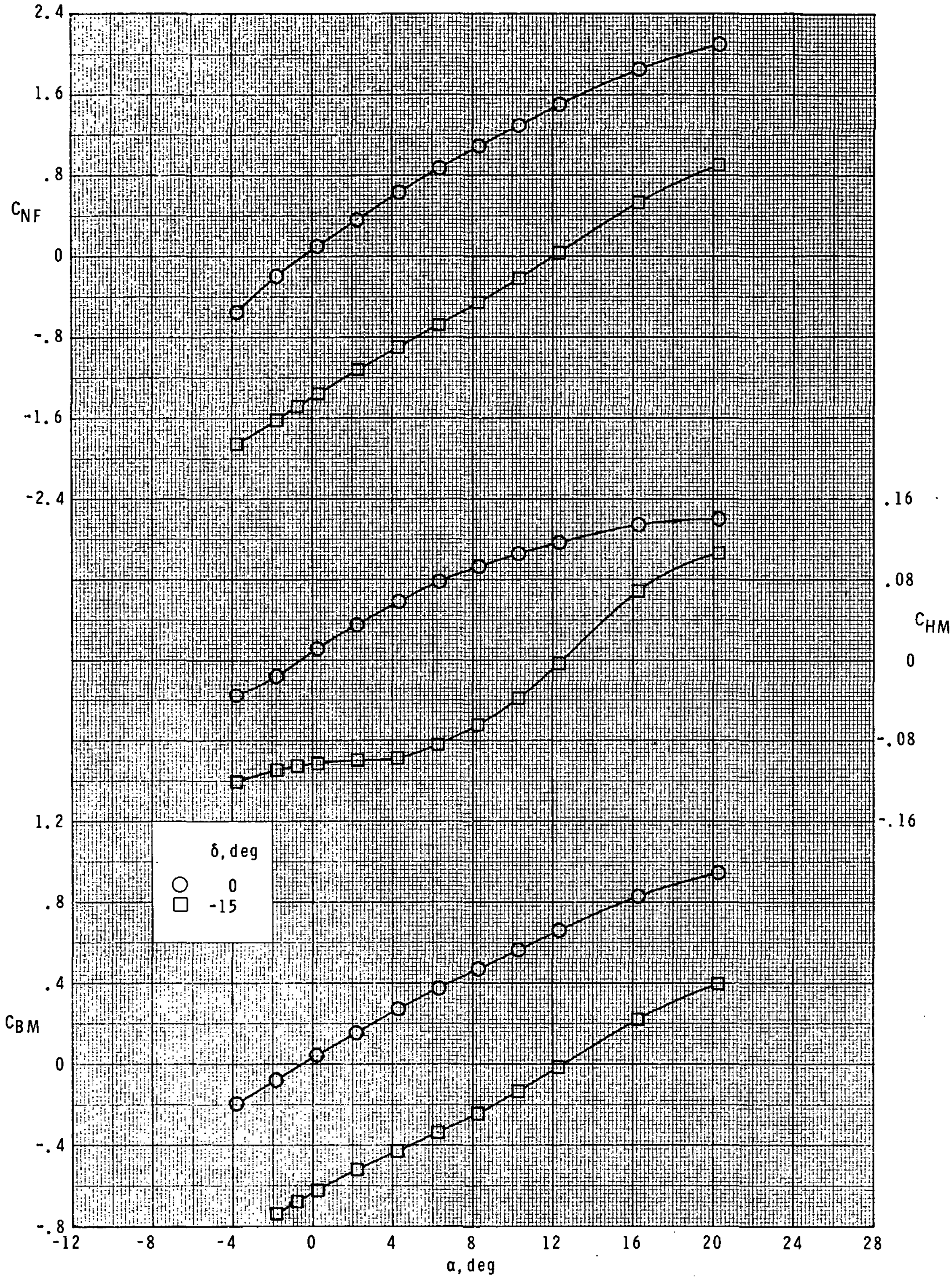

(d) M = 1.60; $\phi_f = 90°$; $\phi = 0°$.

Figure 3.- Continued.

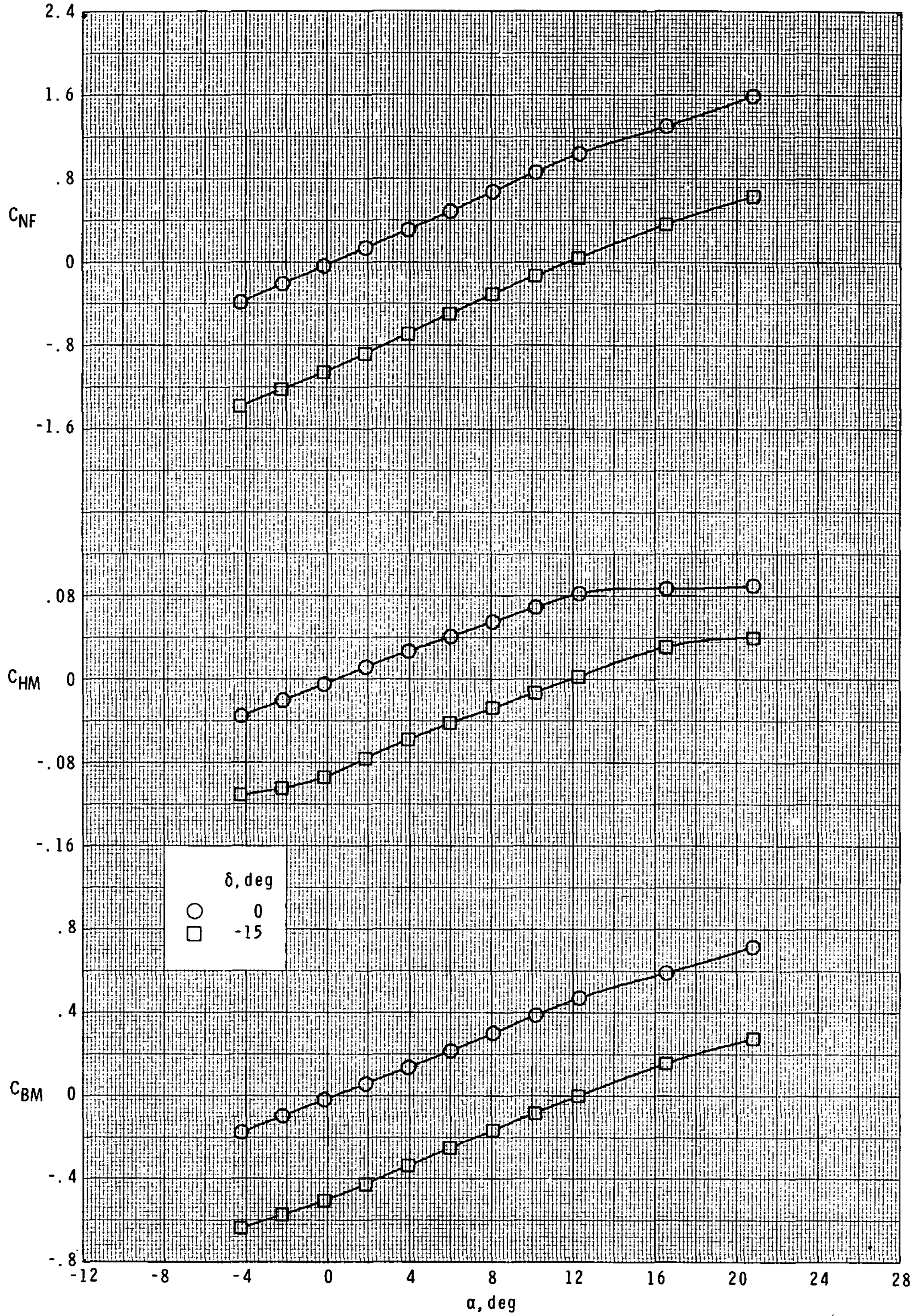

(e) $M = 2.36$; $\phi_f = 90^\circ$; $\phi = 0^\circ$.

Figure 3.- Continued.

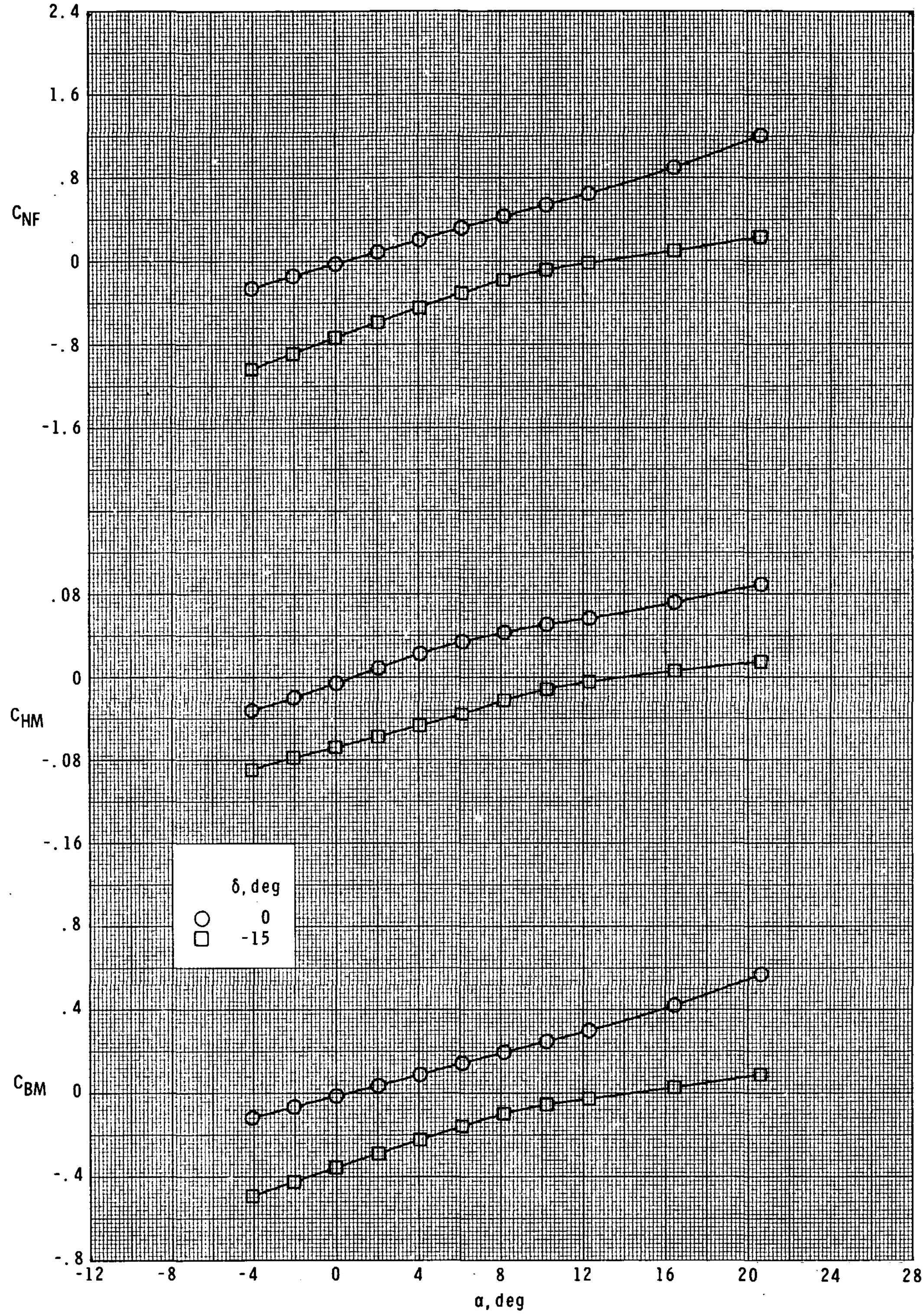

(f) $M = 3.70$; $\phi_f = 90^\circ$; $\phi = 0^\circ$.

Figure 3.- Continued.

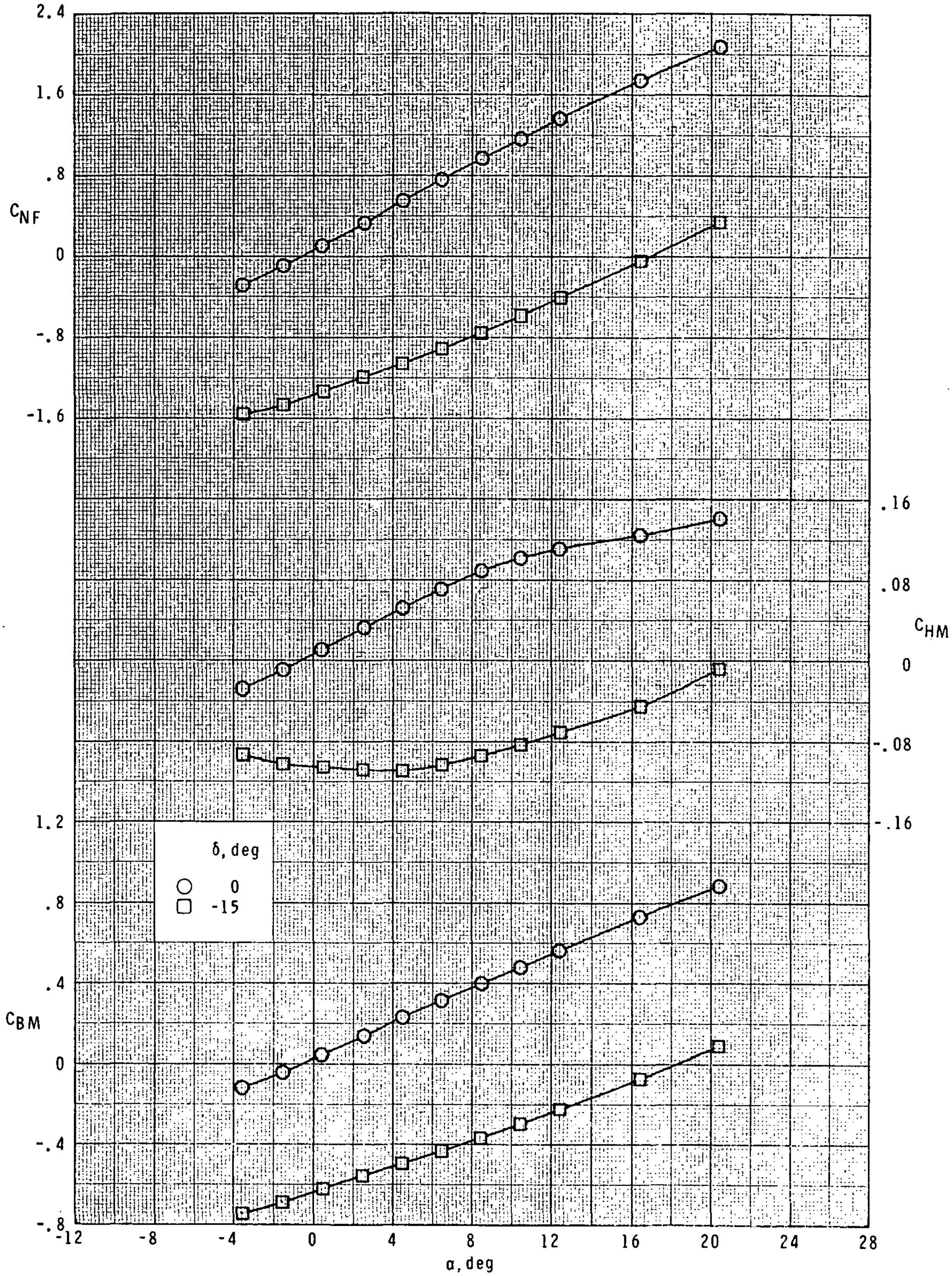

(g) M = 1.60; ϕ_f = 135°; ϕ = 45°.

Figure 3.- Continued.

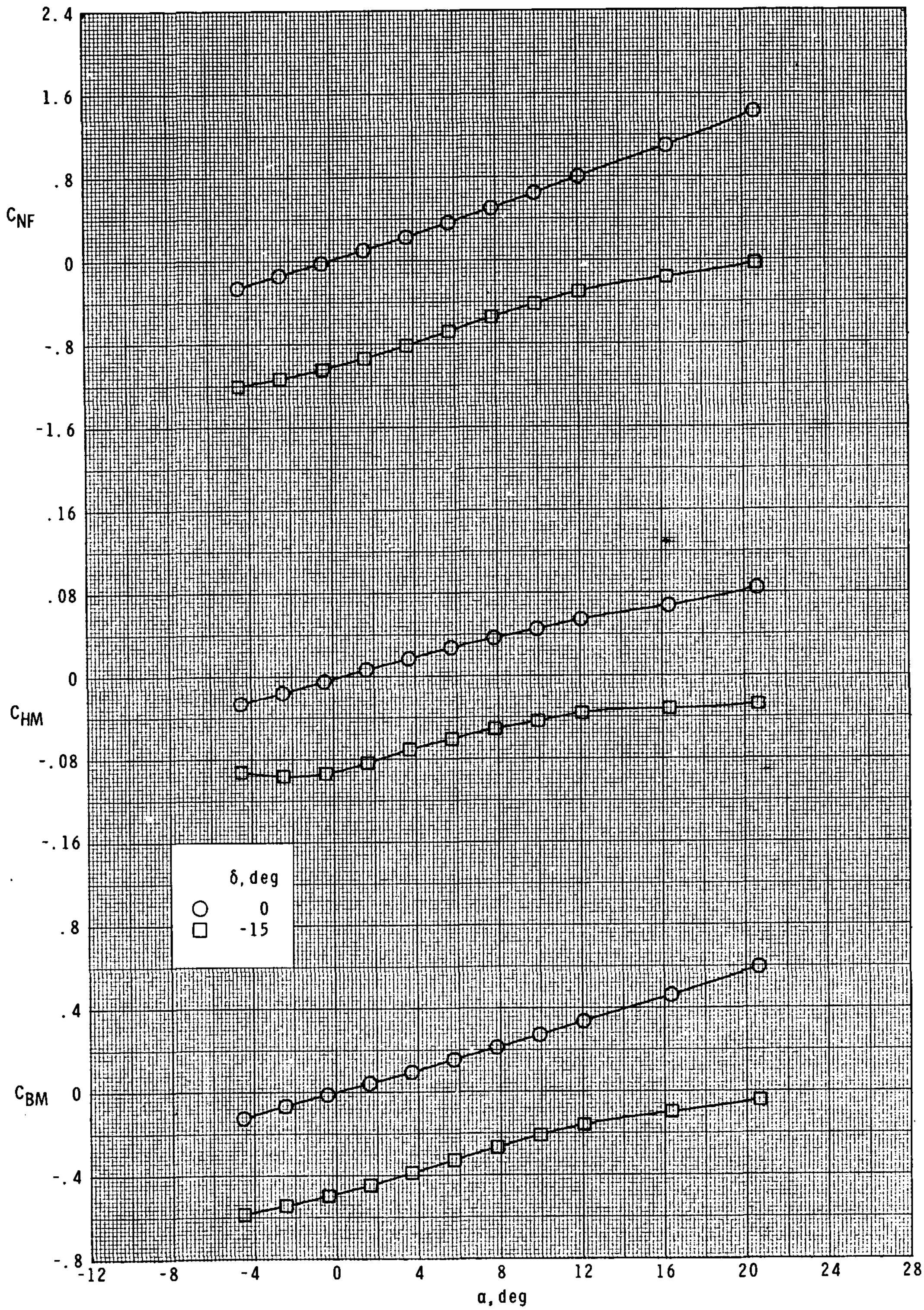

(h) $M = 2.36$; $\phi_f = 135^\circ$; $\phi = 45^\circ$.

Figure 3.- Continued.

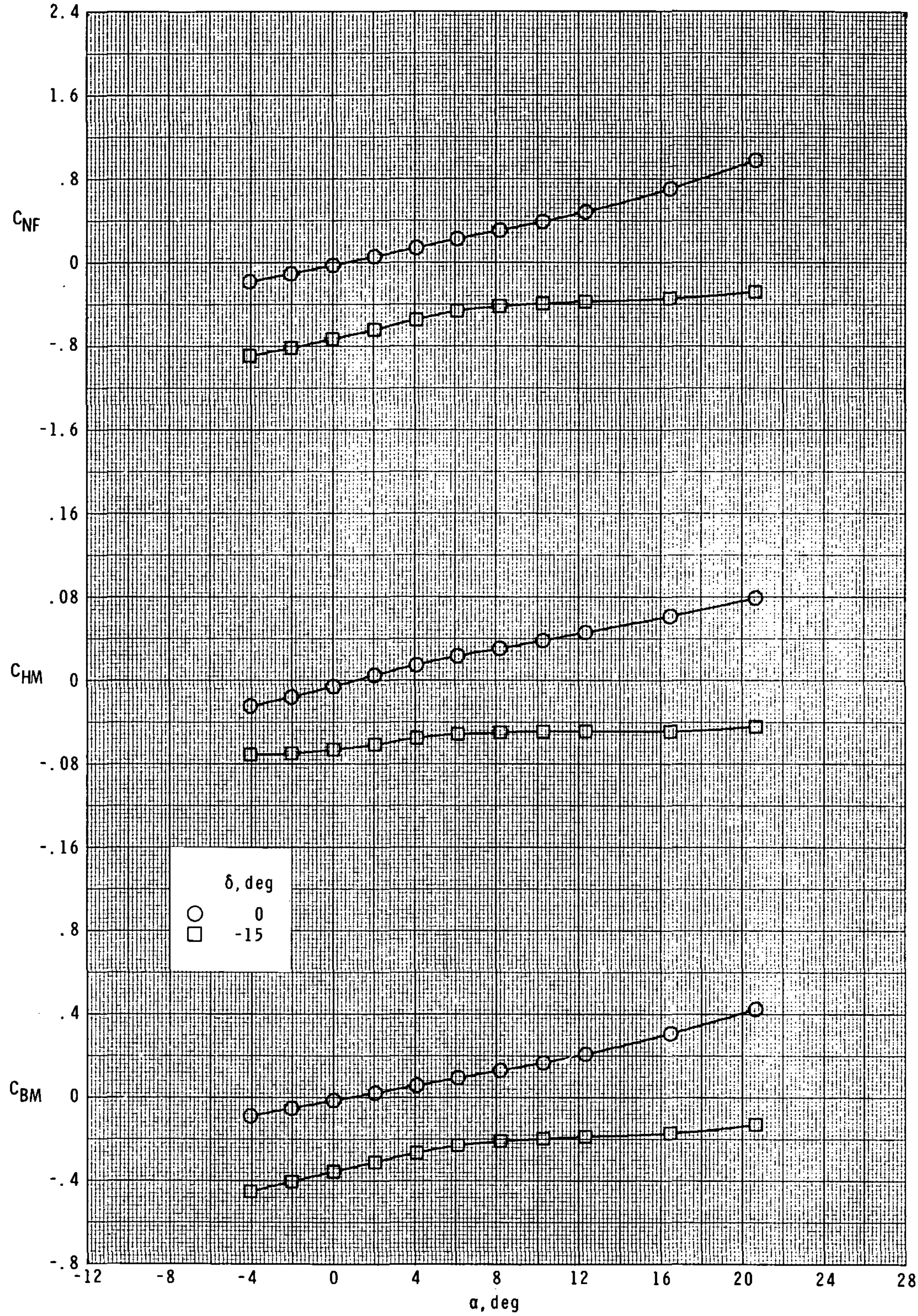

(i) M = 3.70; $\phi_f = 135^{\circ}$; $\phi = 45^{\circ}$.

Figure 3.- Concluded.

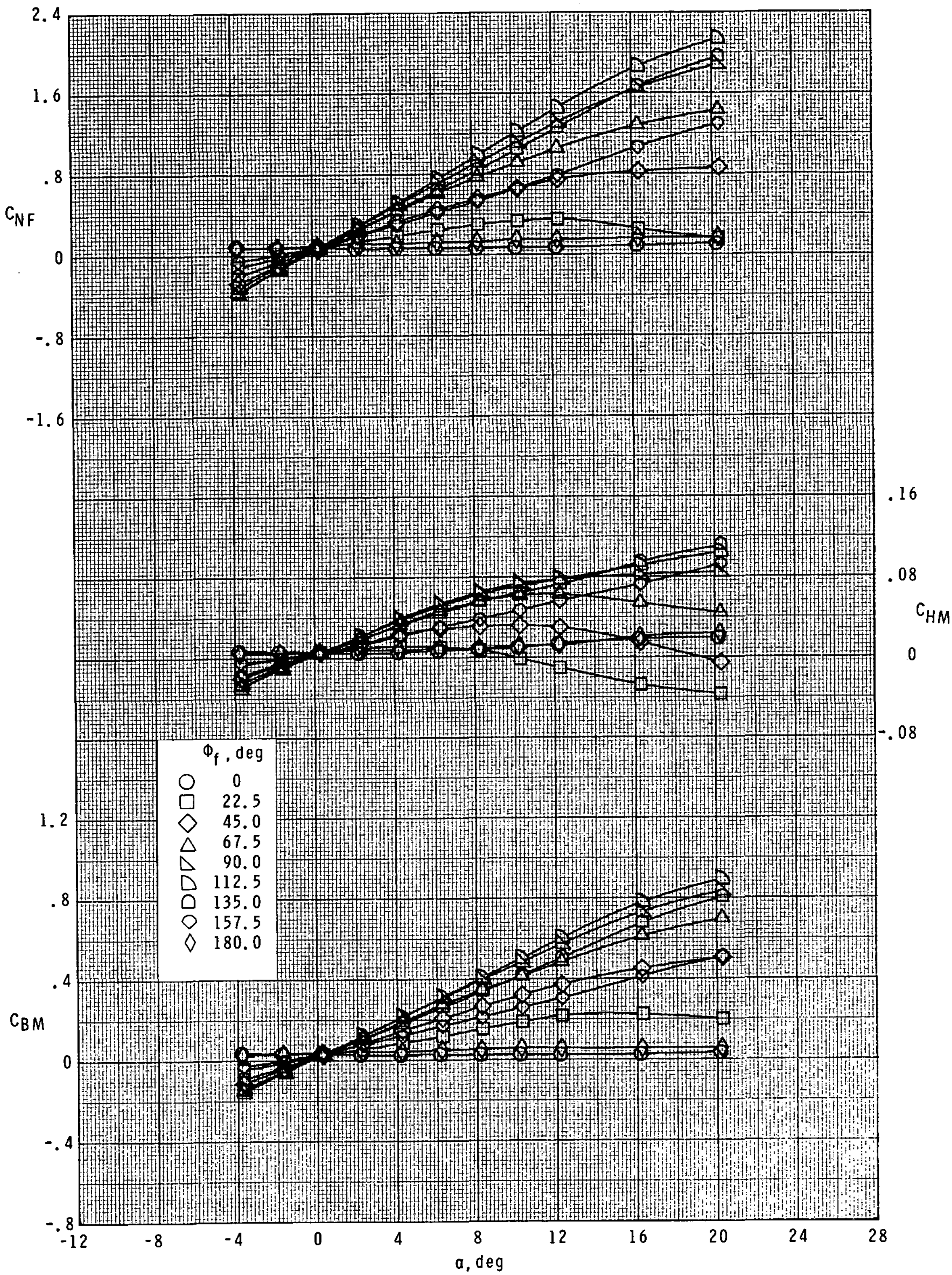

(a) M = 1.60.

Figure 4.- Effect of tail roll orientation on tail loads for T_B at $\delta = 0^{\circ}$.

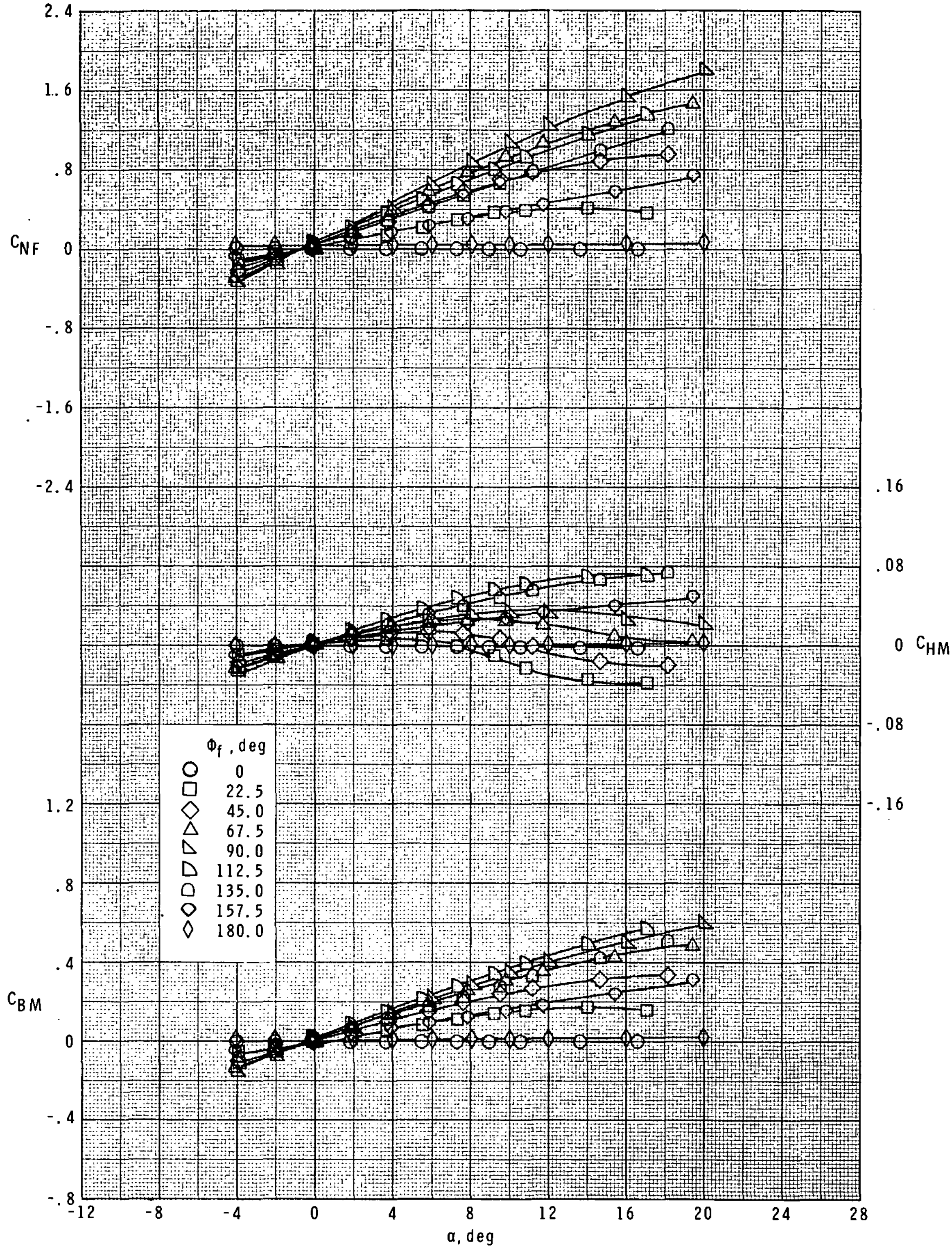

(b) M = 2.36.

Figure 4.- Continued.

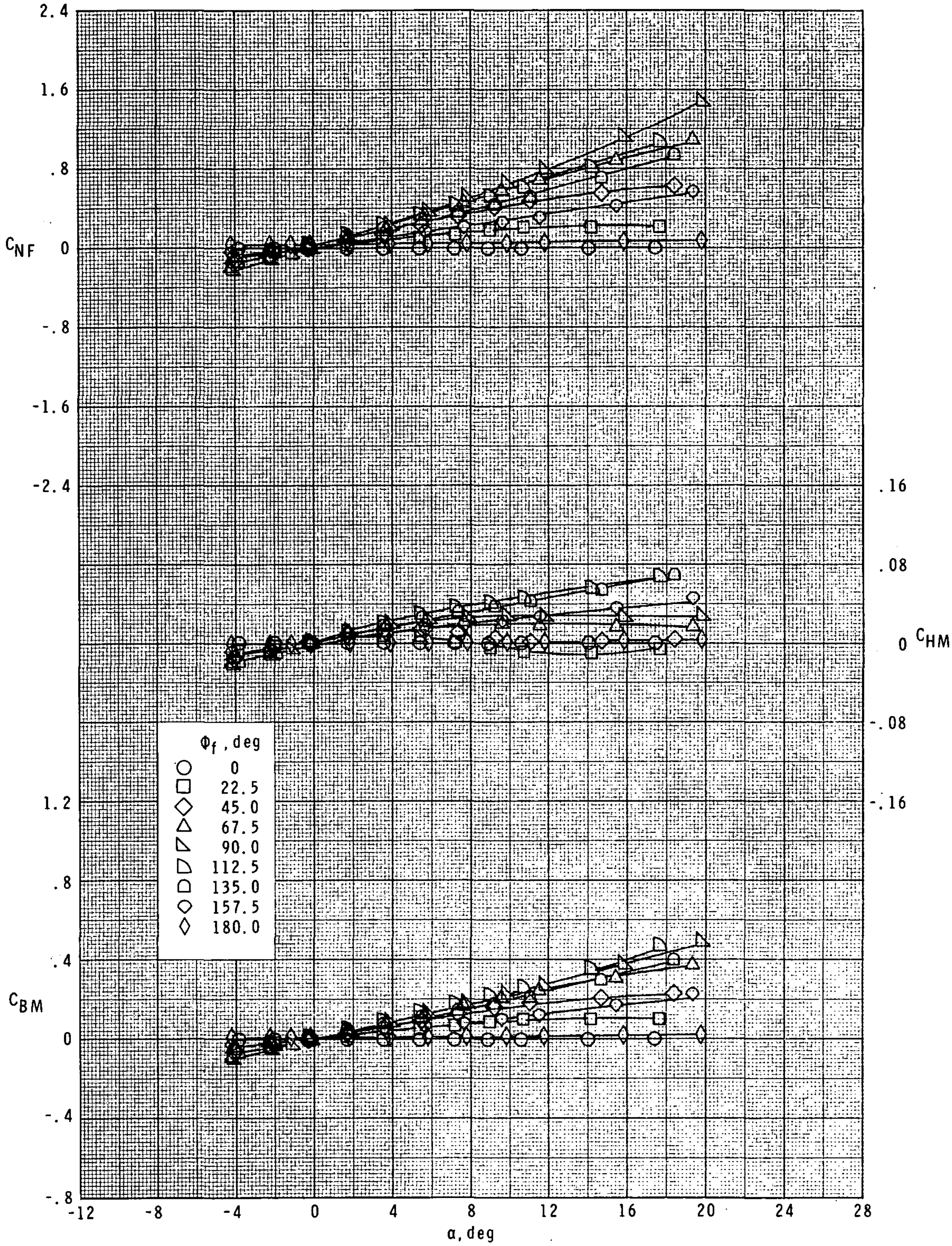

(c) M = 3.70.

Figure 4.- Concluded.

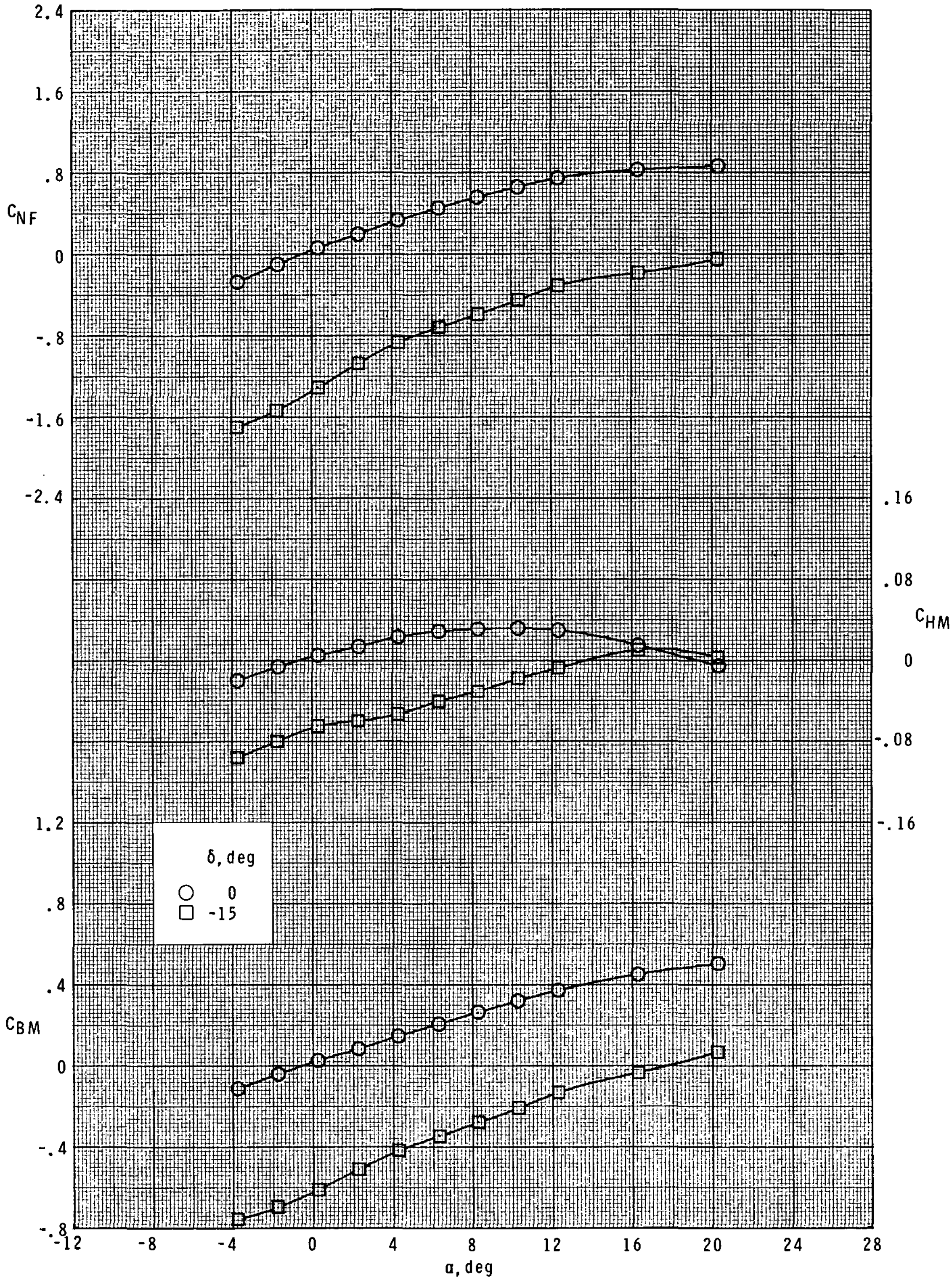

(a) $M = 1.60$; $\phi_f = 45°$; $\phi = 45°$.

Figure 5.- Effect of tail deflection on tail loads for T_B.

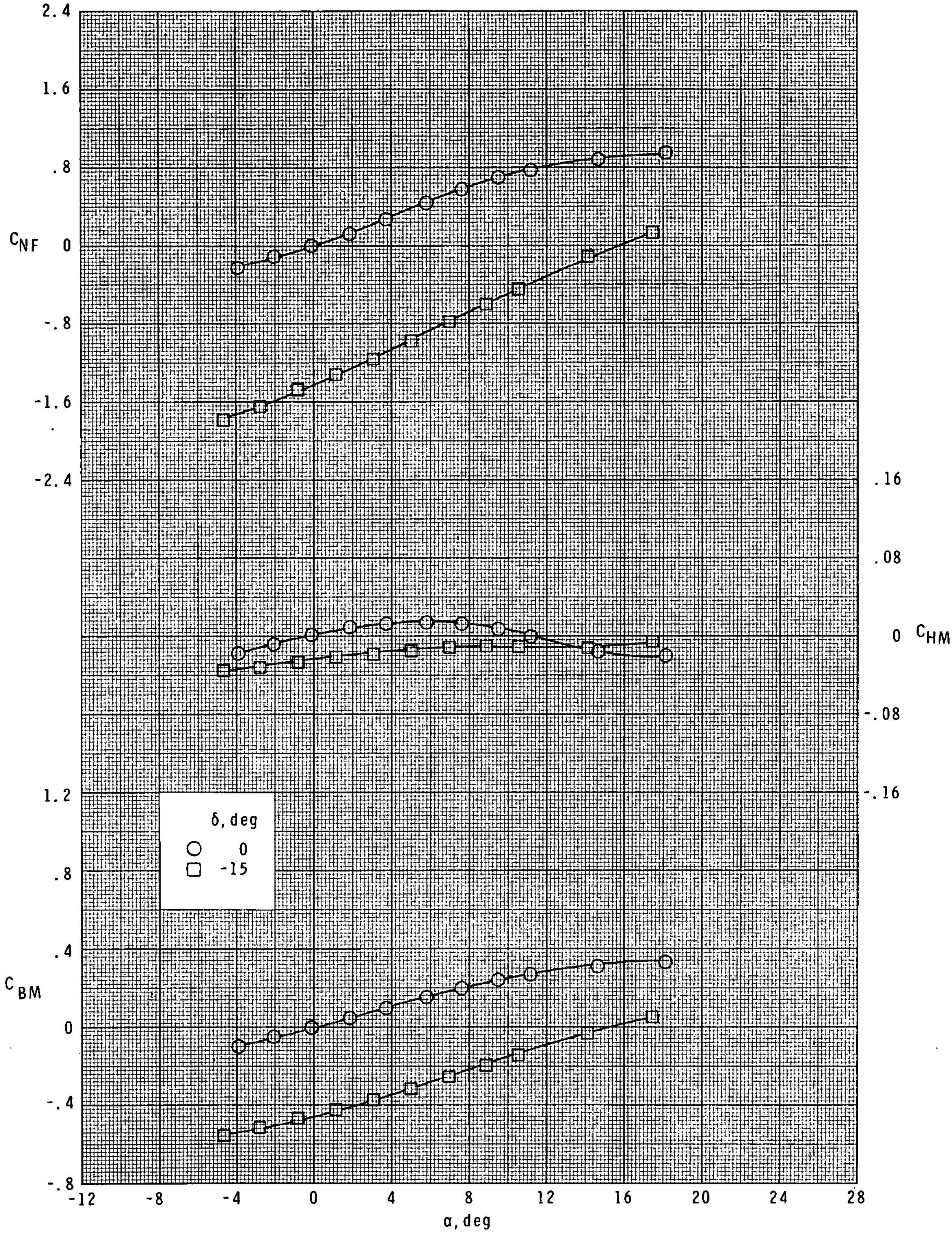

(b) $M = 2.36$; $\phi_f = 45^\circ$; $\phi = 45^\circ$.

Figure 5.- Continued.

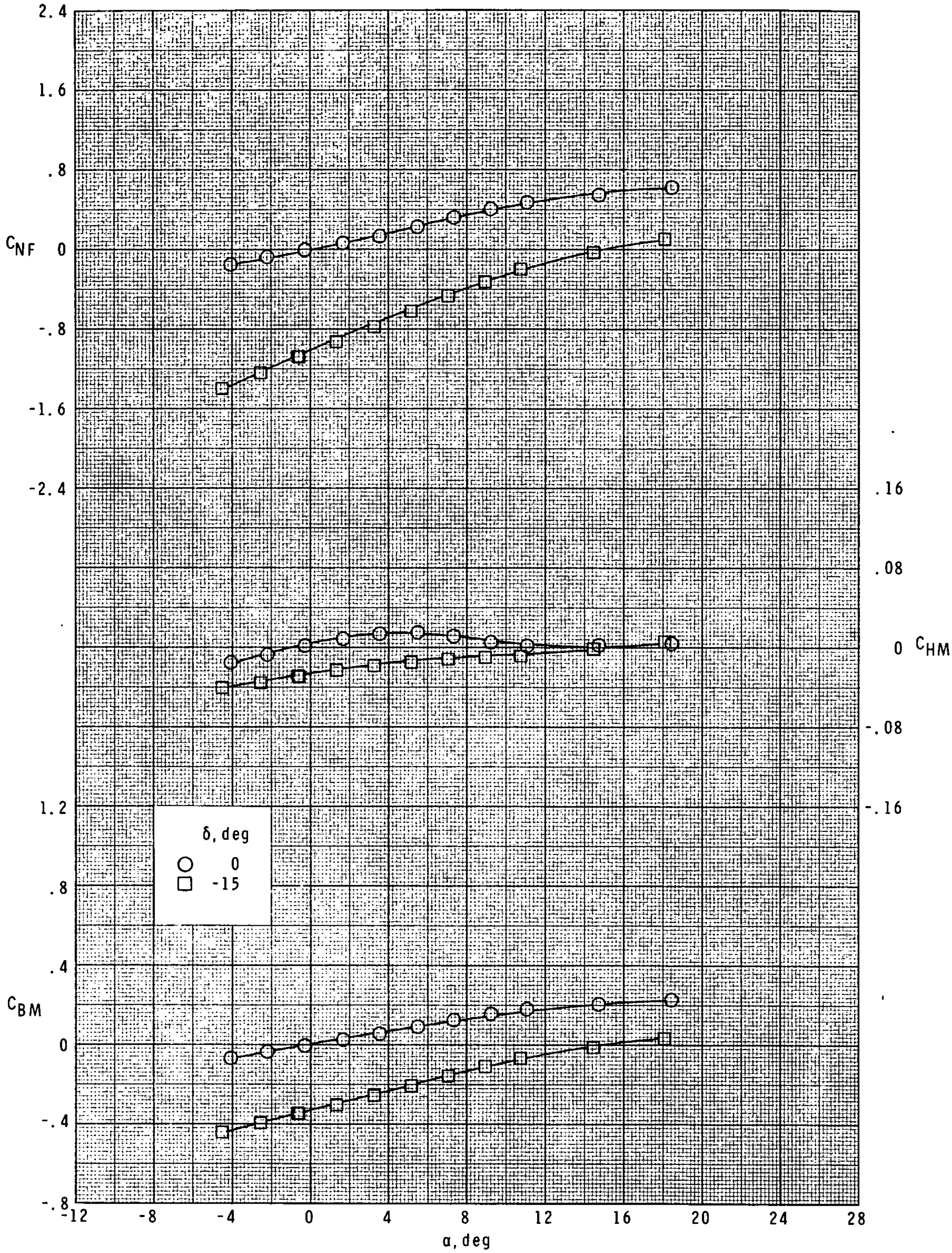

(c) M = 3.70; ϕ_f = 45°; ϕ = 45°.

Figure 5.- Continued.

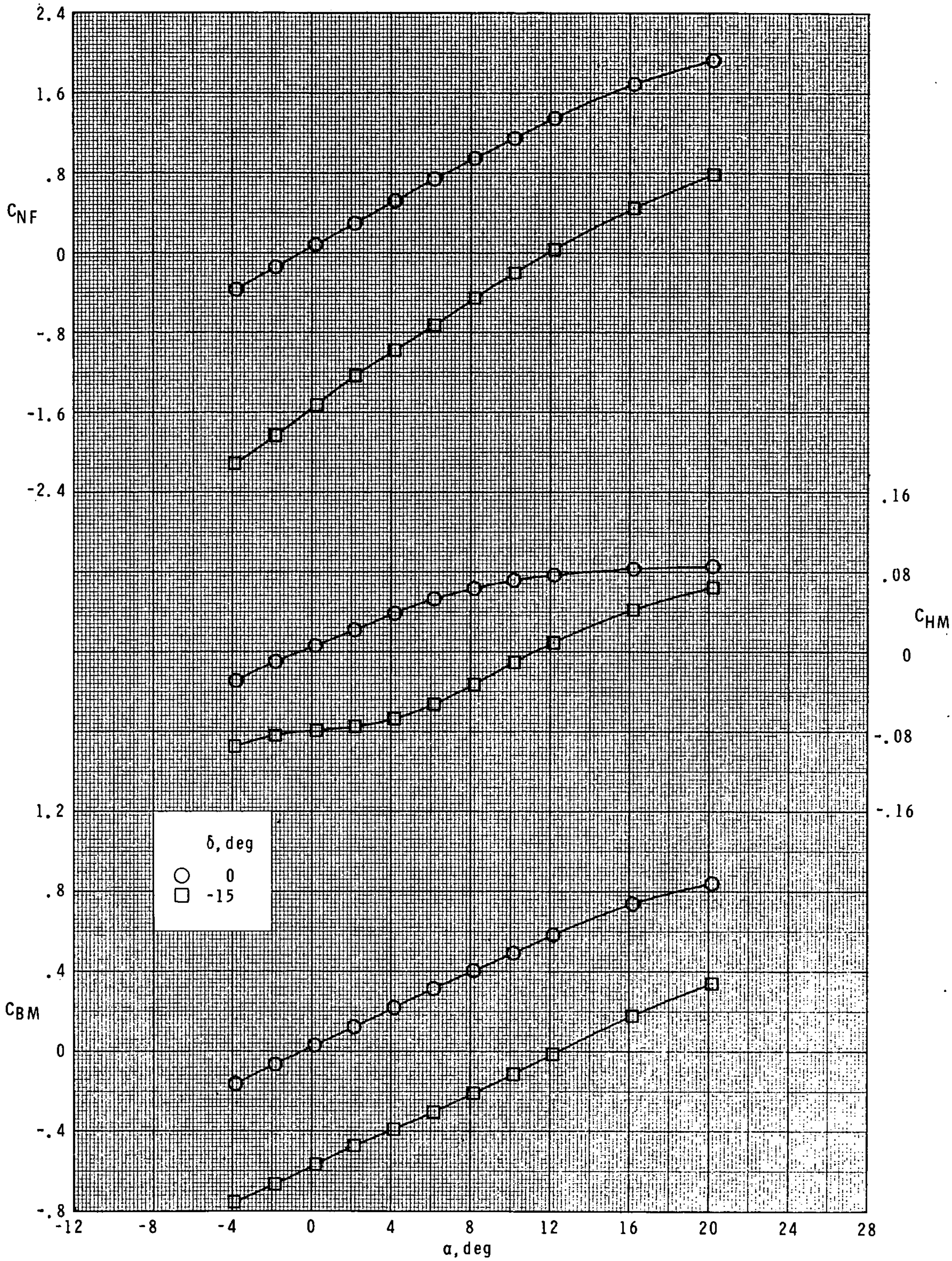

(d) M = 1.60; $\phi_f = 90^{\circ}$; $\phi = 0^{\circ}$.

Figure 5.- Continued.

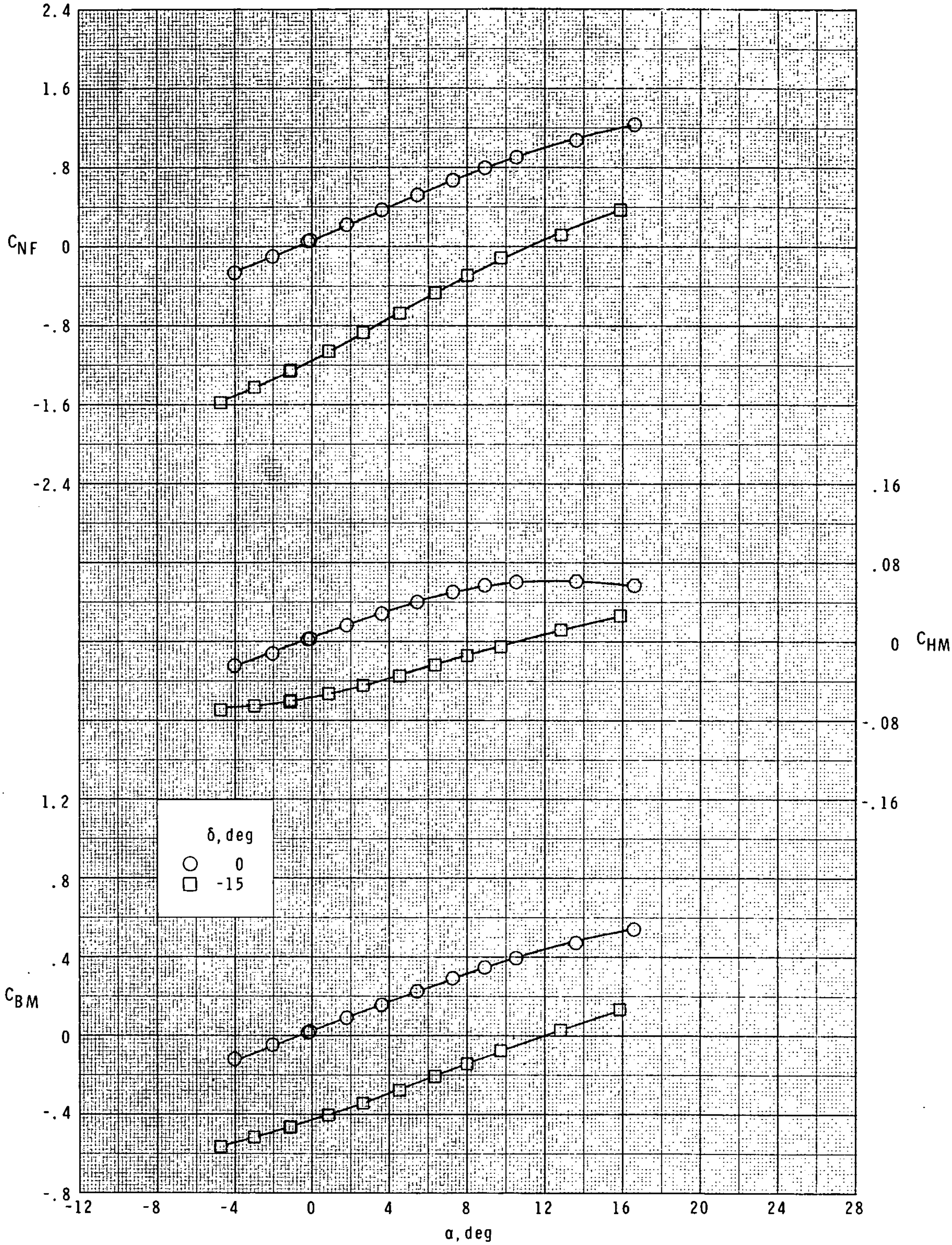

(e) $M = 2.36$; $\phi_f = 90^\circ$; $\phi = 0^\circ$.

Figure 5.- Continued.

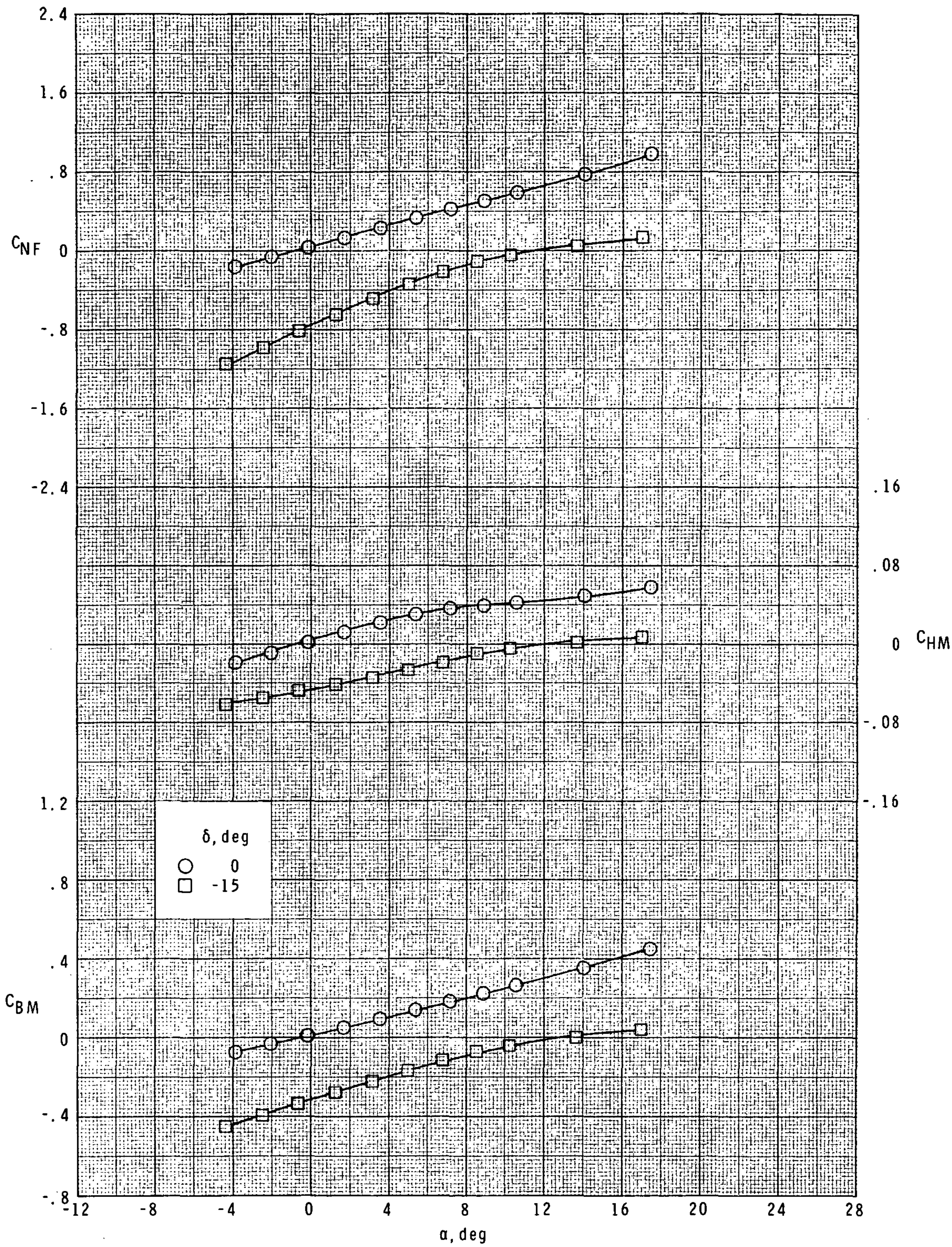

(f) $M = 3.70$; $\phi_f = 90^\circ$; $\phi = 0^\circ$.

Figure 5.- Continued.

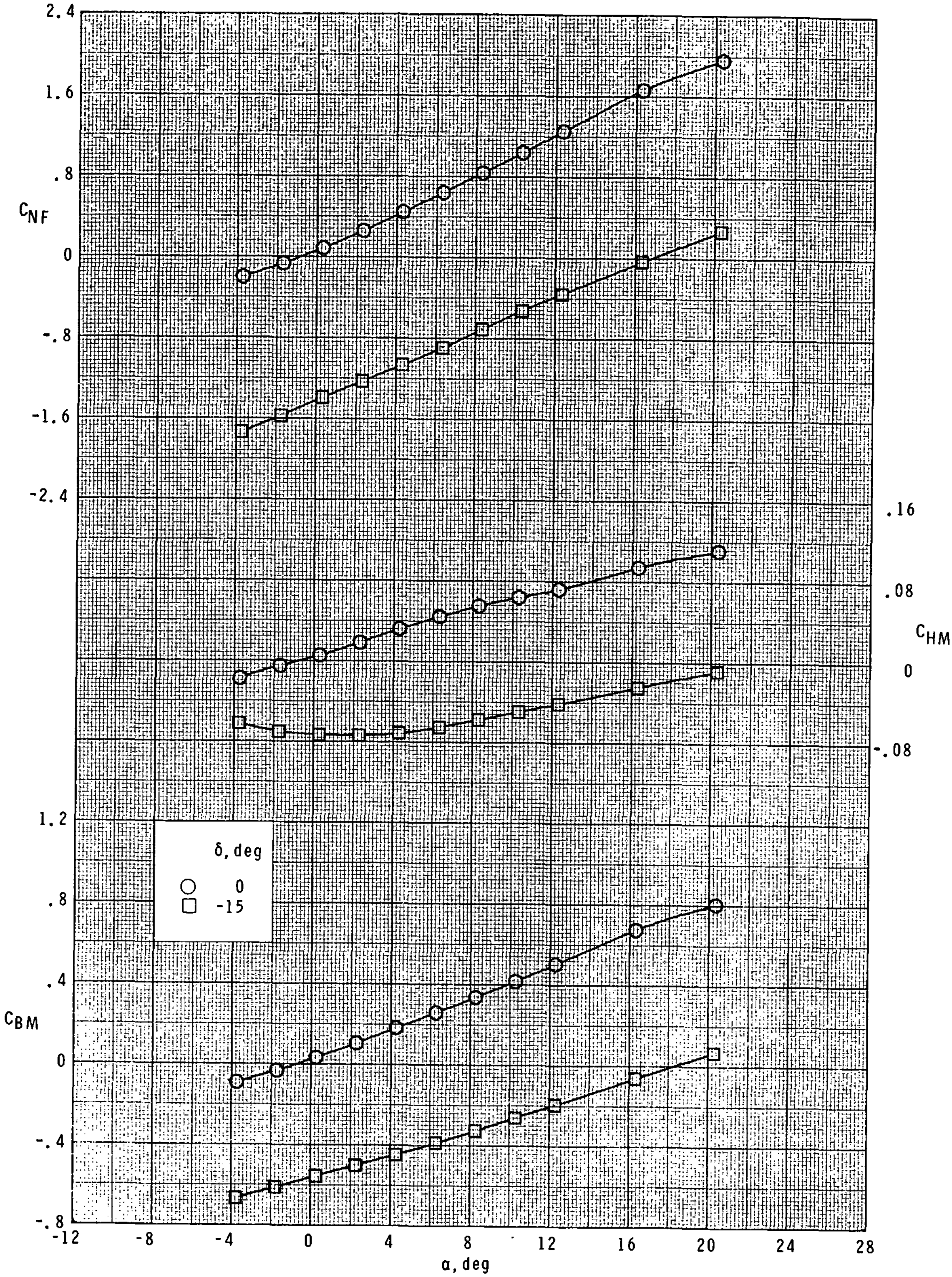

(g) $M = 1.60$; $\phi_f = 135^{\circ}$; $\phi = 45^{\circ}$.

Figure 5.- Continued.

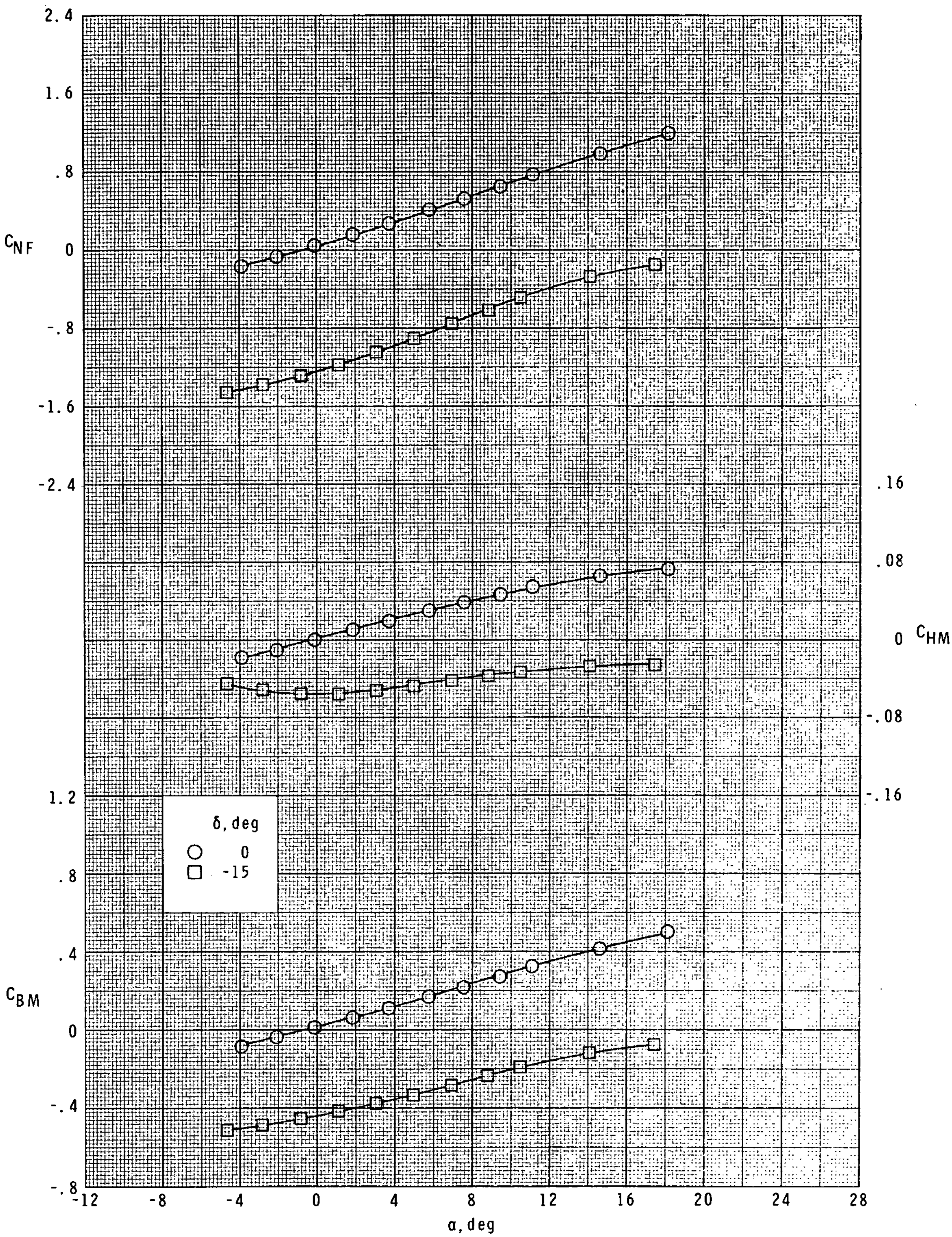

(h) M = 2.36; ϕ_f = 135°; ϕ = 45°.

Figure 5.- Continued.

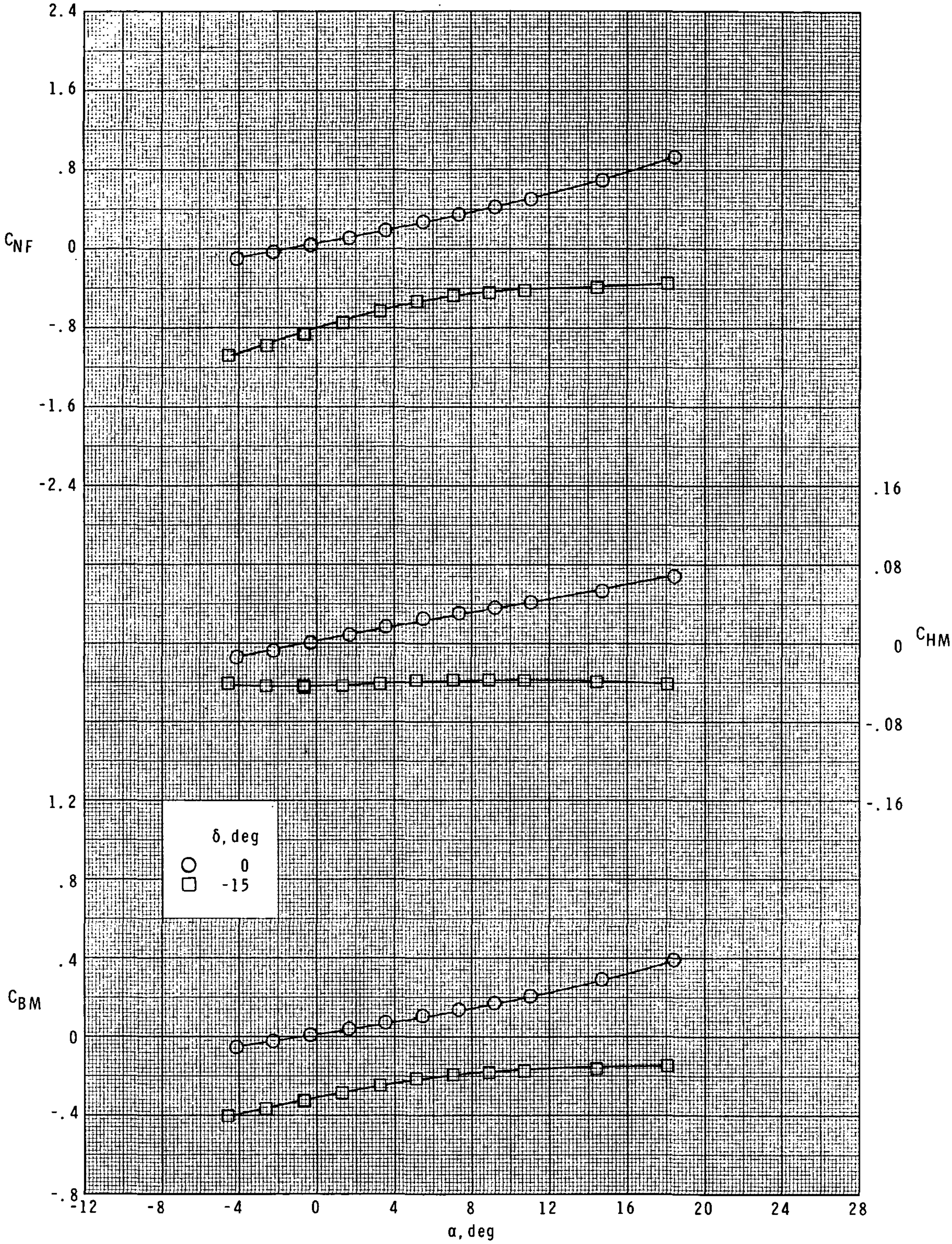

(i) M = 3.70; ϕ_f = 135°; ϕ = 45°.

Figure 5.- Concluded.

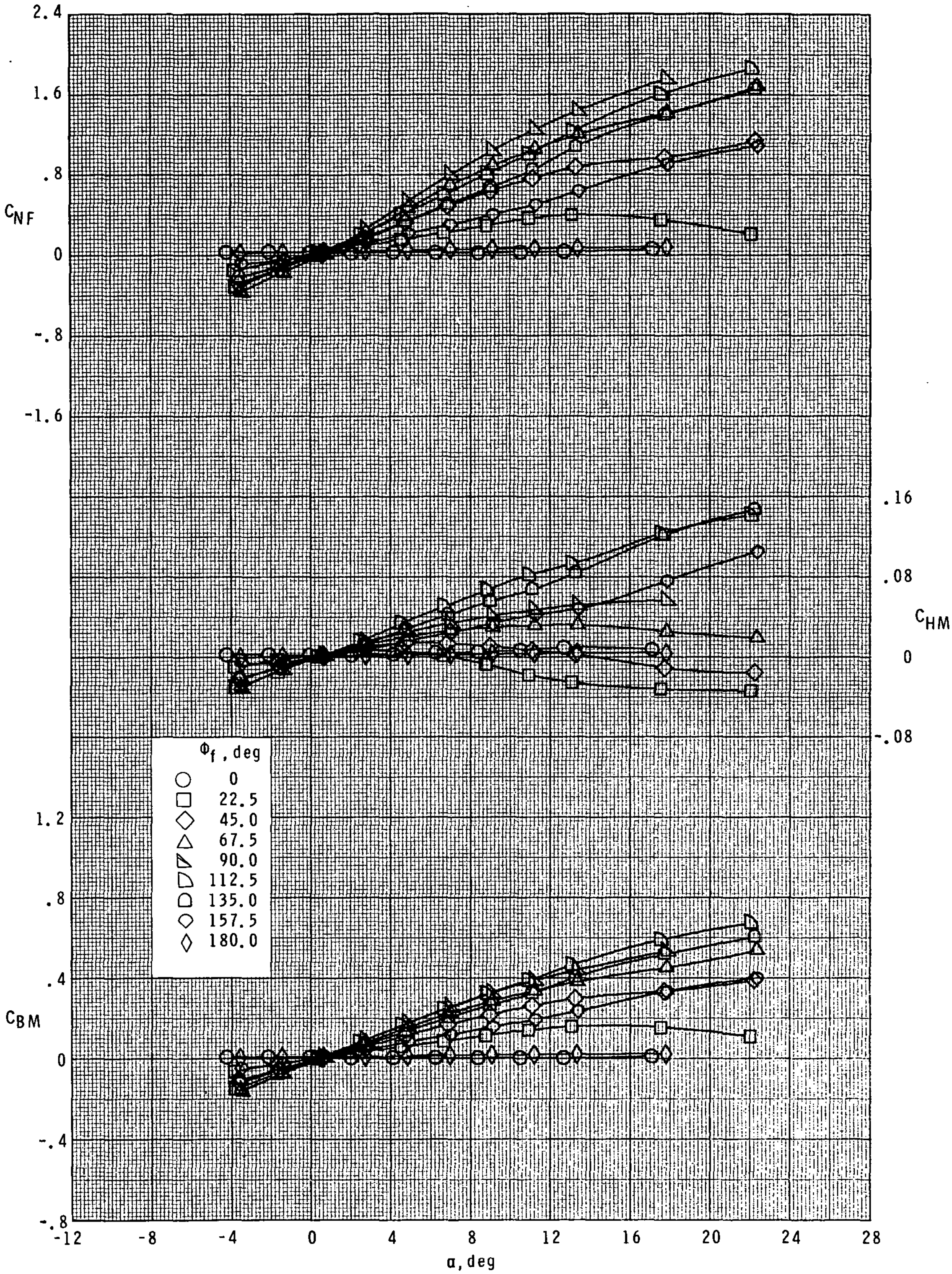

(a) M = 1.60.

Figure 6.- Effect of tail roll orientation on tail loads for T_C at $\delta = 0^{\circ}$.

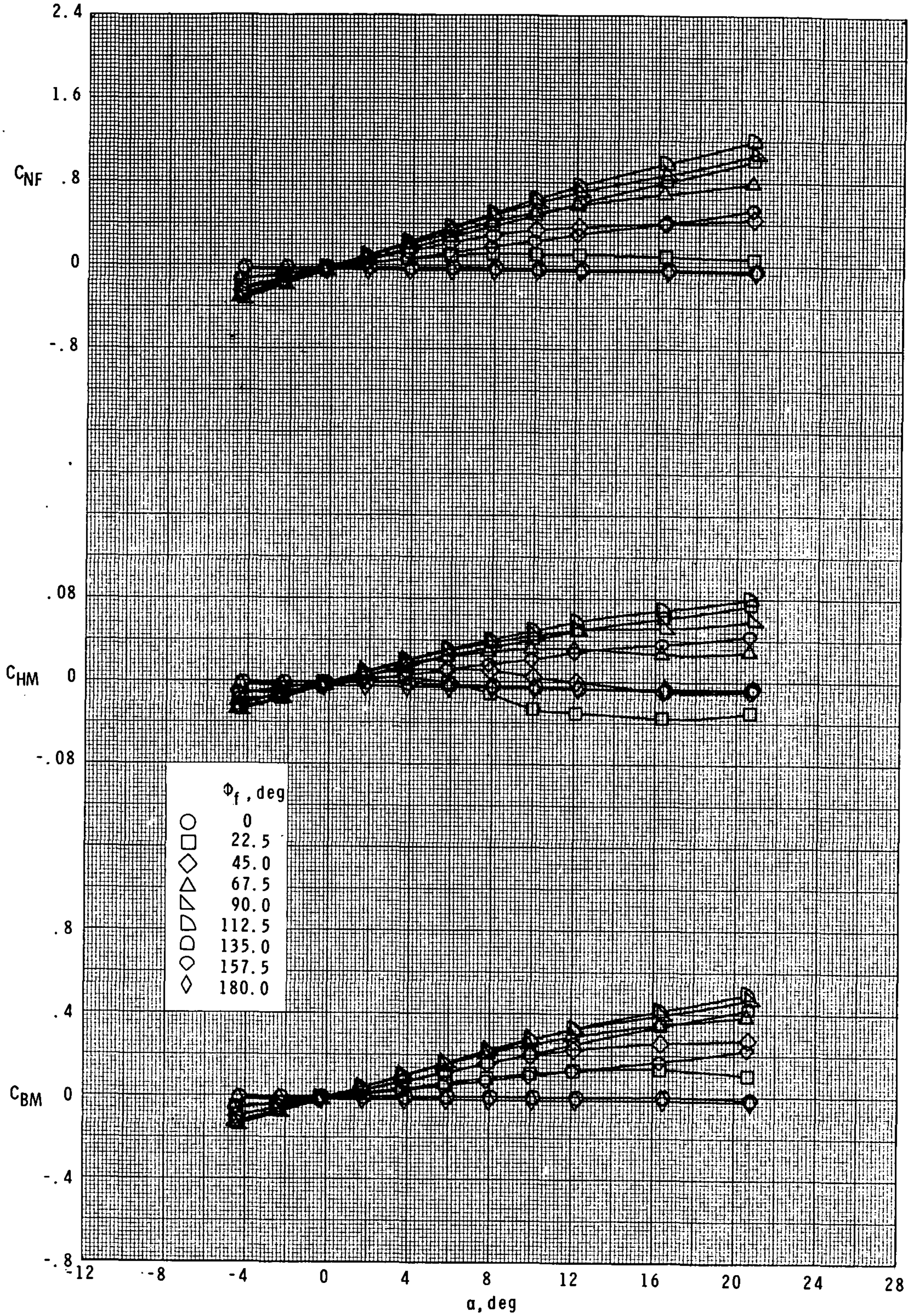

(b) M = 2.36.

Figure 6.- Continued.

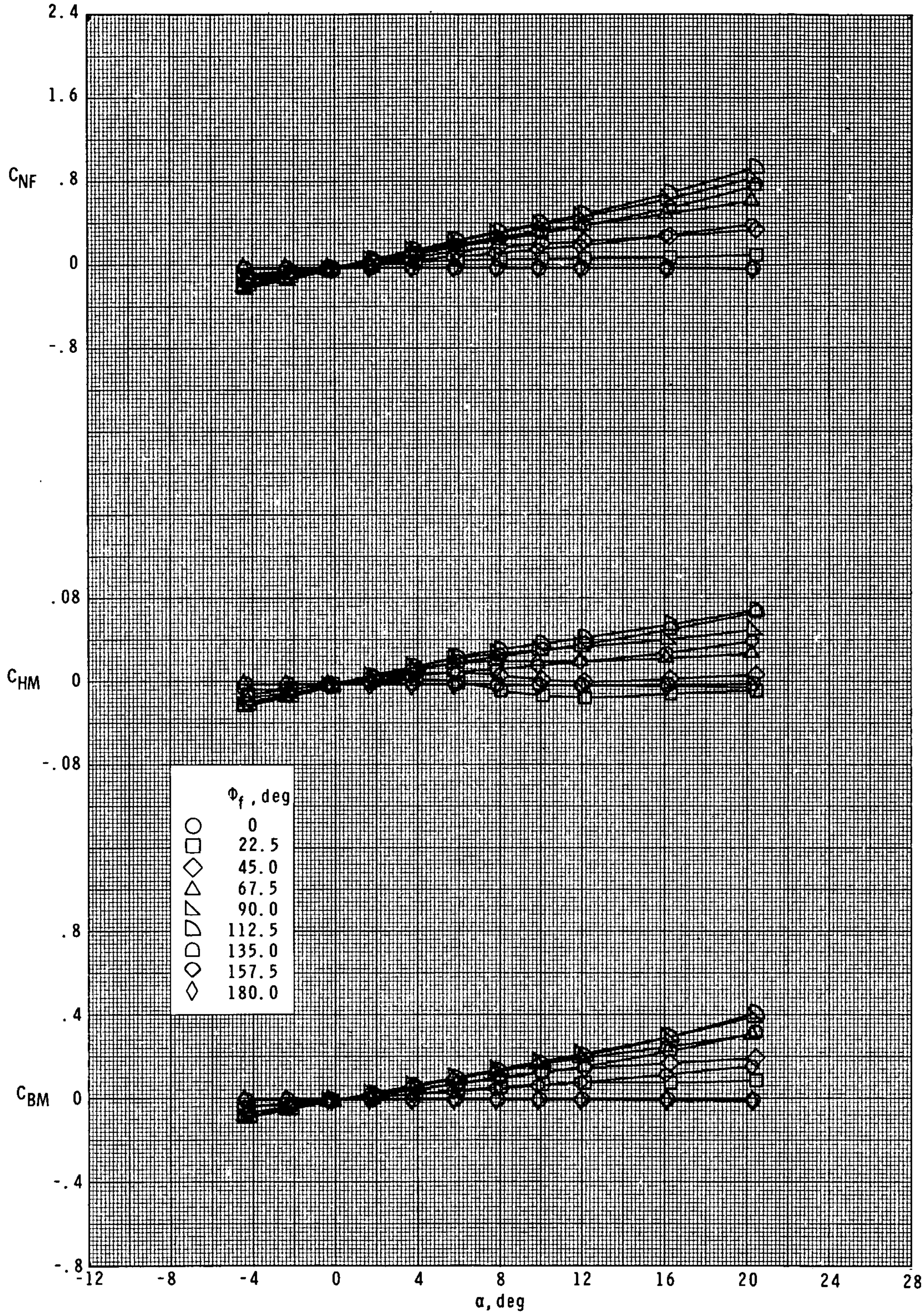

(c) M = 3.70.

Figure 6.- Concluded.

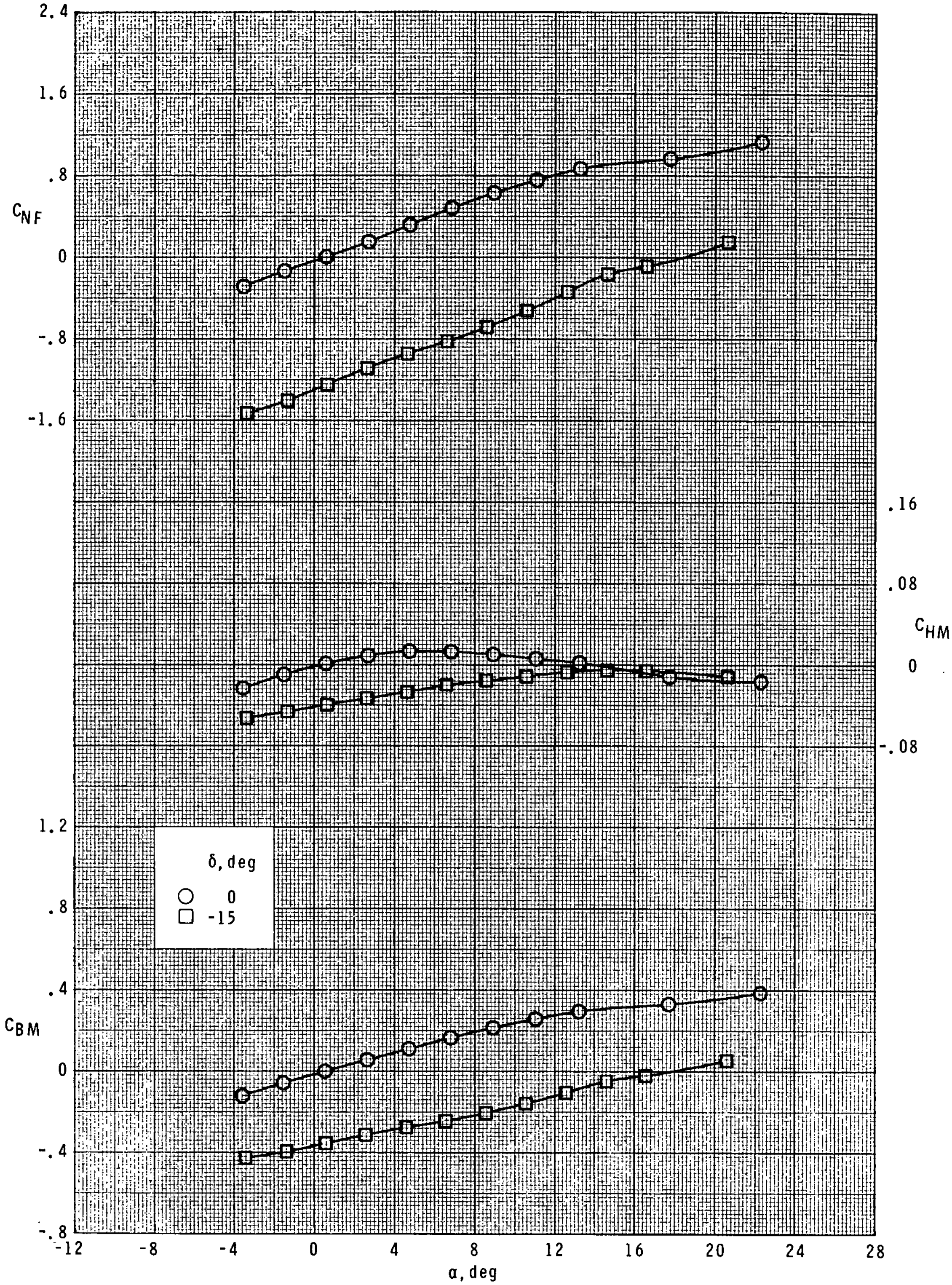

(a) $M = 1.60$; $\phi_f = 45^\circ$; $\phi = 45^\circ$.

Figure 7.- Effect of tail deflection on tail loads for T_C.

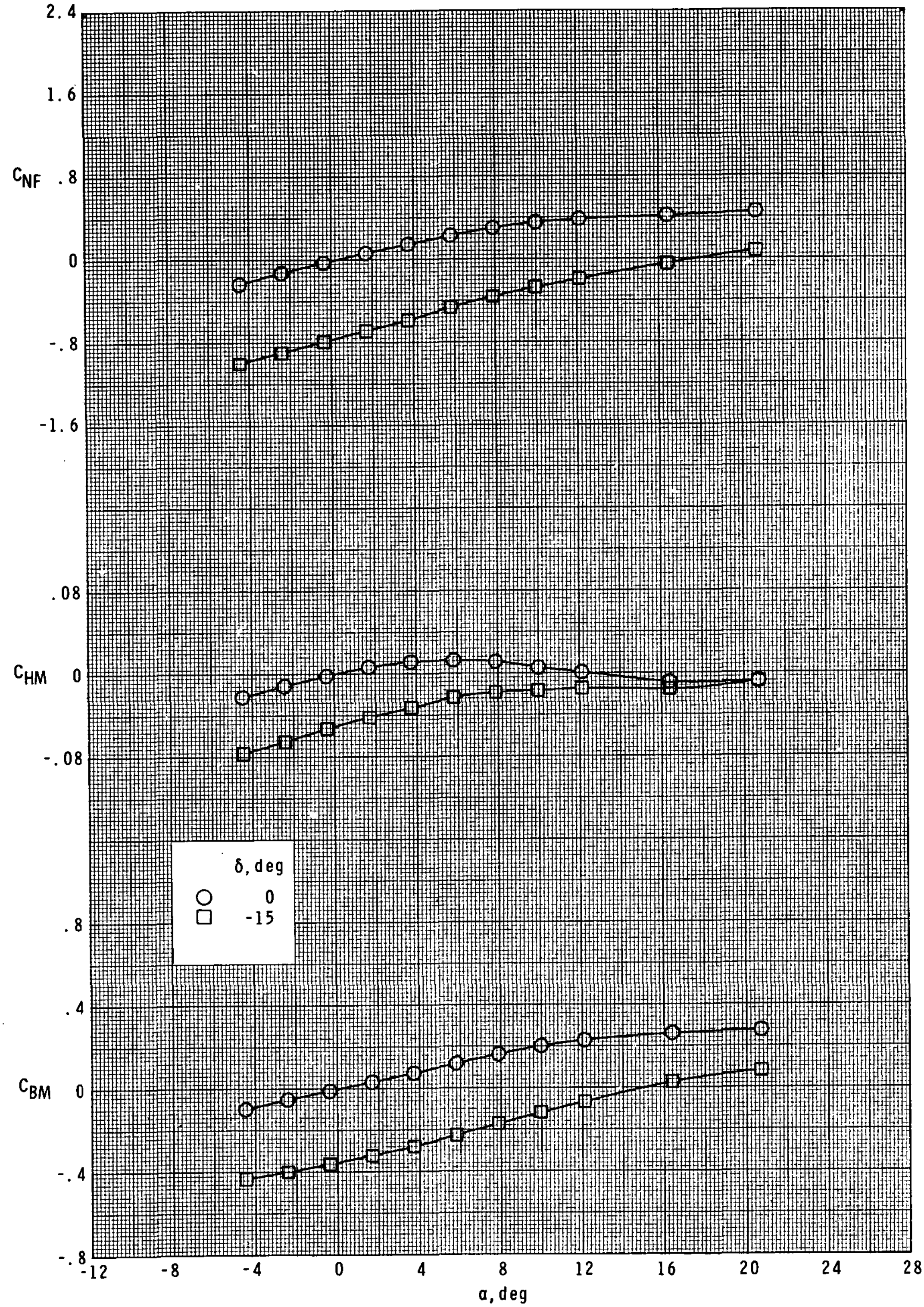

(b) $M = 2.36$; $\phi_f = 45^o$; $\phi = 45^o$.

Figure 7.- Continued.

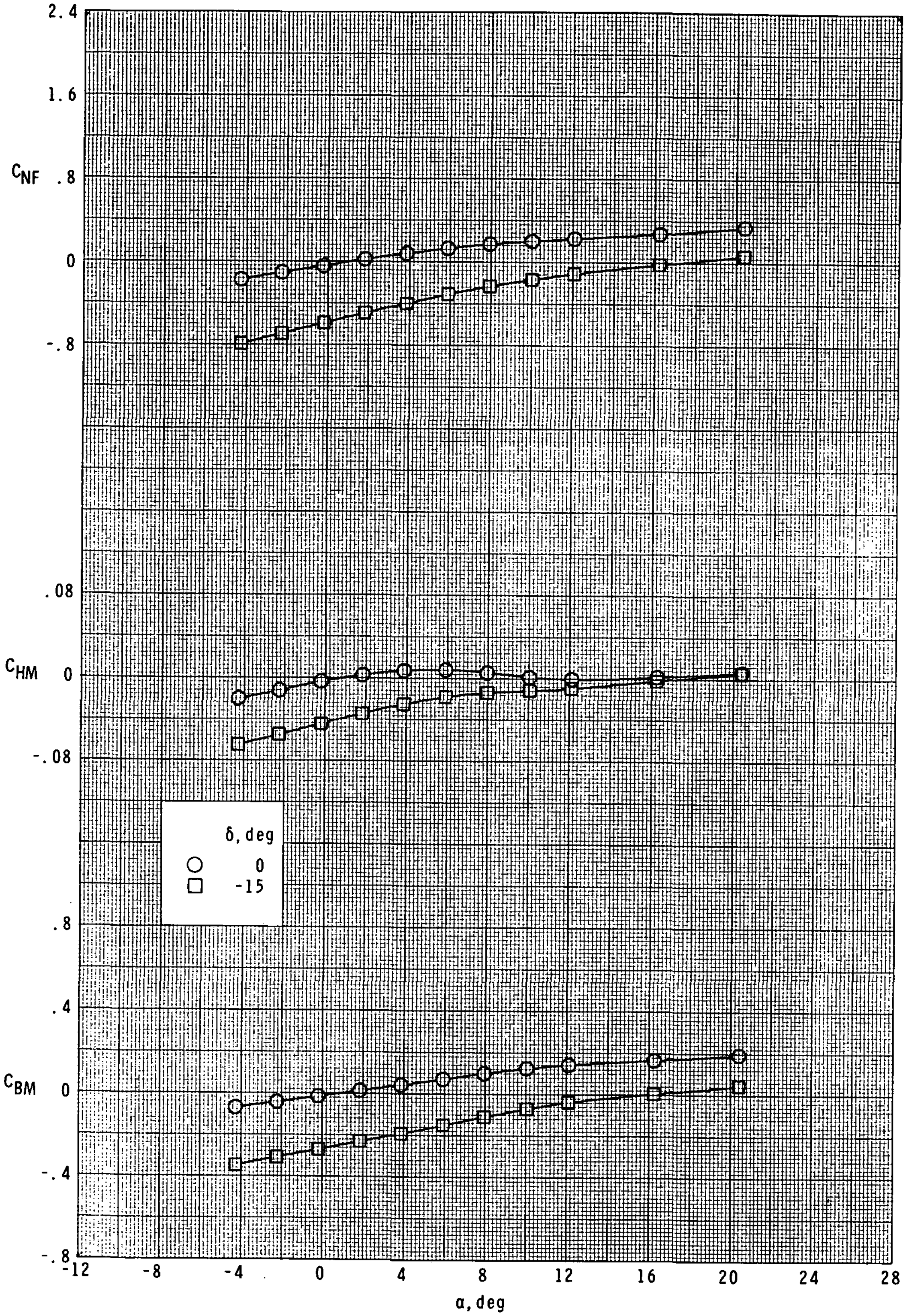

(c) M = 3.70; $\phi_f = 45^\circ$; $\phi = 45^\circ$.

Figure 7.- Continued.

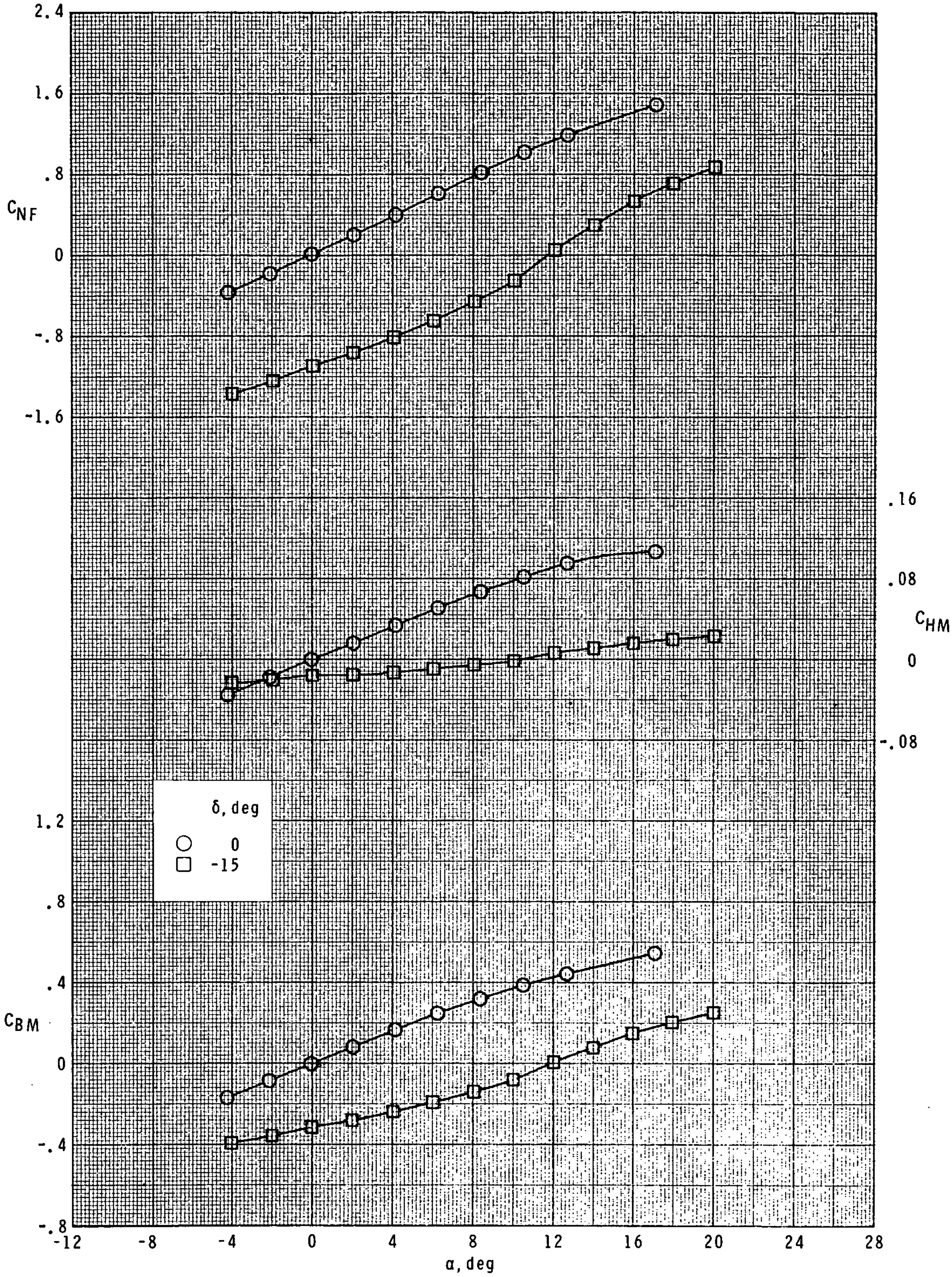

(d) $M = 1.60$; $\phi_f = 90^\circ$; $\phi = 0^\circ$.

Figure 7.- Continued.

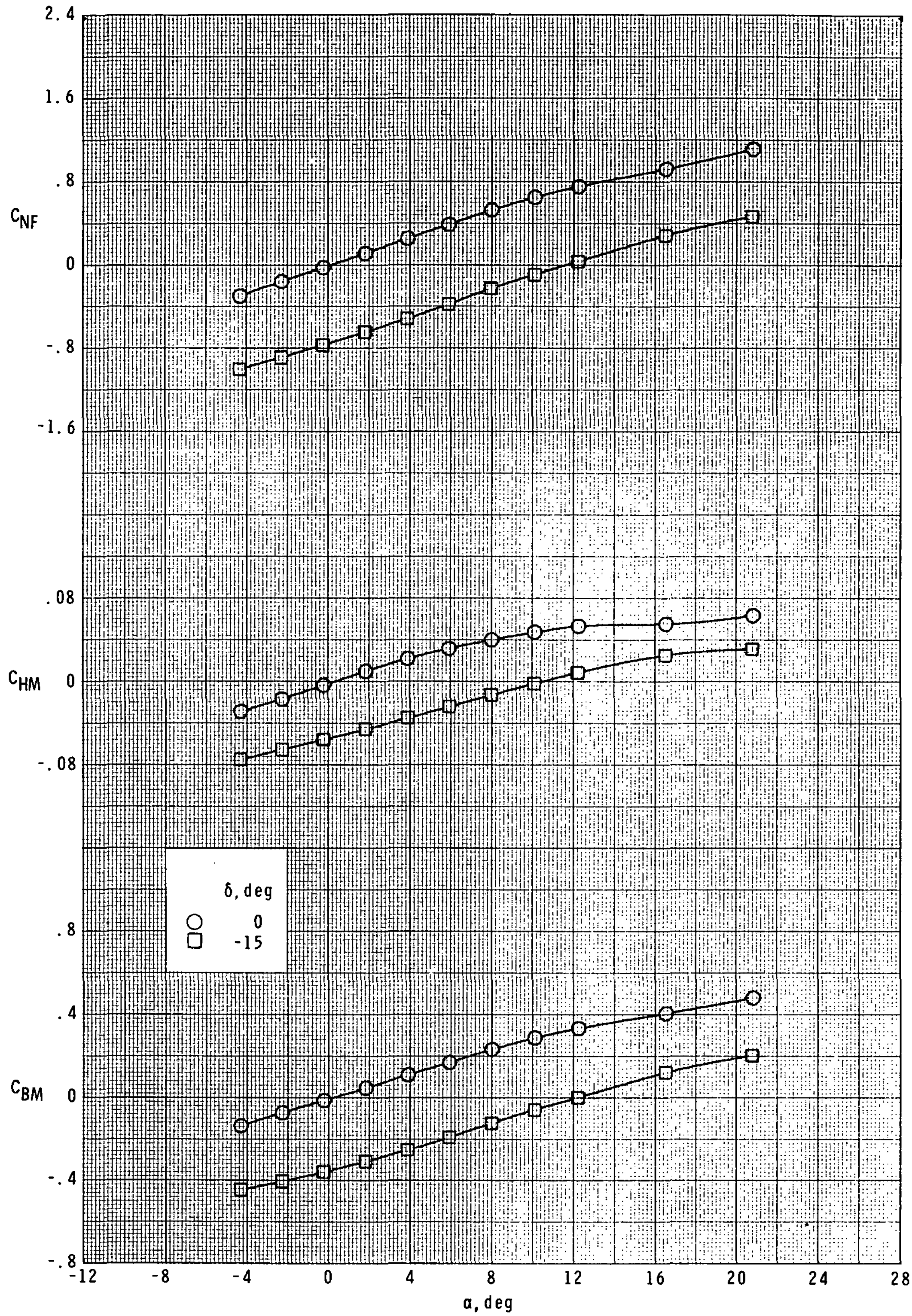

(e) M = 2.36; $\phi_f = 90°$; $\phi = 0°$.

Figure 7.- Continued.

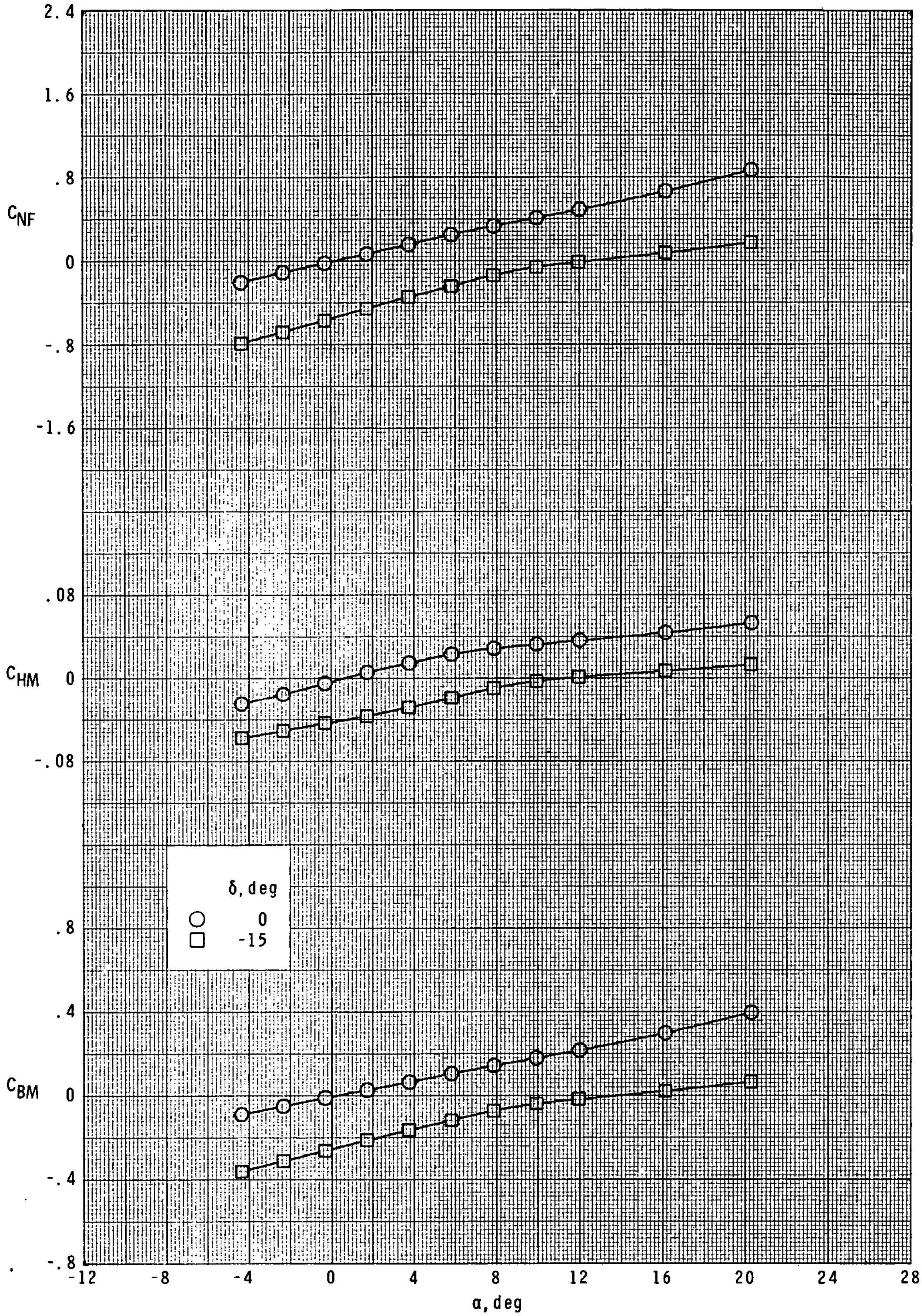

(f) $M = 3.70$; $\phi_f = 90^{\circ}$; $\phi = 0^{\circ}$.

Figure 7.- Continued.

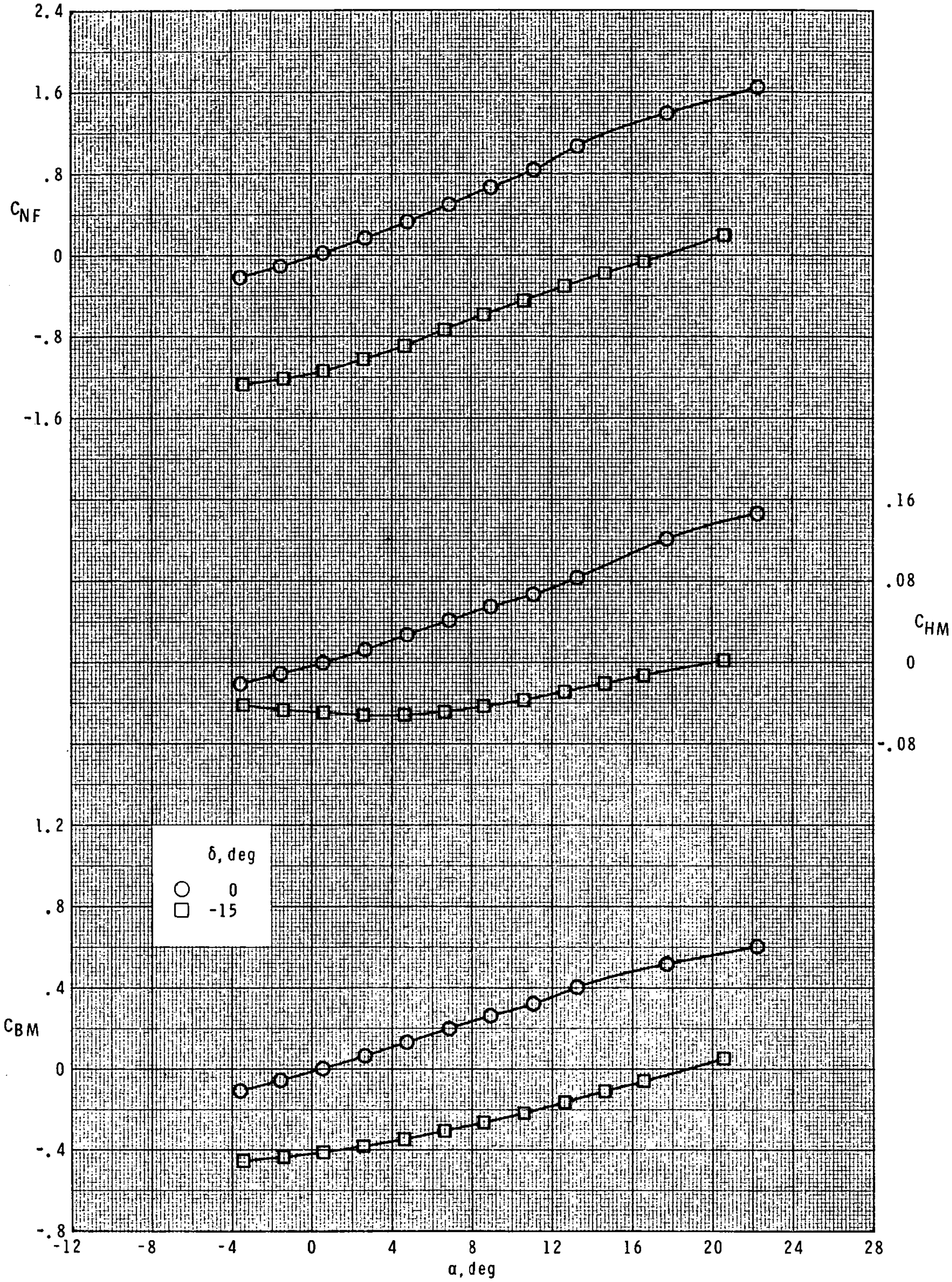

(g) M = 1.60; $\phi_f = 135^\circ$; $\phi = 45^\circ$.

Figure 7.- Continued.

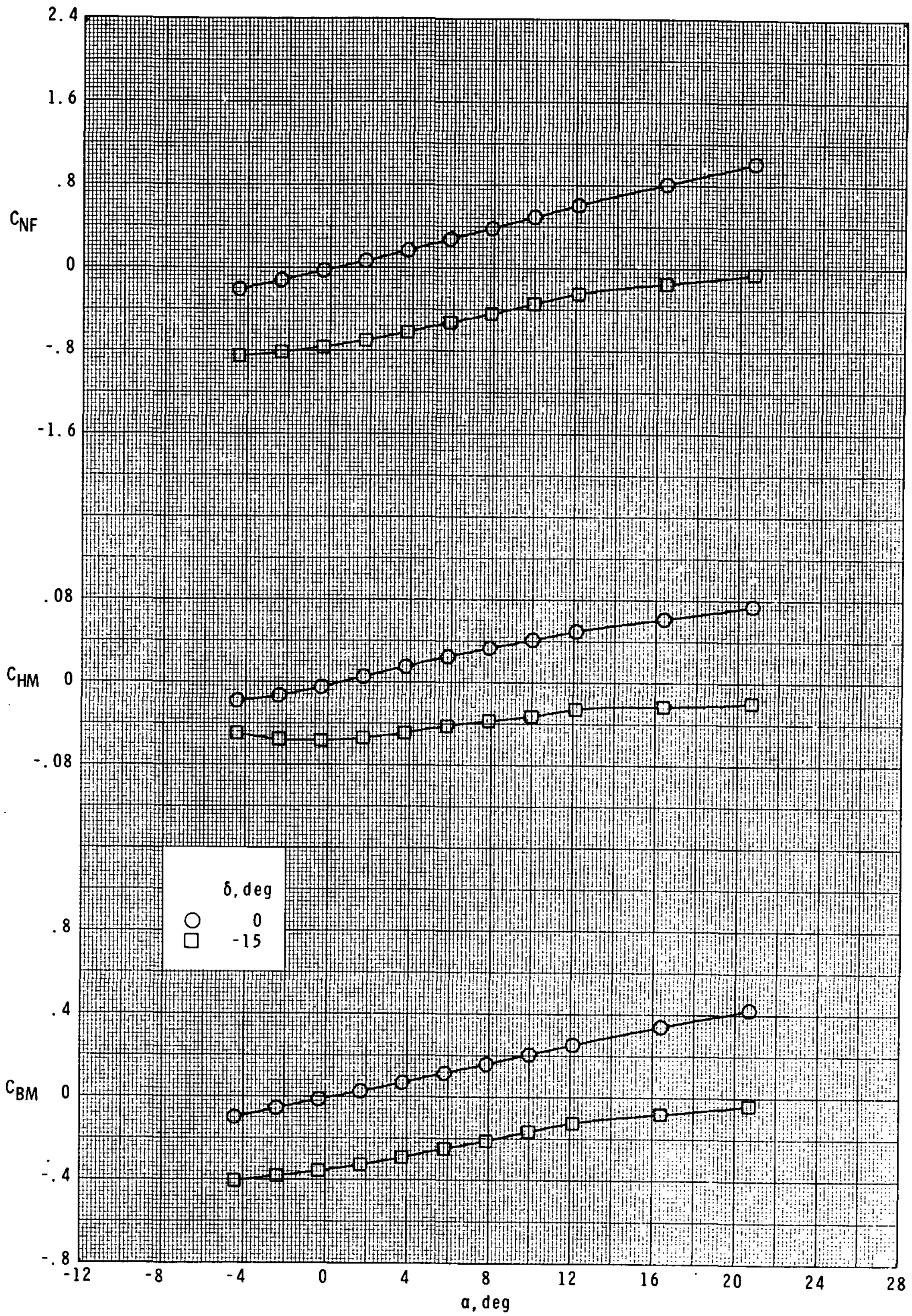

(h) M = 2.36; ϕ_f = 135°; ϕ = 45°.

Figure 7.- Continued.

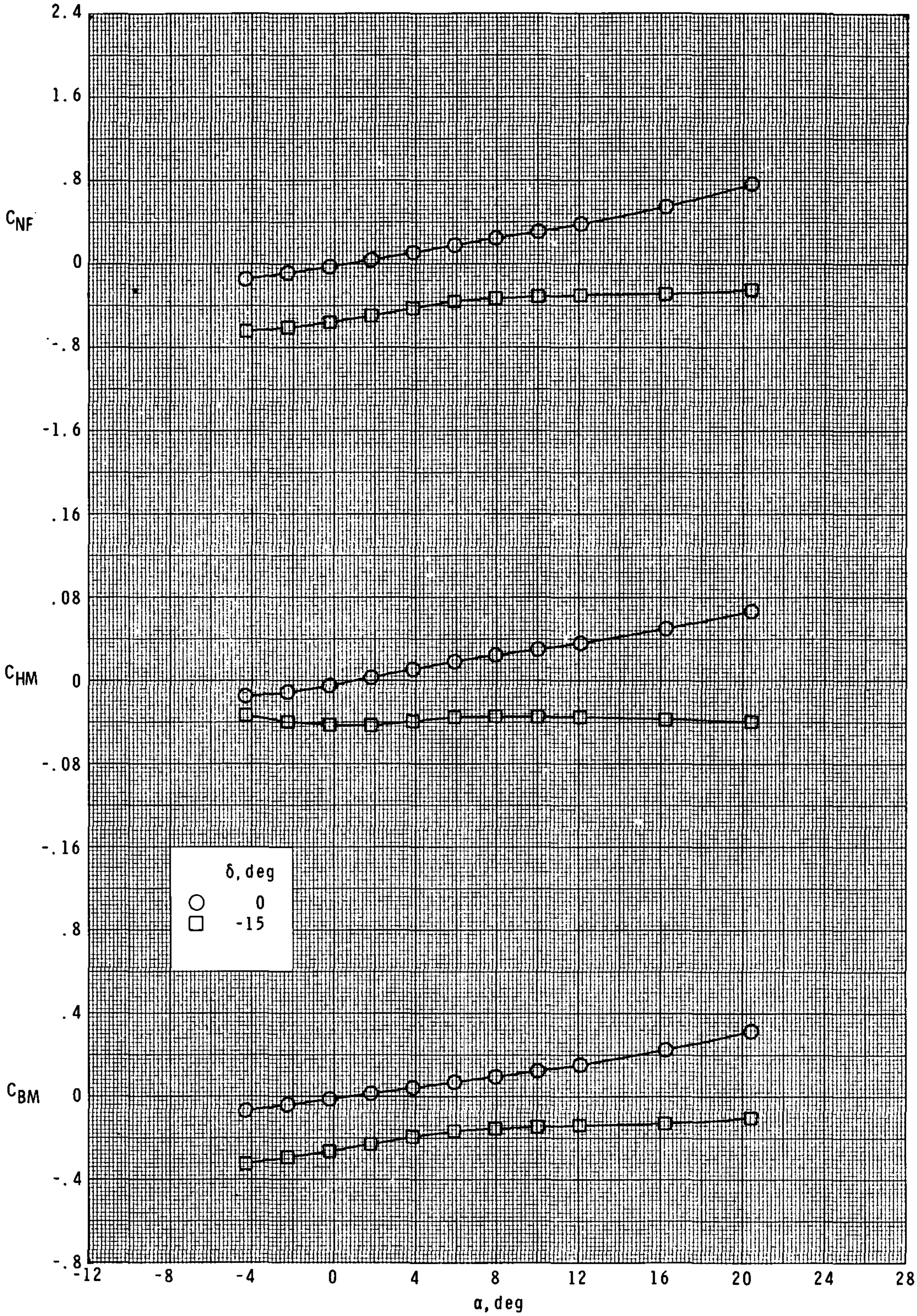

(i) $M = 3.70$; $\phi_f = 135^{\circ}$; $\phi = 45^{\circ}$.

Figure 7.- Concluded.

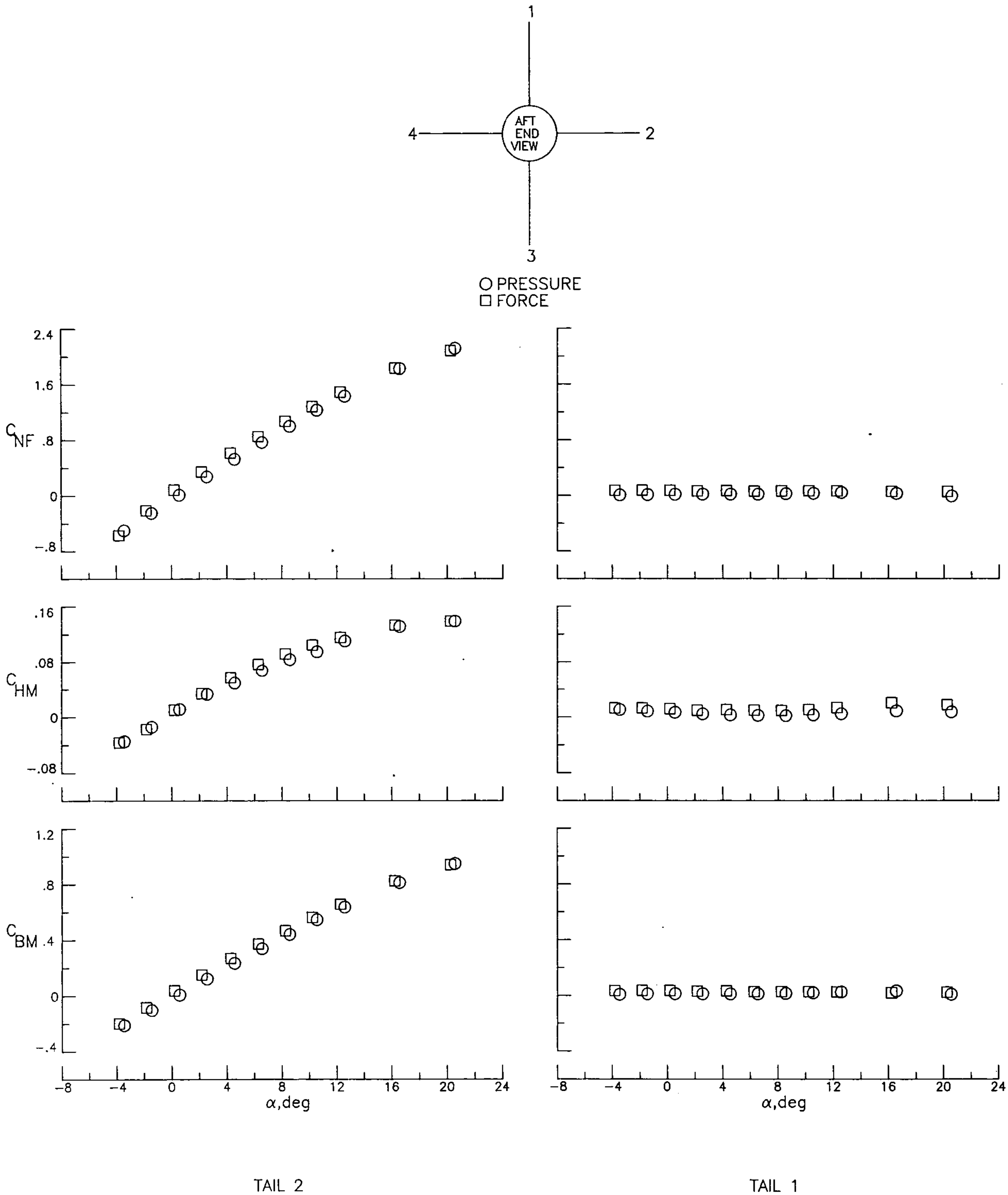

(a) $\phi = 0^{\circ}$.

Figure 8.- Comparison of balance-measured and pressure-integrated panel loads for T_A at $\delta = 0^{\circ}$ and $M = 1.60$.

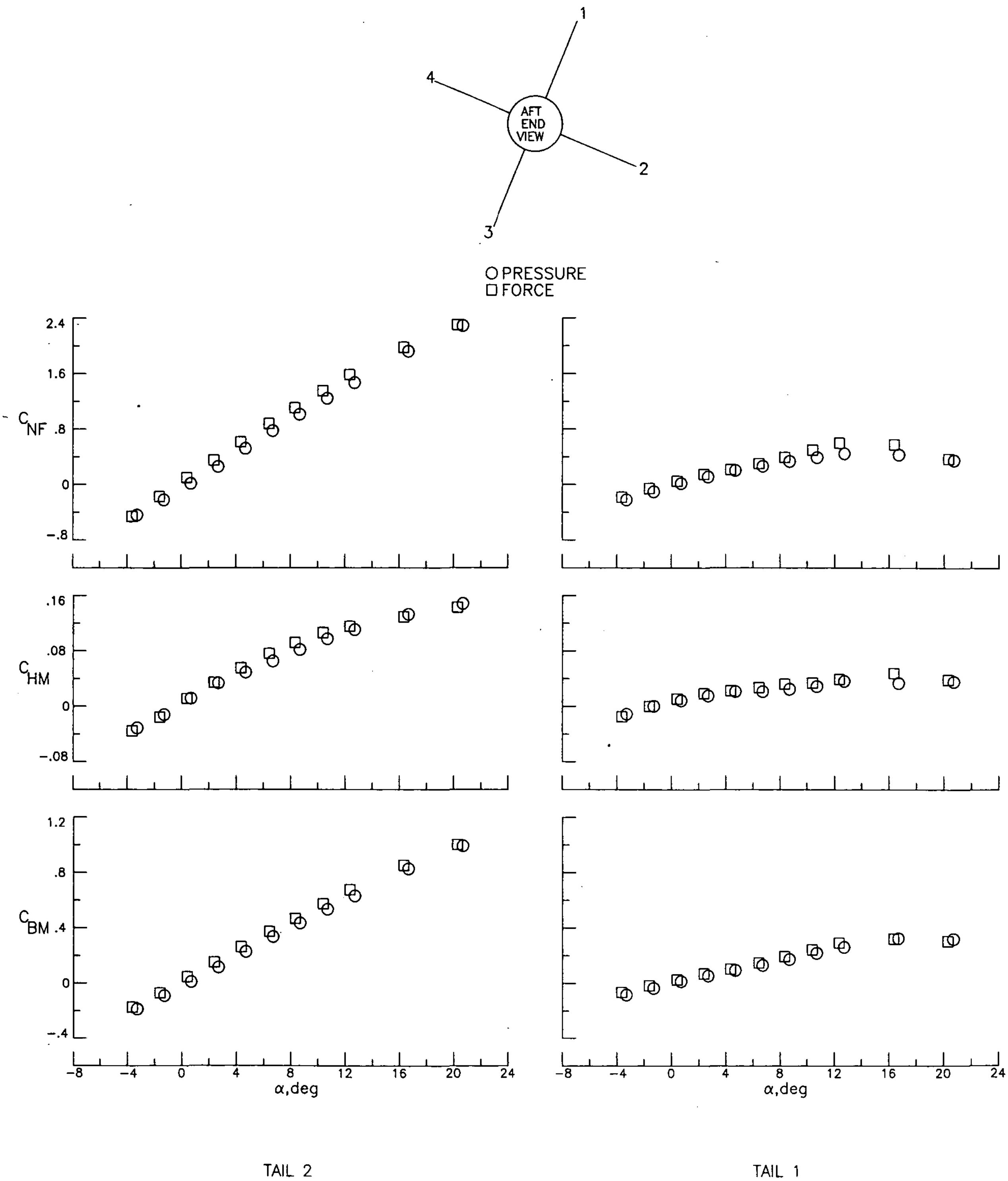

(b) $\phi = 22.5^{\circ}$.

Figure 8.- Continued.

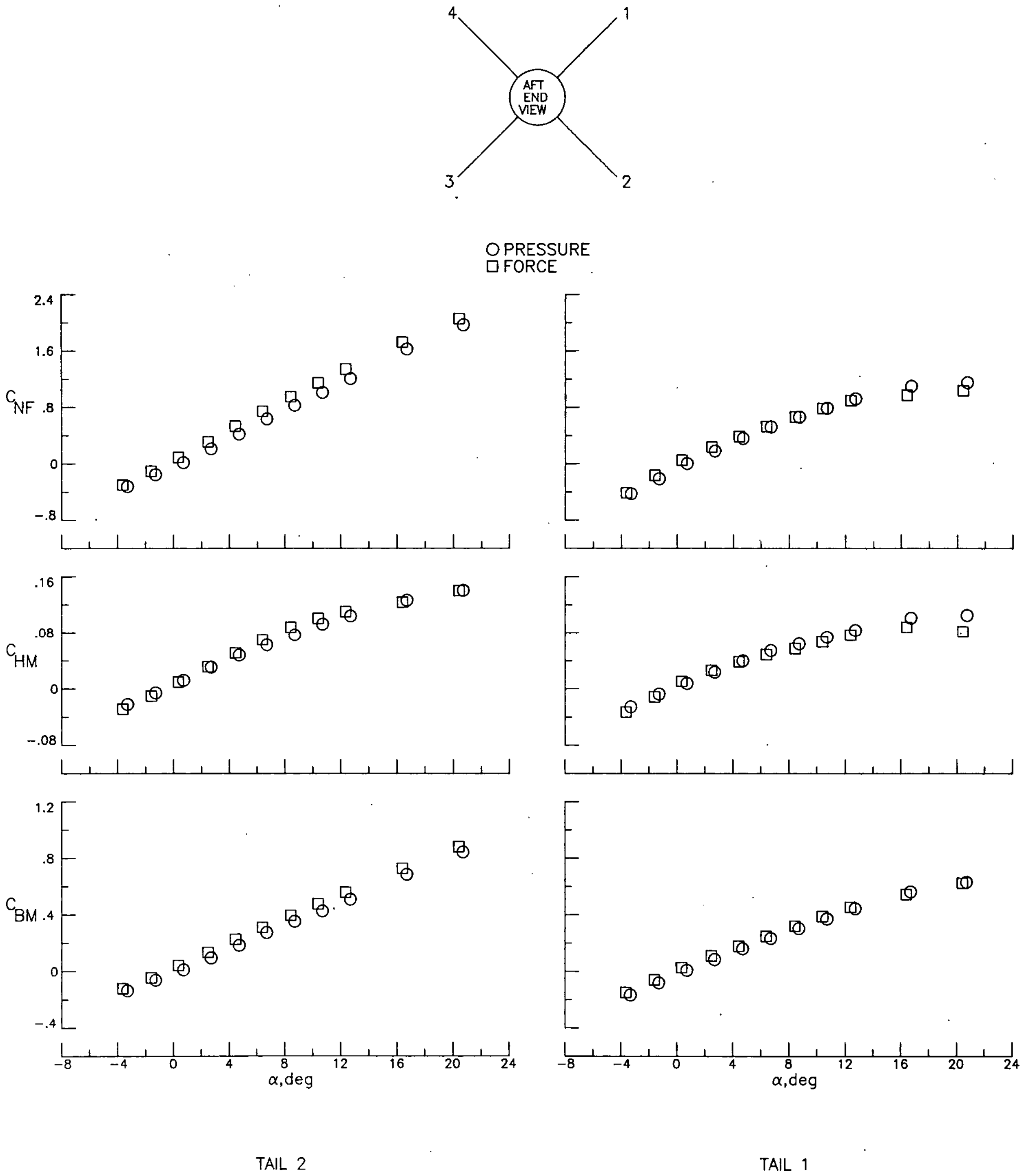

(c) $\phi = 45^{\circ}$.

Figure 8.- Continued.

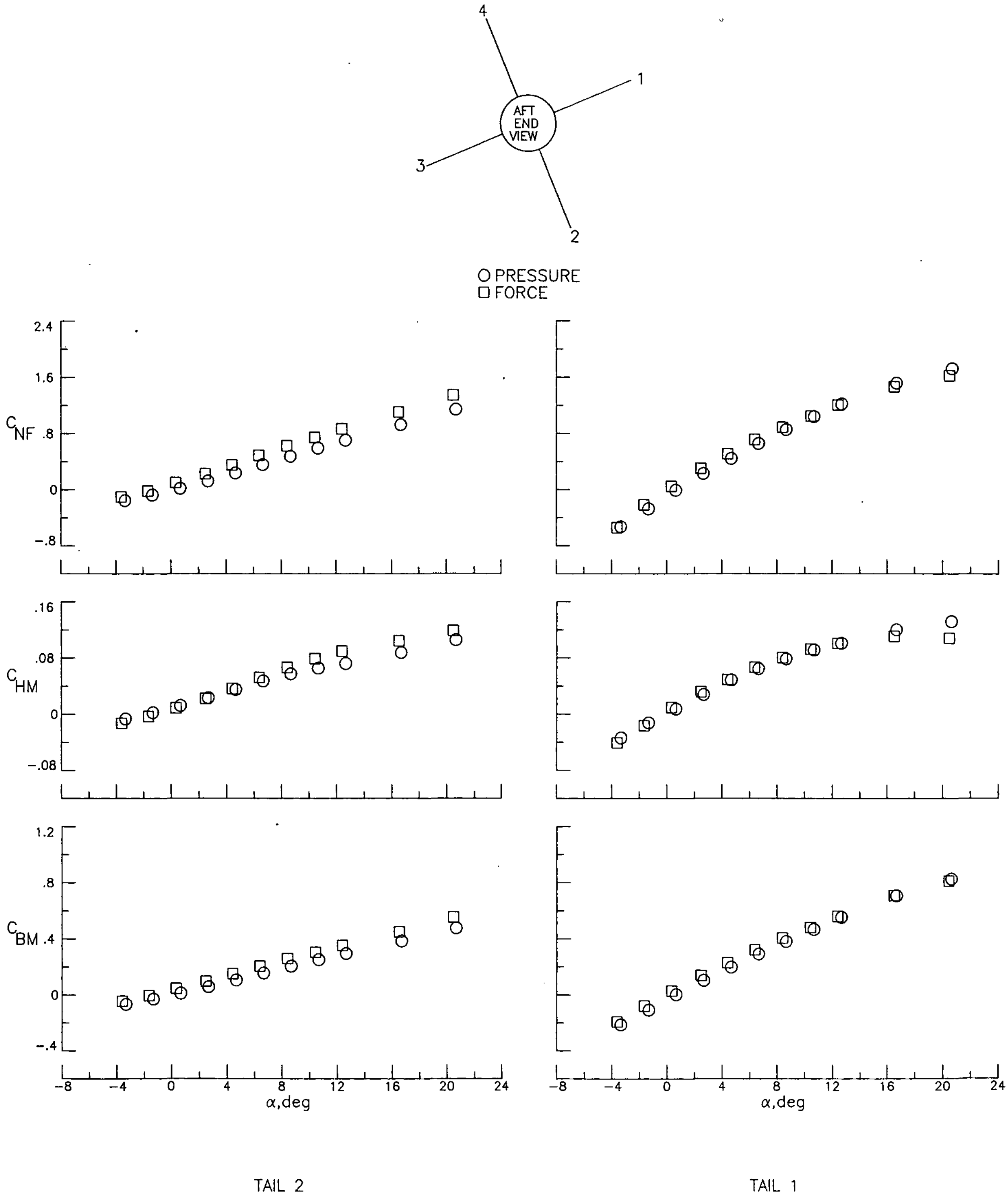

(d) $\phi = 67.5^{\circ}$.

Figure 8.- Continued.

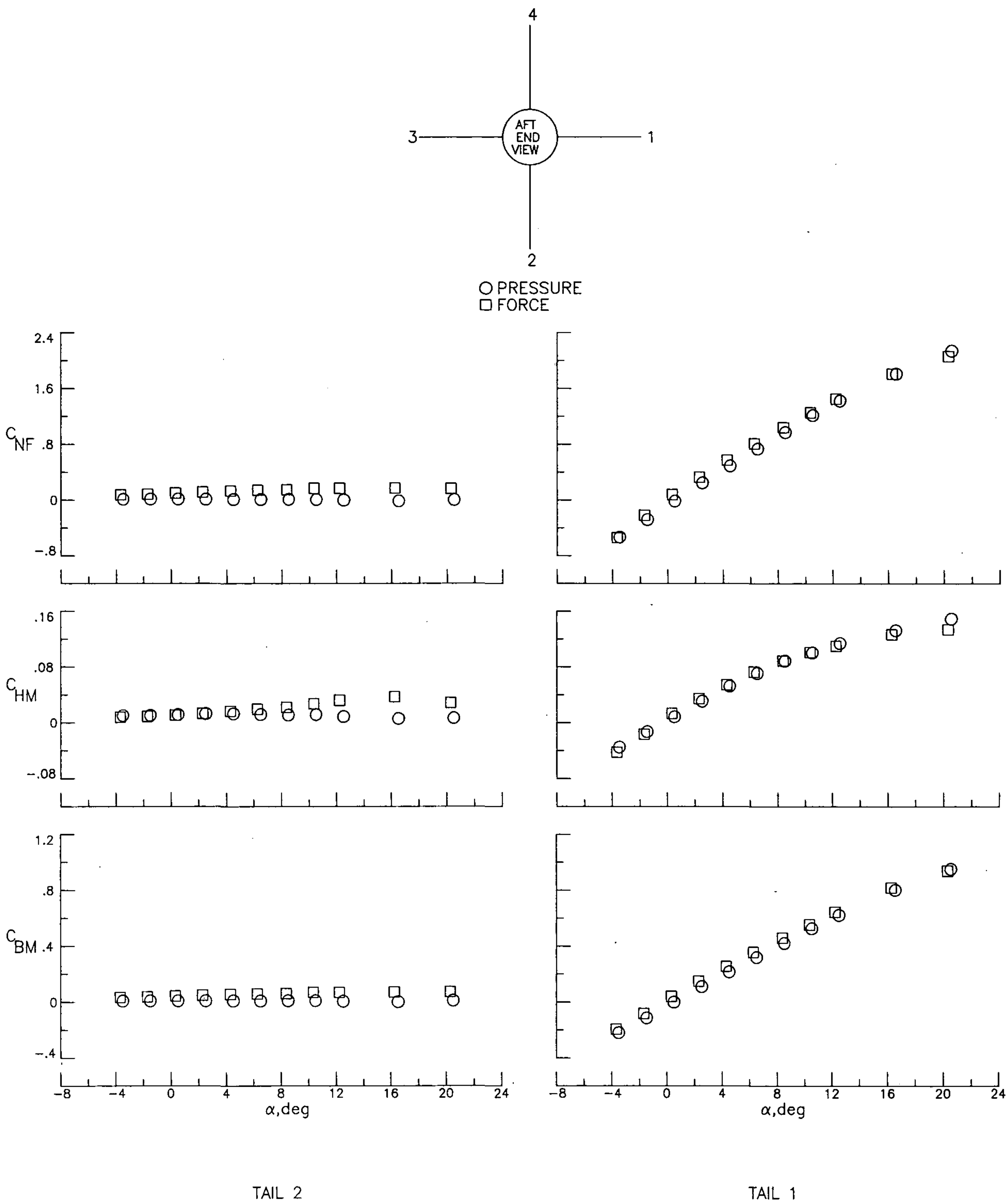

(e) $\phi = 90^{\circ}$.

Figure 8.- Concluded.

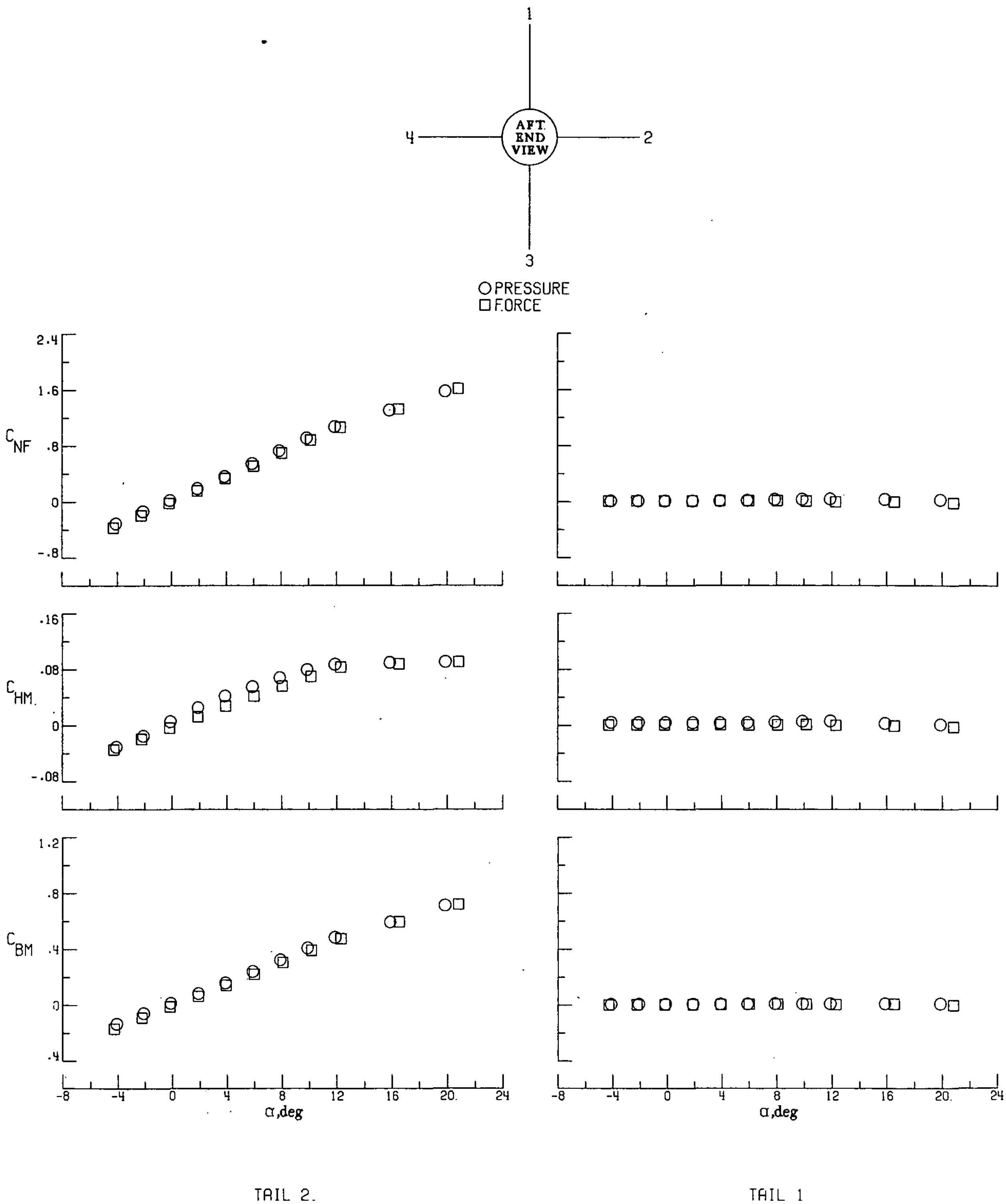

(a) $\phi = 0^{\circ}$.

Figure 9.- Comparison of balance-measured and pressure-integrated panel loads for T_A at $\delta = 0^{\circ}$ and $M = 2.36$.

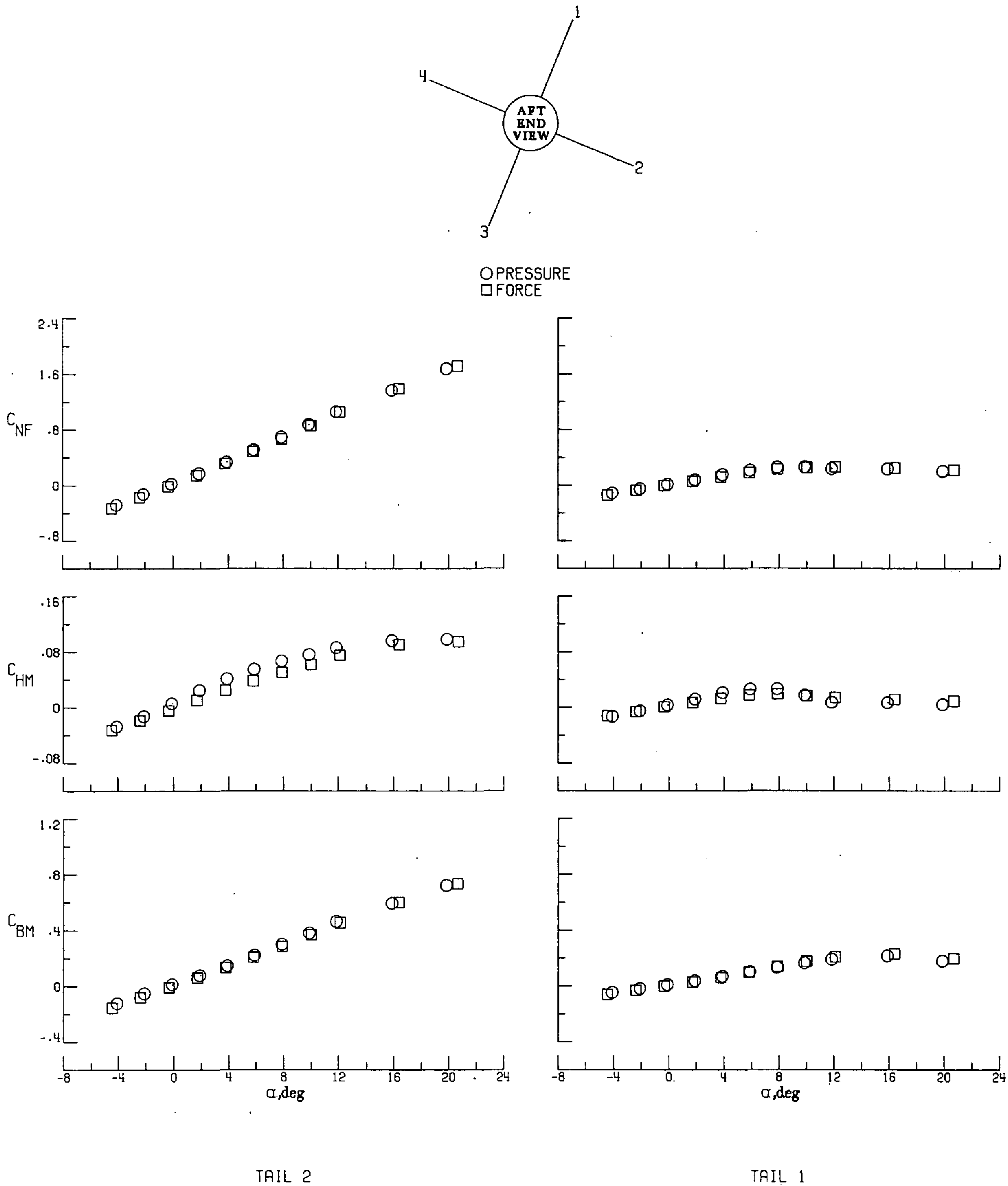

(b) $\phi = 22.5^{\circ}$.

Figure 9.- Continued.

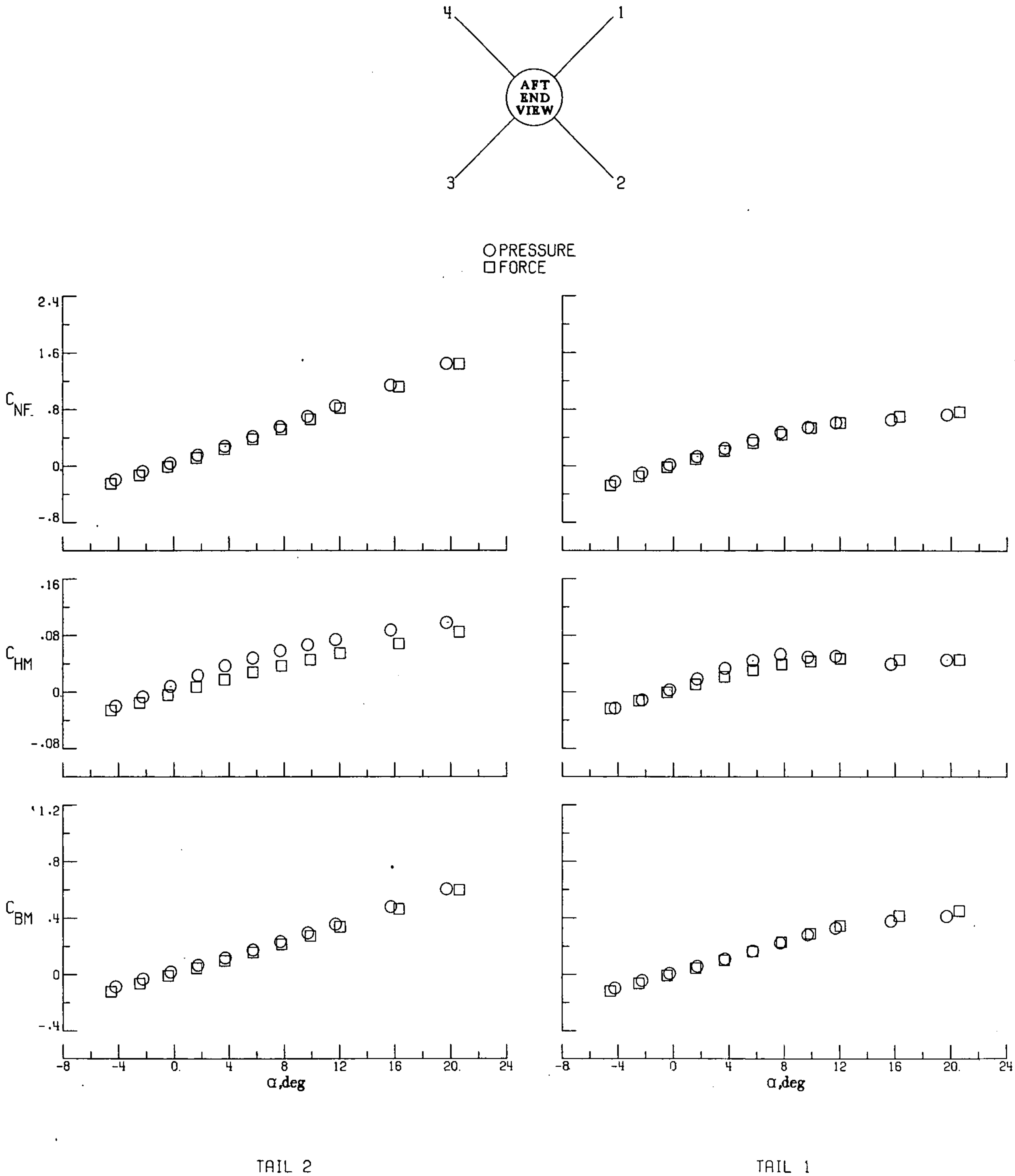

(c) $\phi = 45°$.

Figure 9.- Continued.

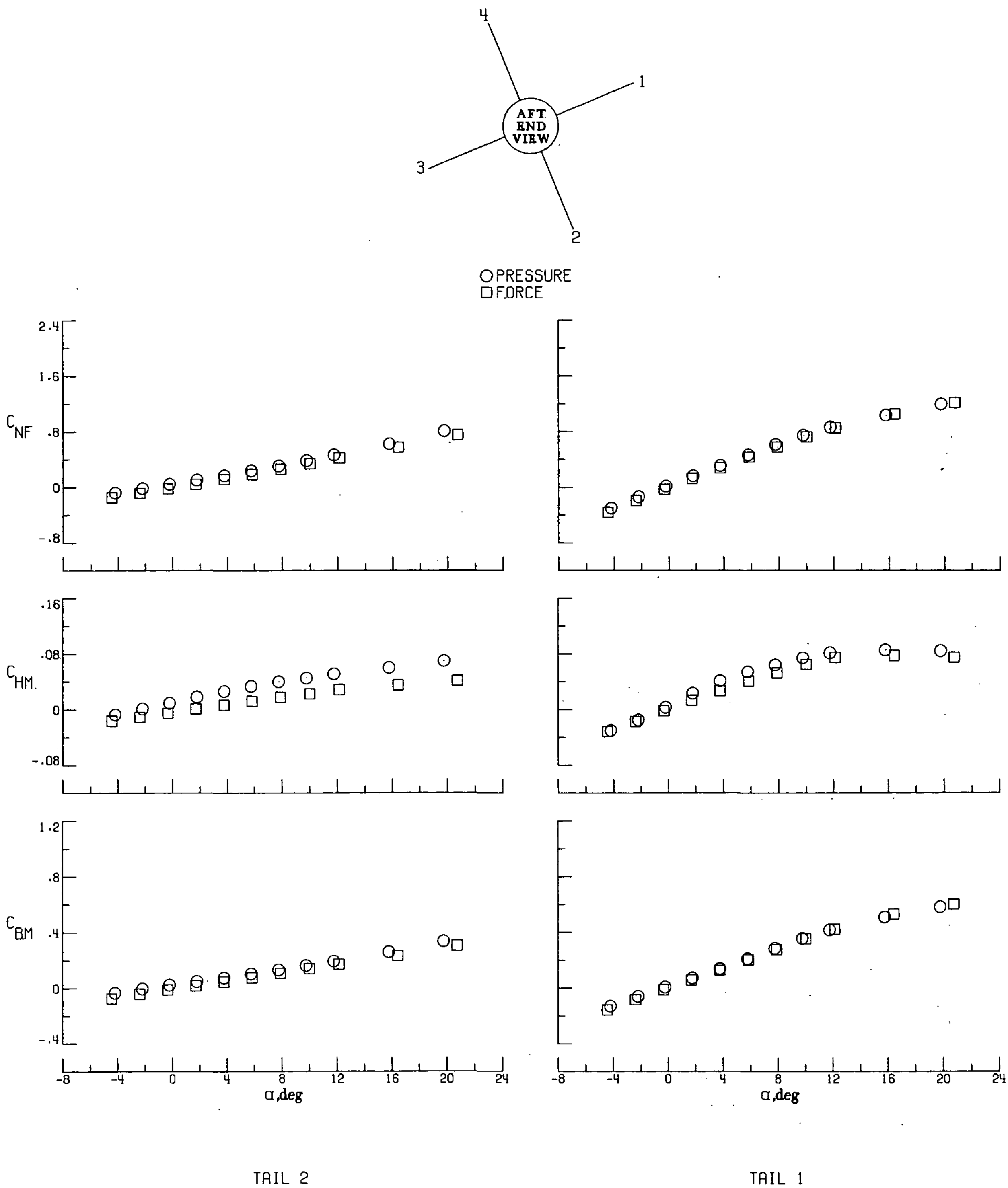

(d) $\phi = 67.5^{\circ}$.

Figure 9.- Continued.

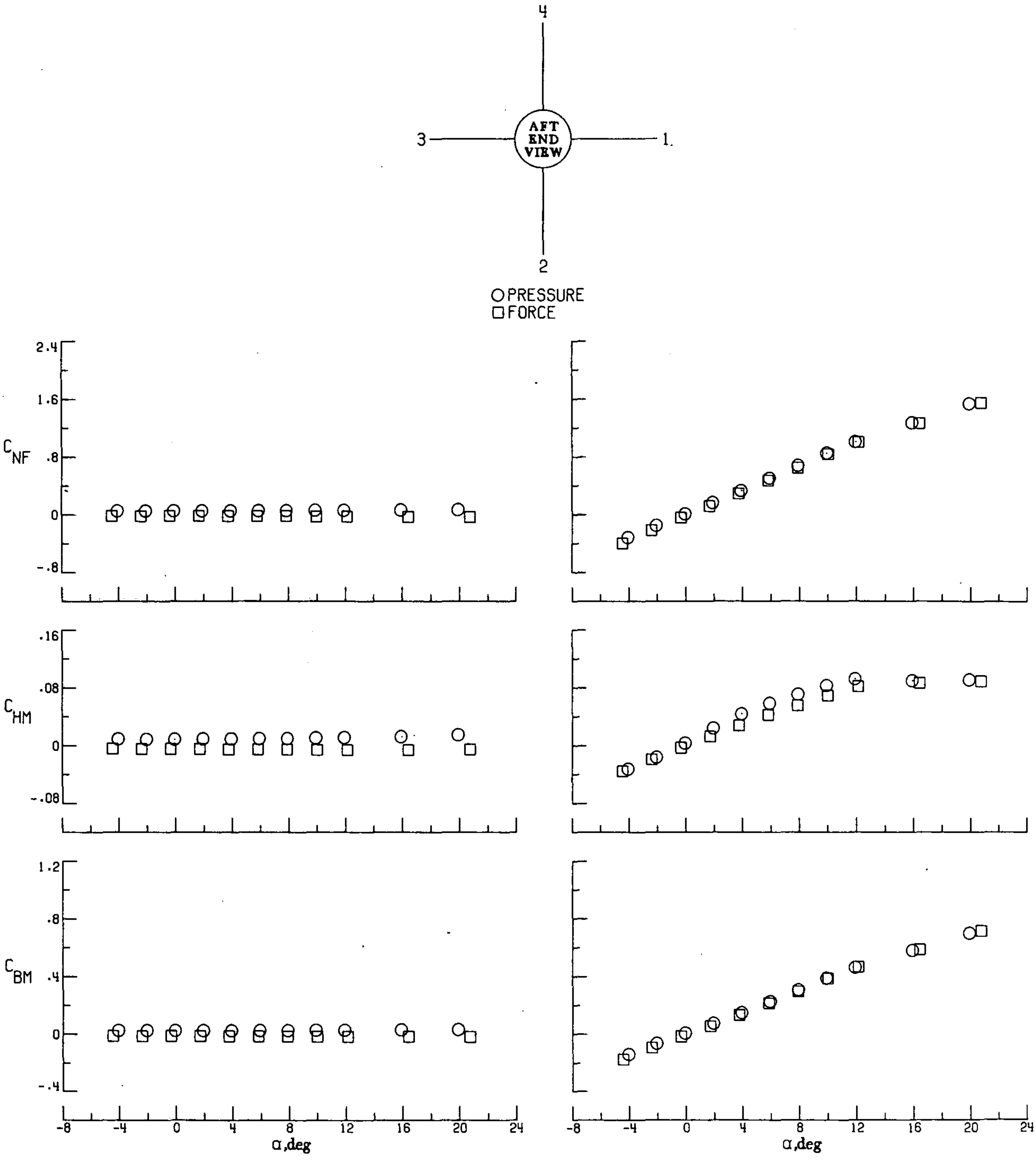

(e) $\phi = 90^{\circ}$.

Figure 9.- Concluded.

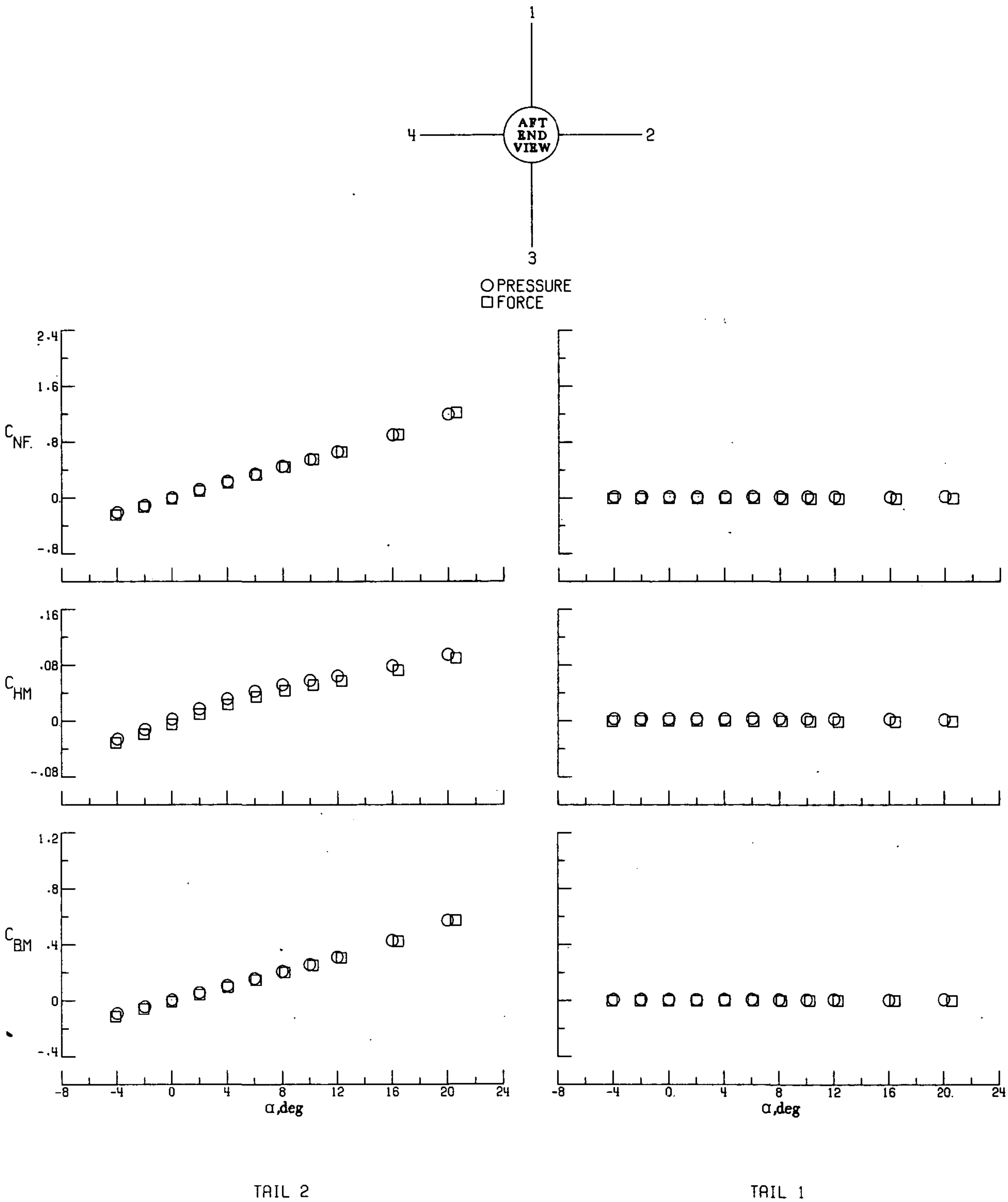

(a) $\phi = 0^{\circ}$.

Figure 10.- Comparison of balance-measured and pressure-integrated panel loads for T_A at $\delta = 0^{\circ}$ and $M = 3.70$.

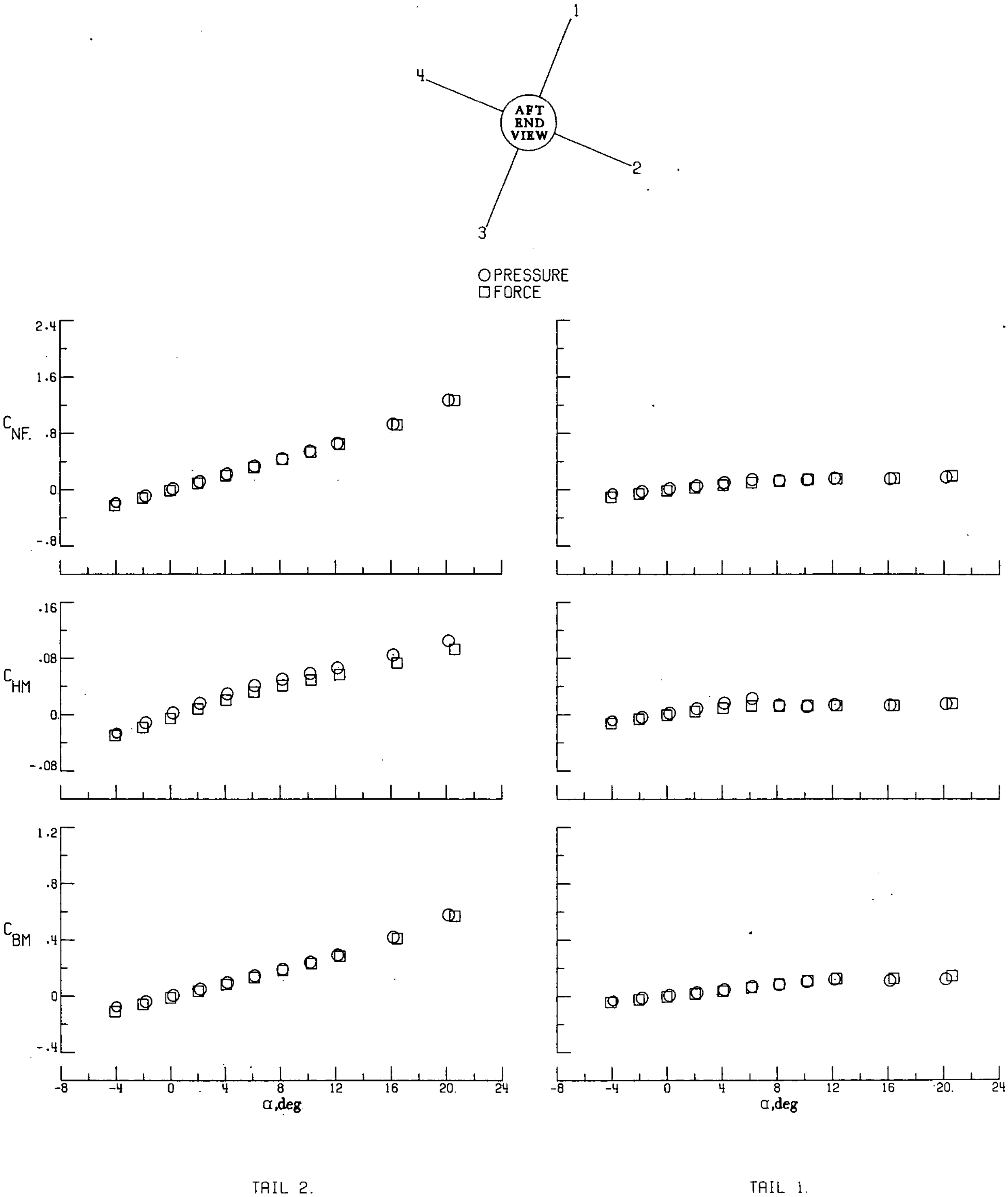

(b) $\phi = 22.5^{\circ}$.

Figure 10.- Continued.

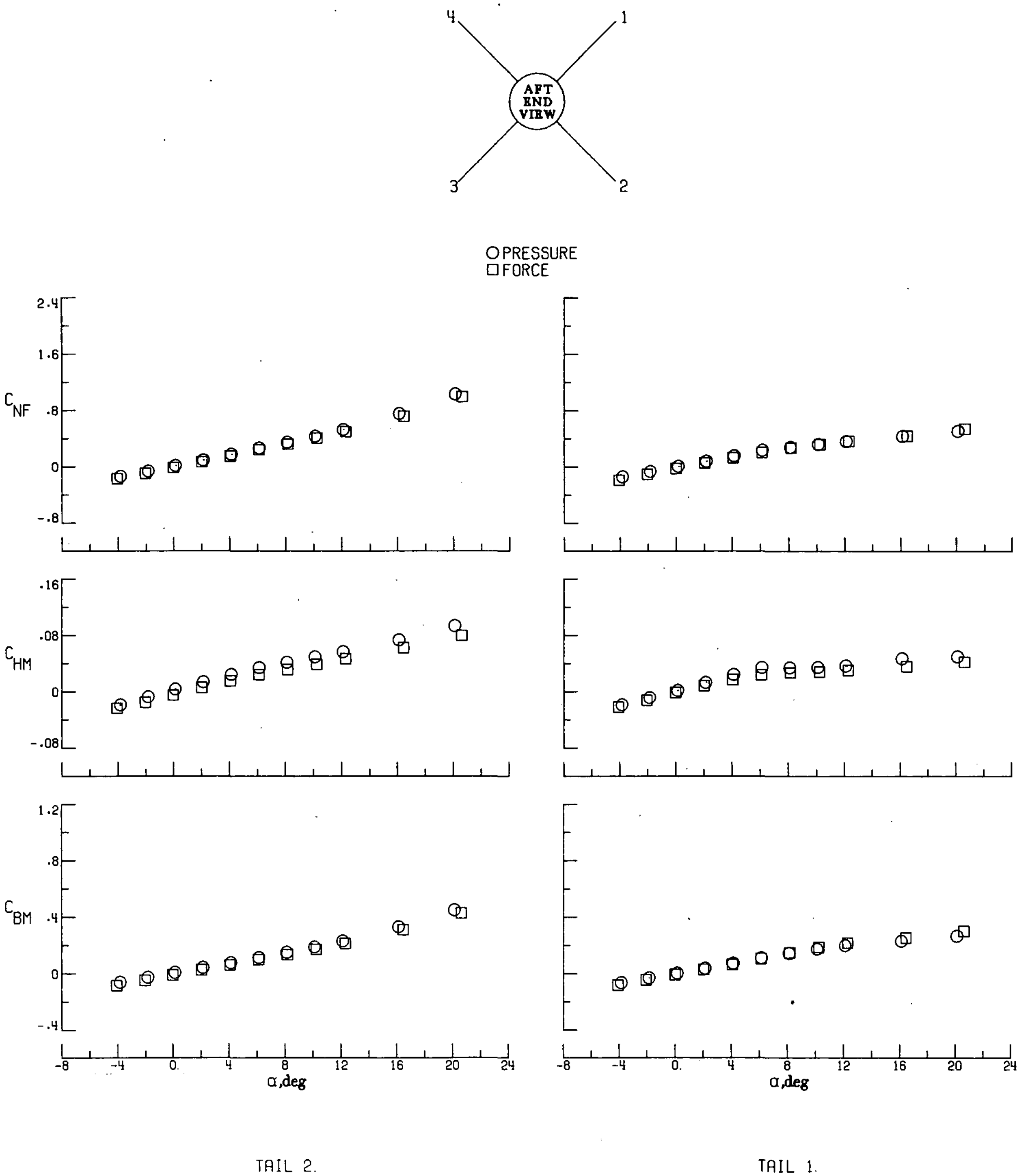

(c) $\phi = 45^{\circ}$.

Figure 10.- Continued.

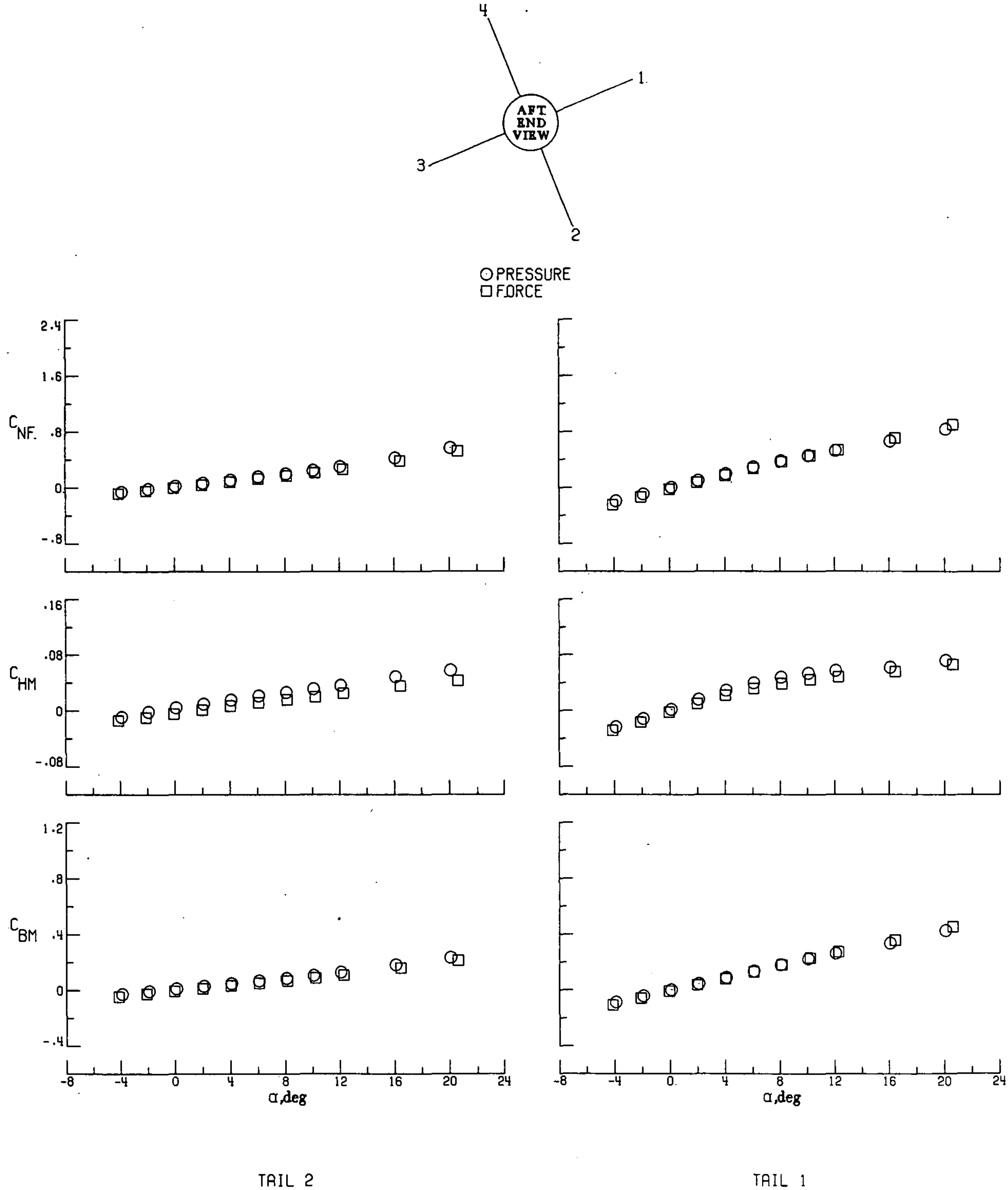

(d) $\phi = 67.5^{\circ}$.

Figure 10.- Continued.

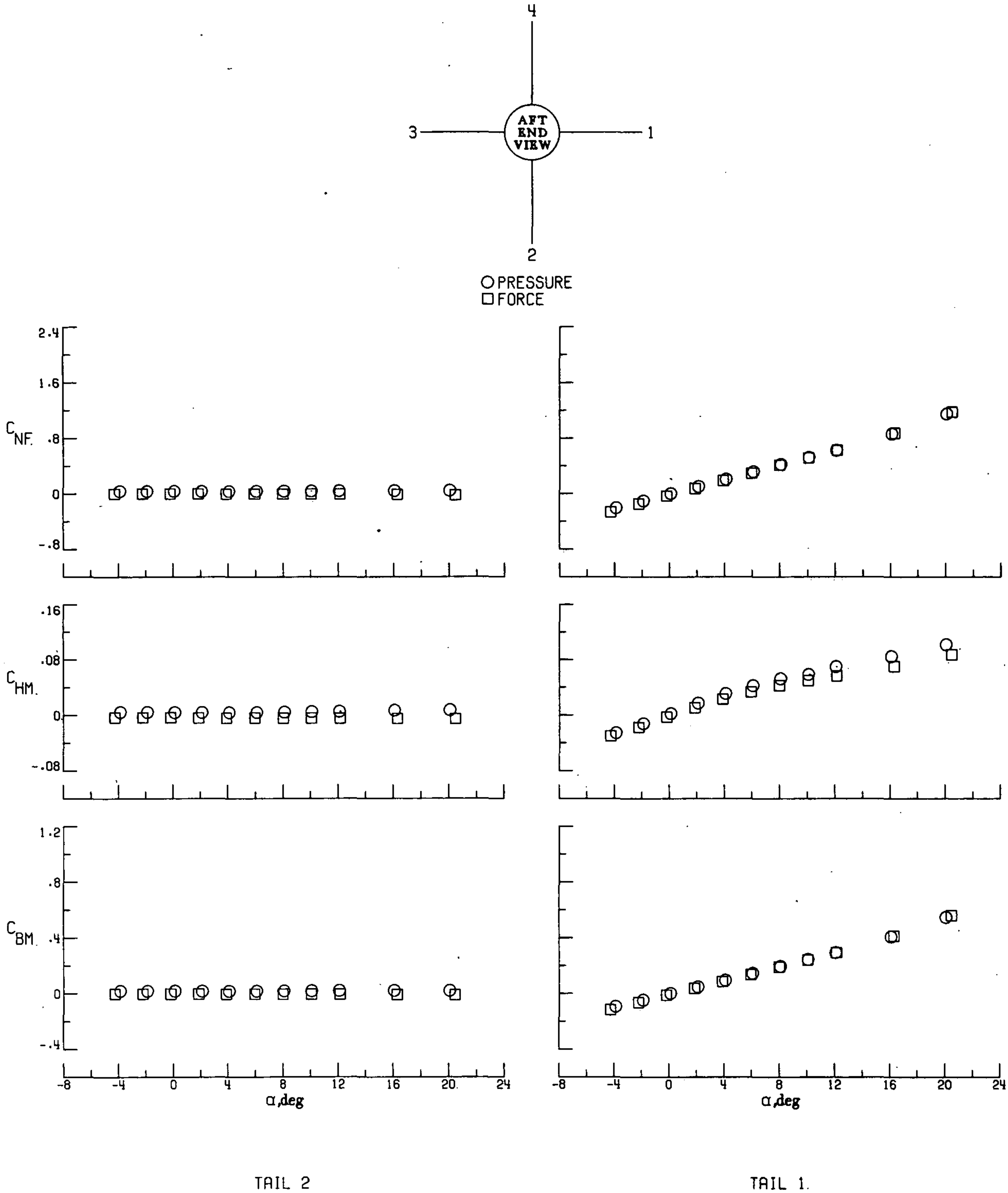

(e) $\phi = 90^{\circ}$.

Figure 10.- Concluded.

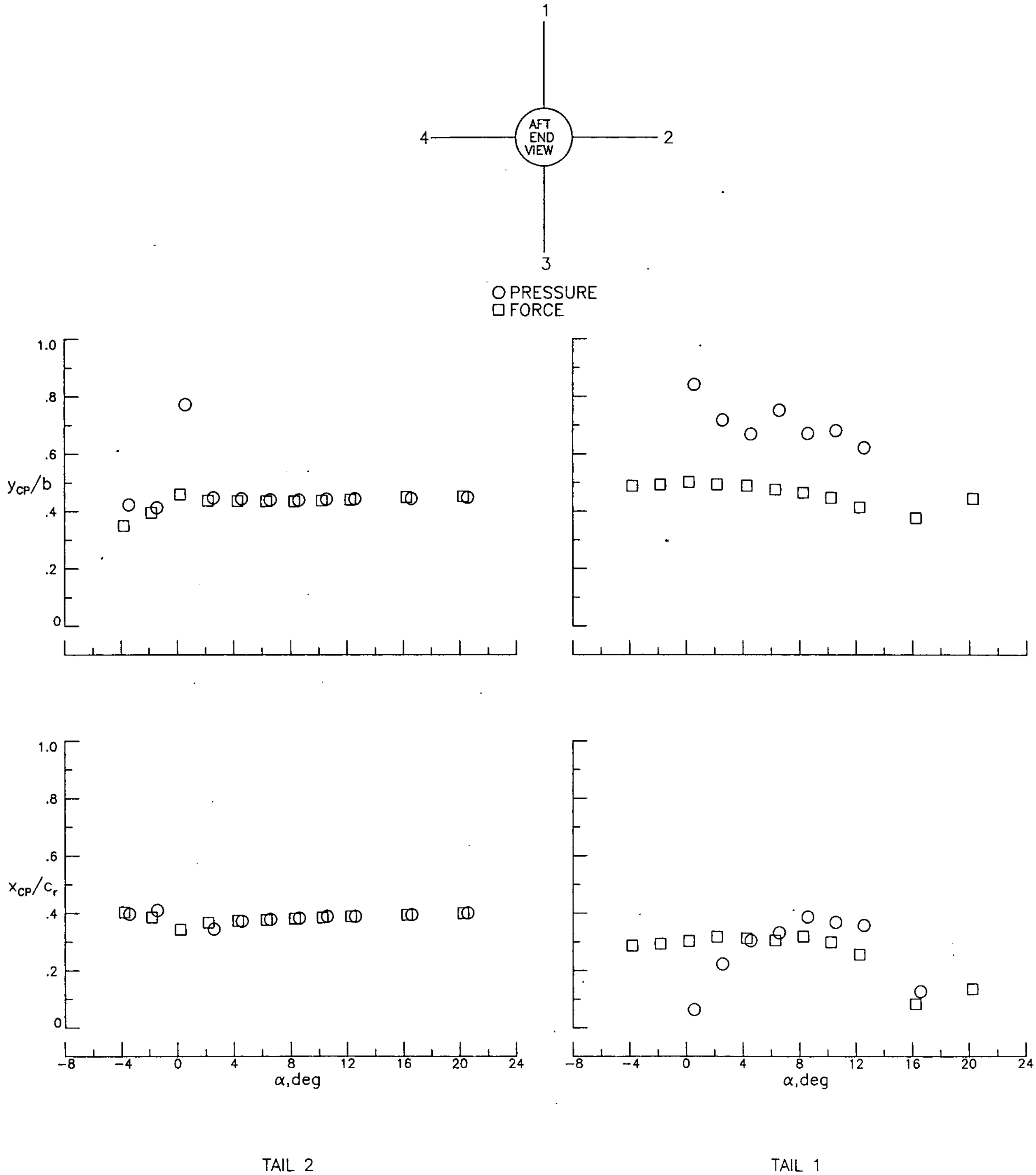

(a) $\phi = 0^{\circ}$.

Figure 11.- Comparison of balance-measured and pressure-integrated centers of pressure for T_A at $\delta = 0^{\circ}$ and $M = 1.60$.

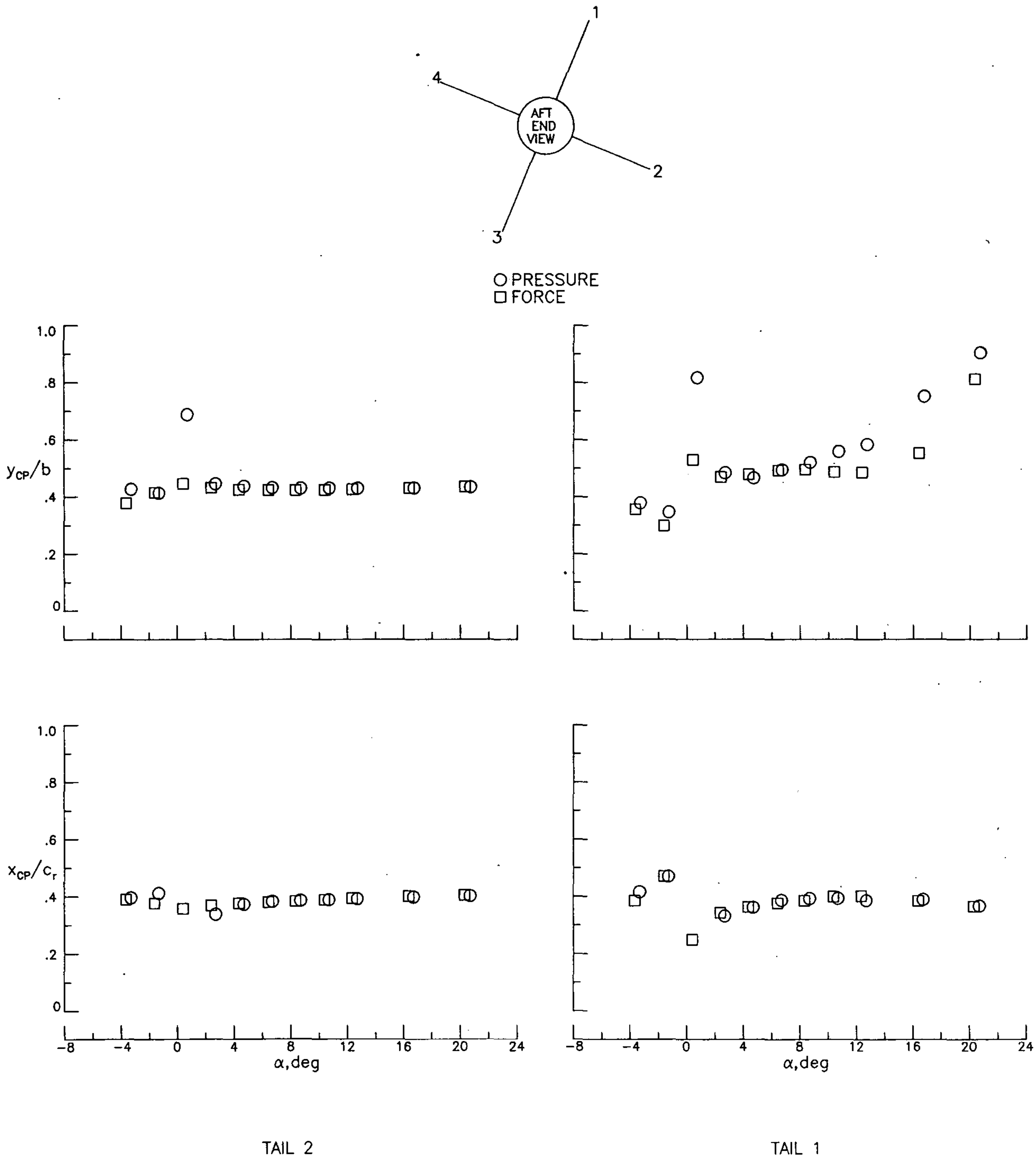

(b) $\phi = 22.5^{\circ}$.

Figure 11.- Continued.

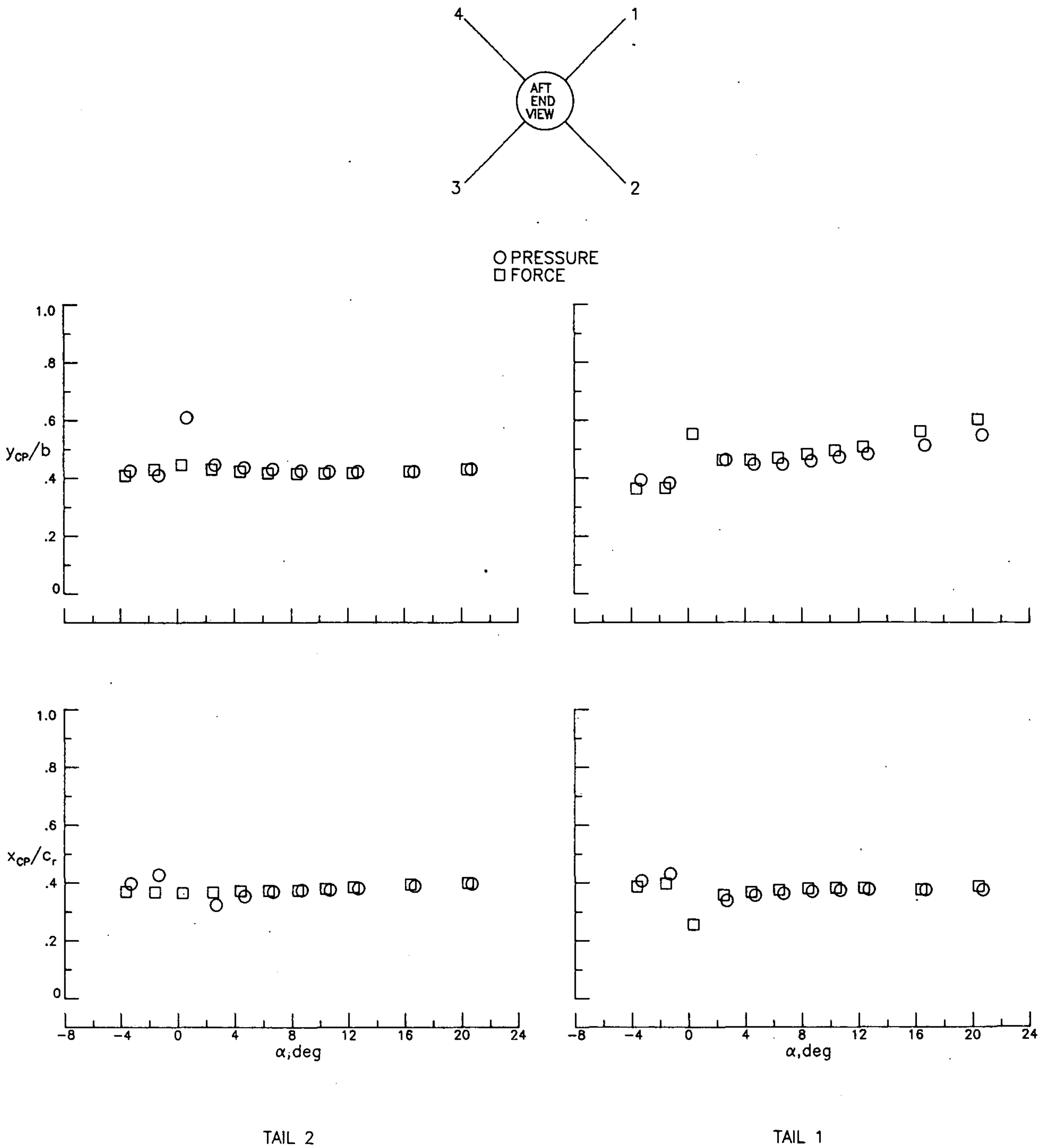

(c) $\phi = 45^{\circ}$.

Figure 11.- Continued.

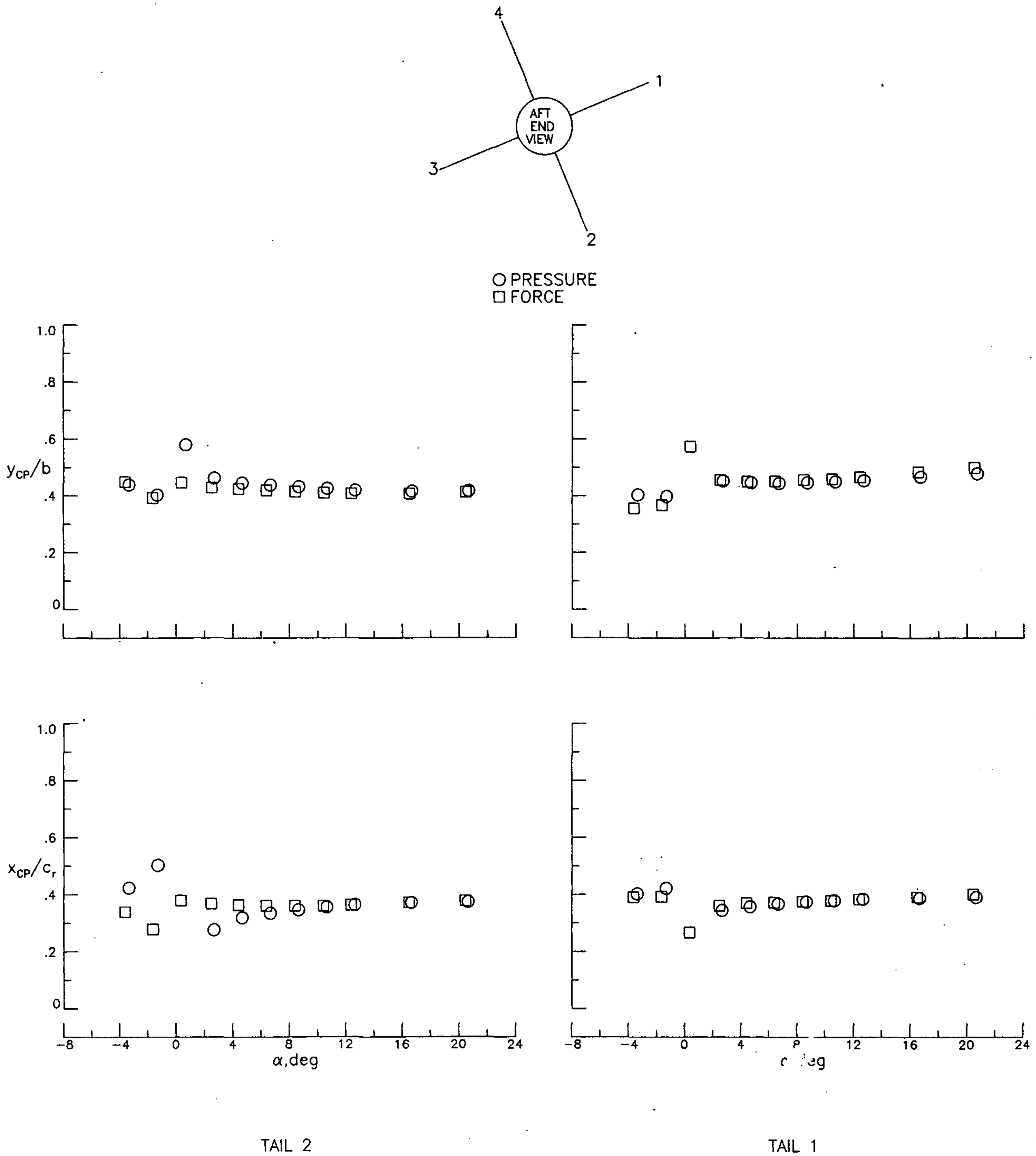

(d) $\phi = 67.5^{\circ}$.

Figure 11.- Continued.

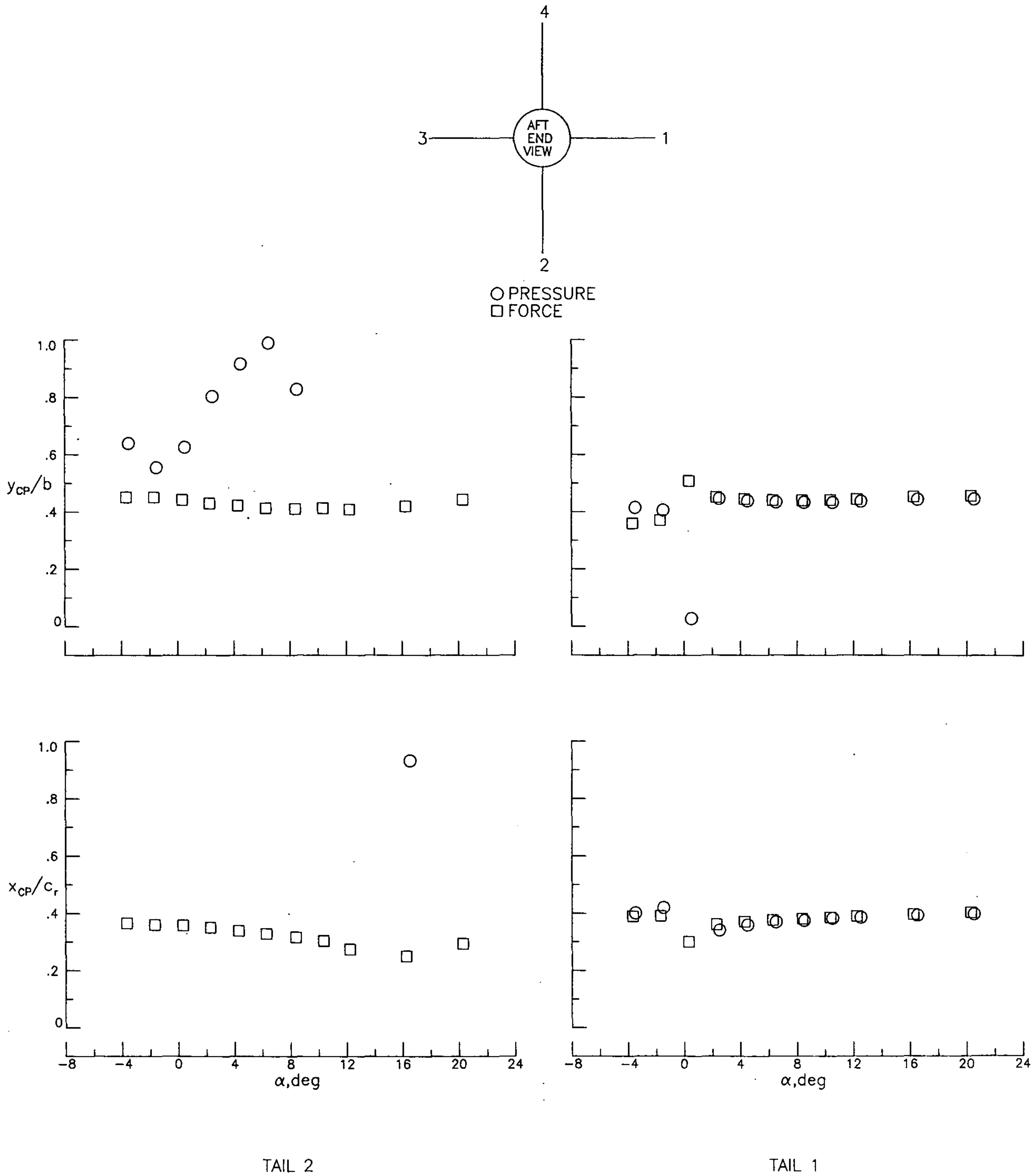

(e) $\phi = 90^{\circ}$.

Figure 11.- Concluded.

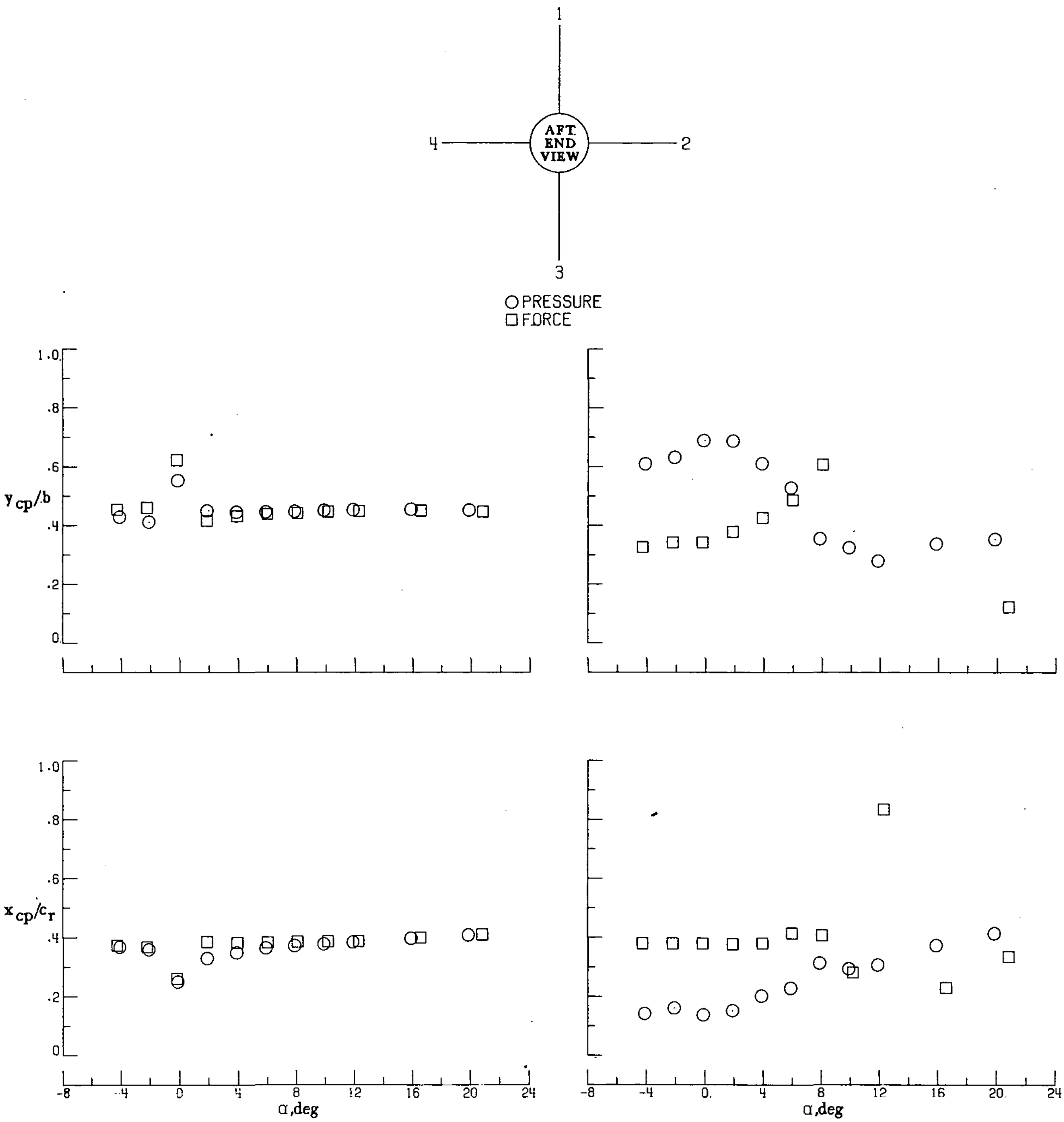

(a) $\phi = 0^{\circ}$.

Figure 12.- Comparison of balance-measured and pressure-integrated centers of pressure for T_A at $\delta = 0^{\circ}$ and $M = 2.36$.

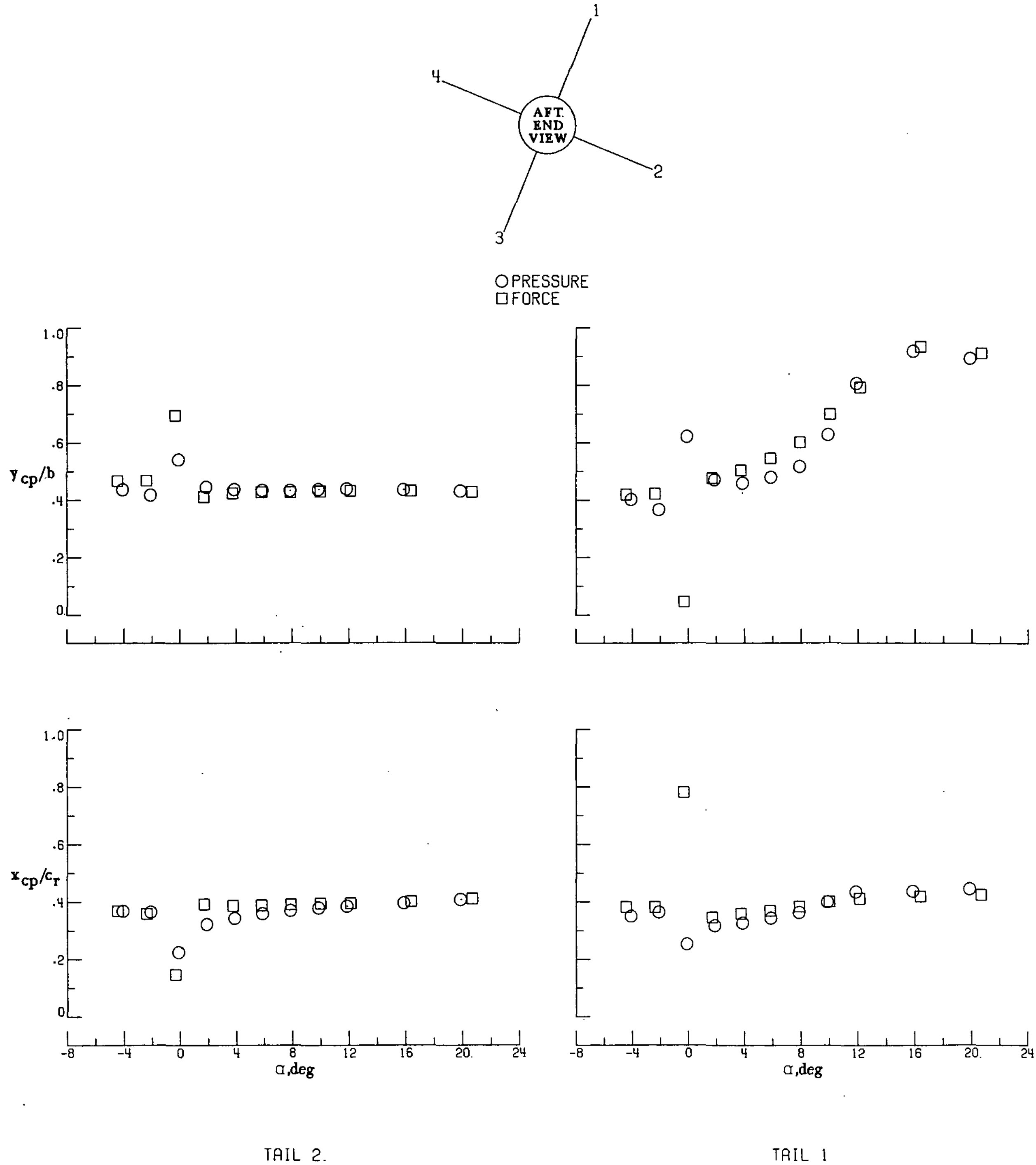

(b) $\phi = 22.5^{\circ}$.

Figure 12.- Continued.

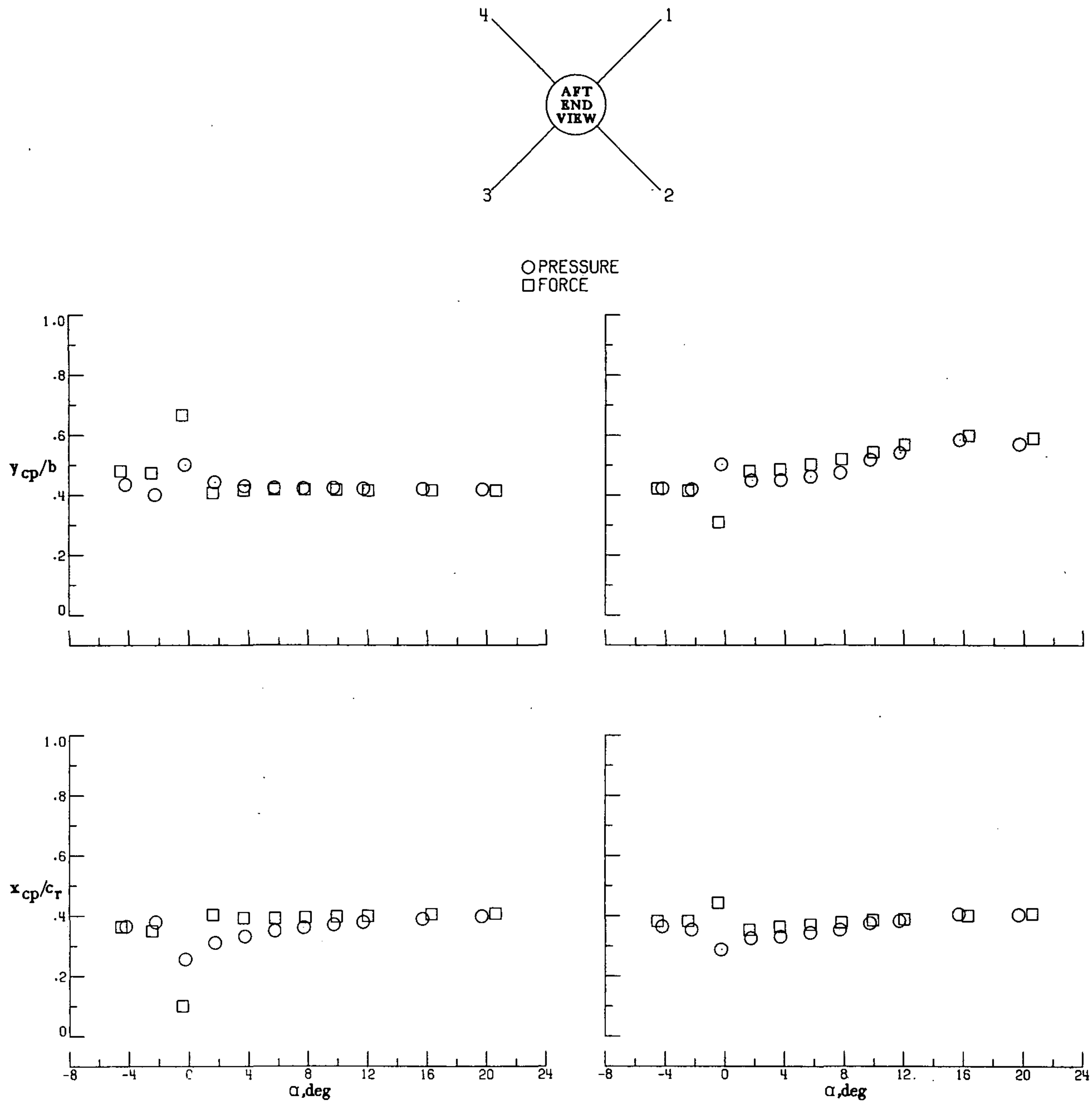

TAIL 2.

TAIL 1

(c) $\phi = 45^{\circ}$.

Figure 12.- Continued.

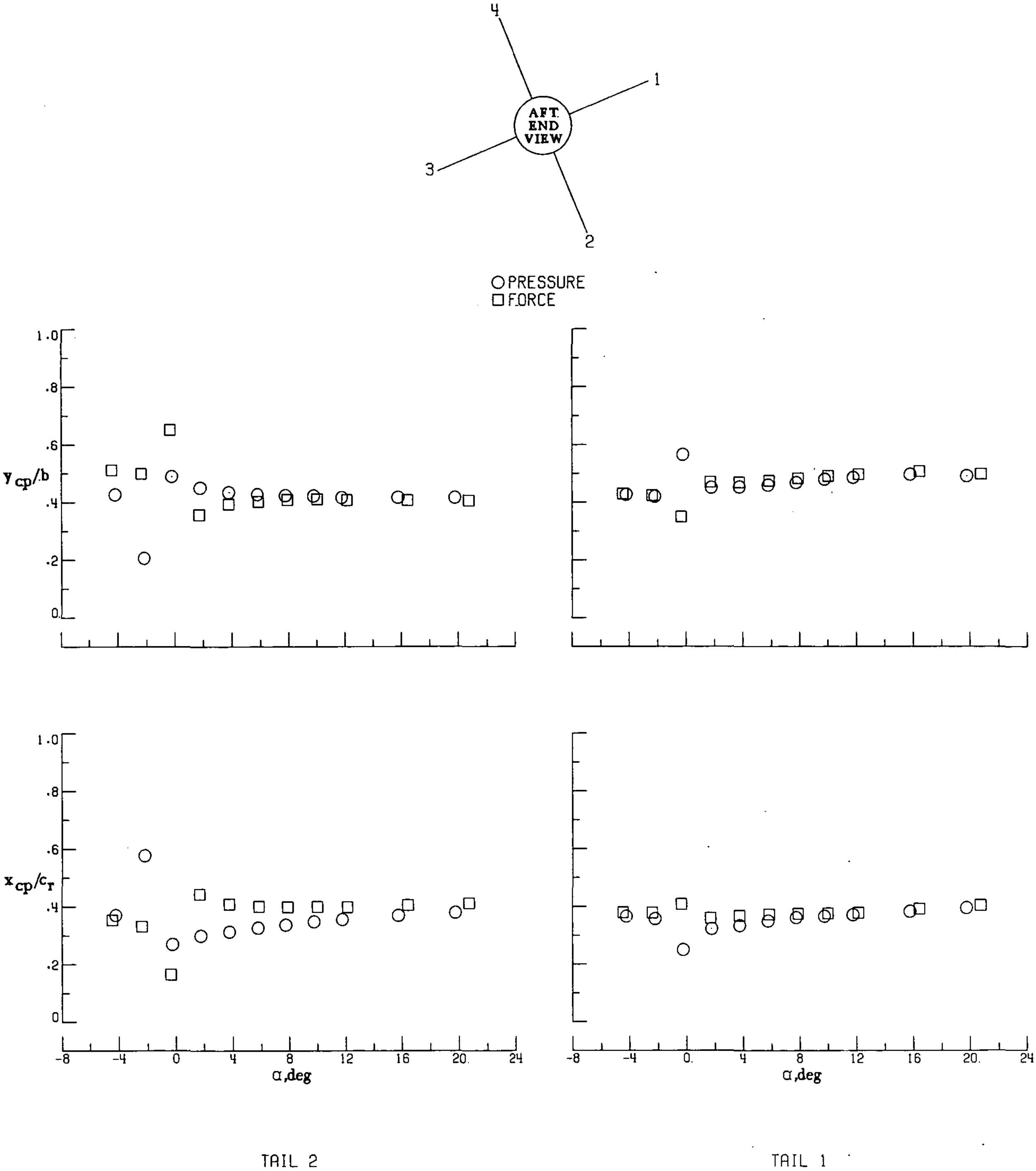

(d) $\phi = 67.5^{\circ}$.

Figure 12.- Continued.

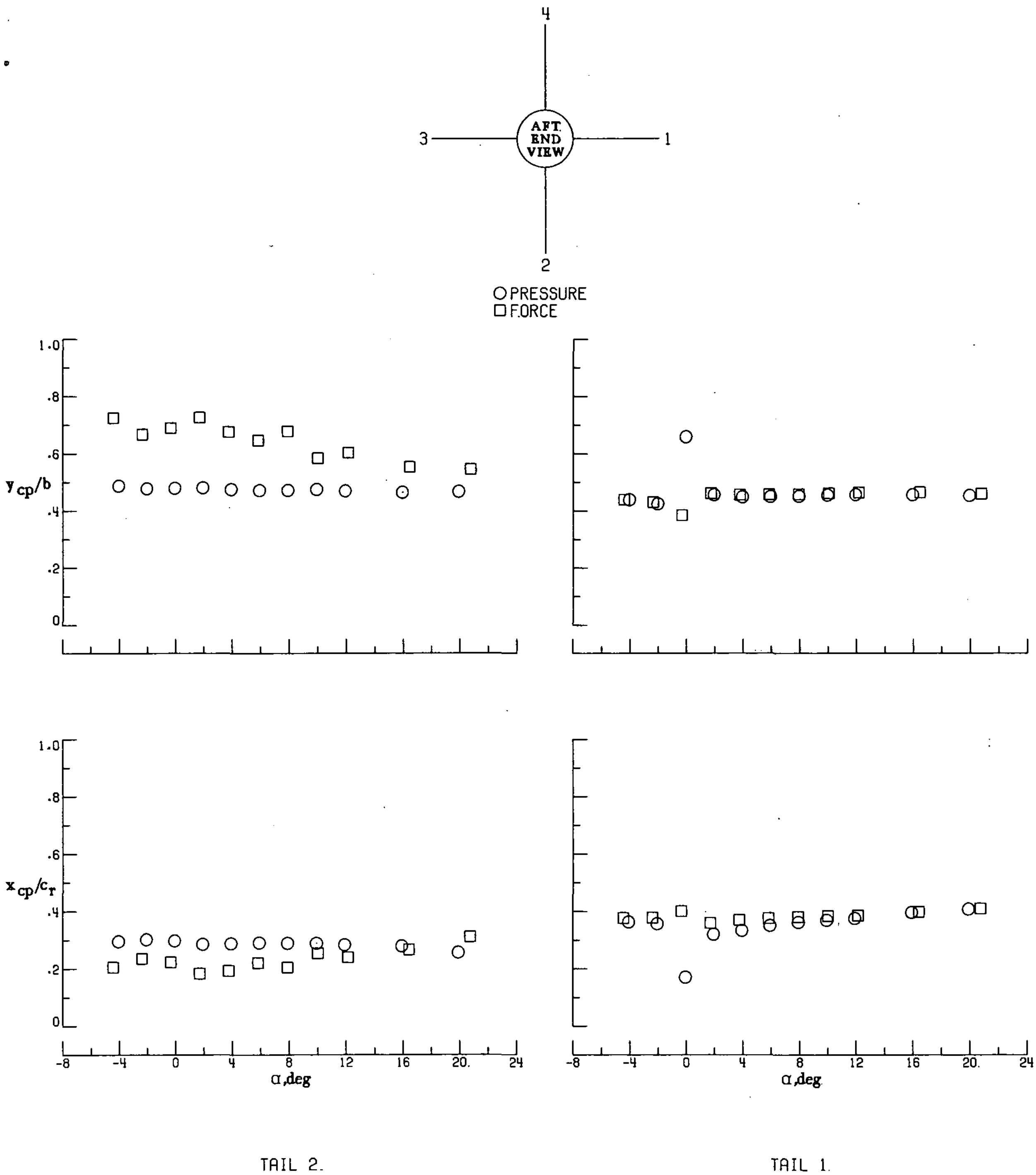

(e) $\phi = 90^{\circ}$.

Figure 12.- Concluded.

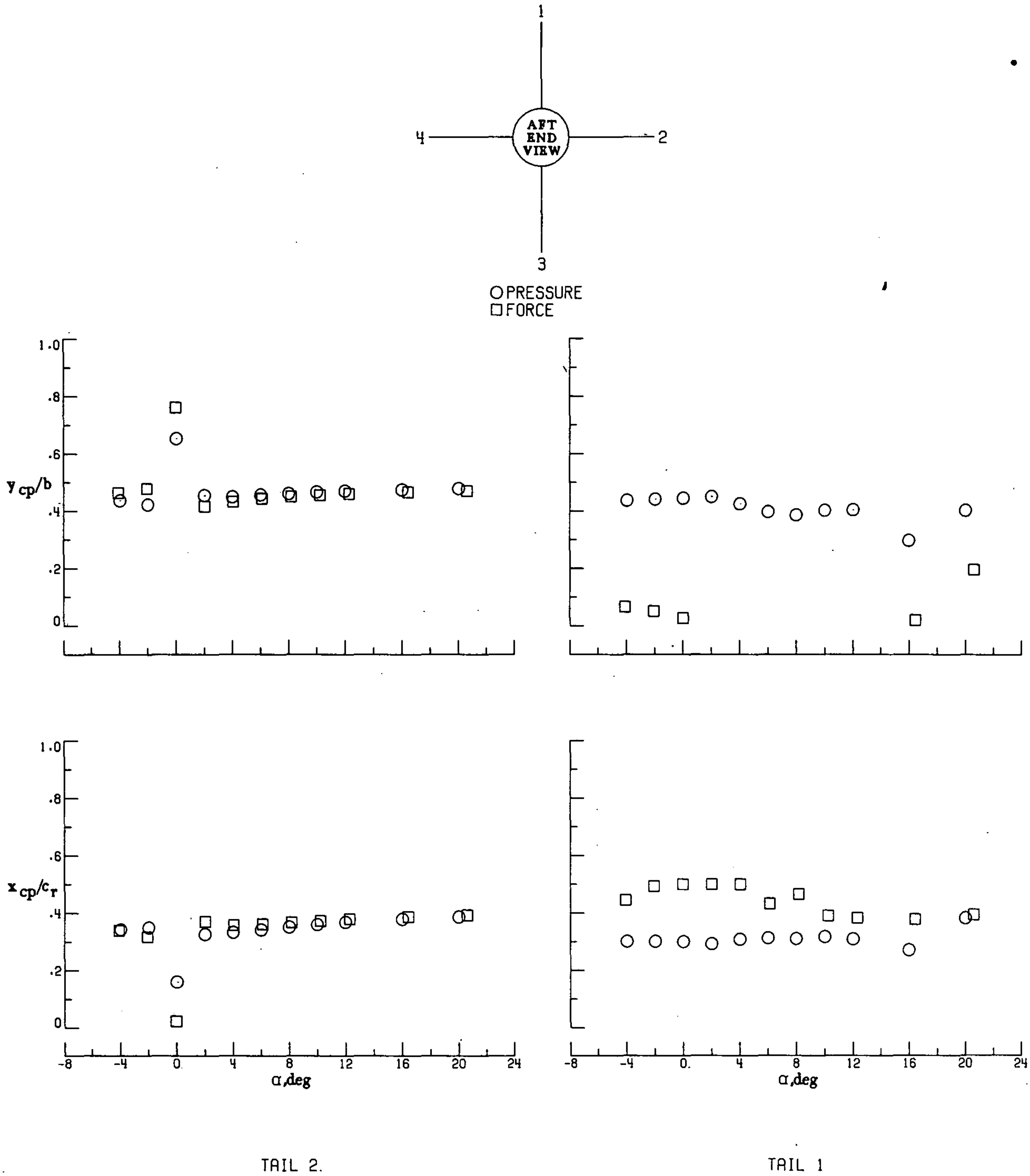

(a) $\phi = 0^{\circ}$.

Figure 13.- Comparison of balance-measured and pressure-integrated centers of pressure for T_A at $\delta = 0^{\circ}$ and $M = 3.70$.

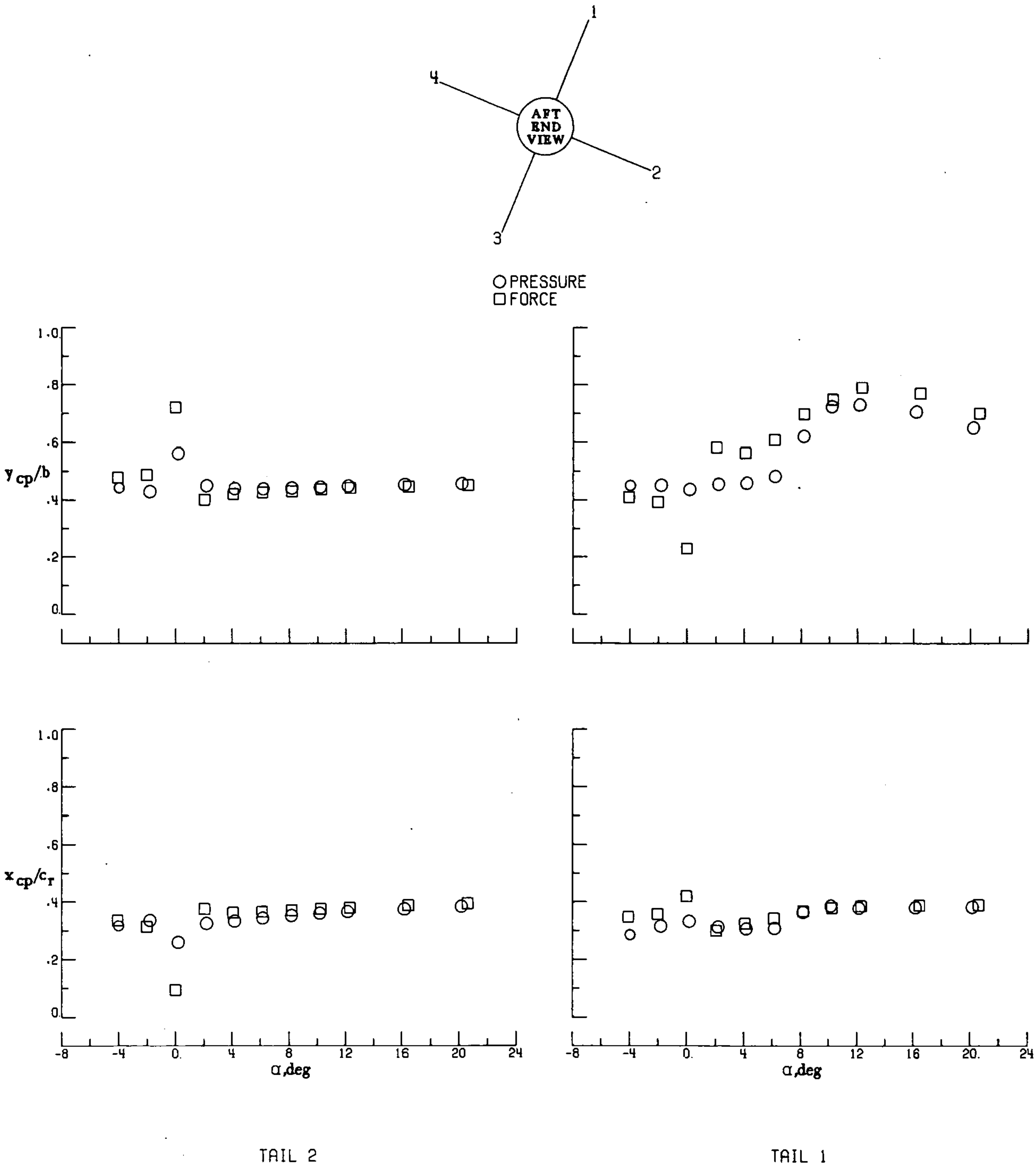

(b) $\phi = 22.5^{\circ}$.

Figure 13.- Continued.

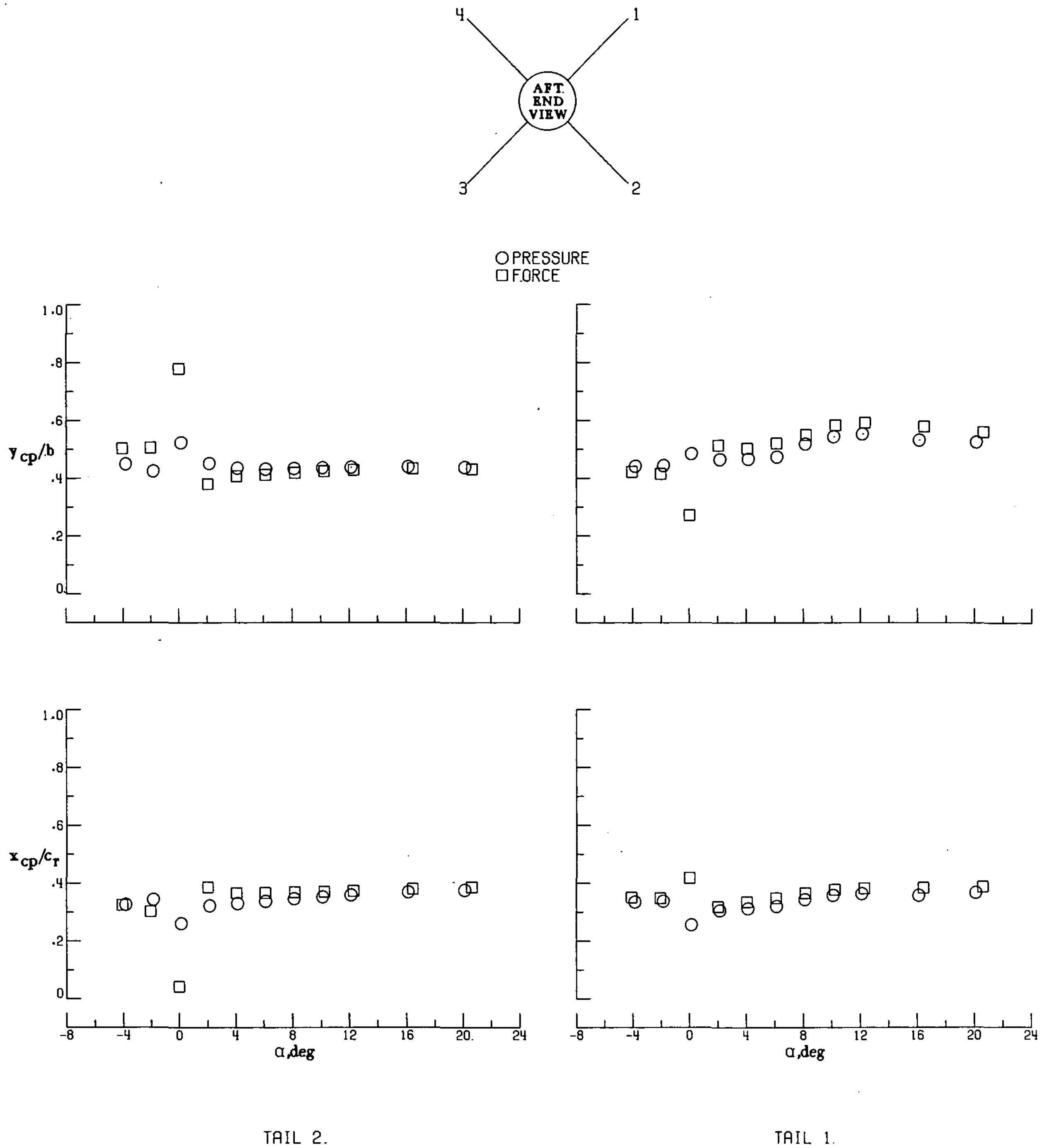

(c) $\phi = 45^{o}$.

Figure 13.- Continued.

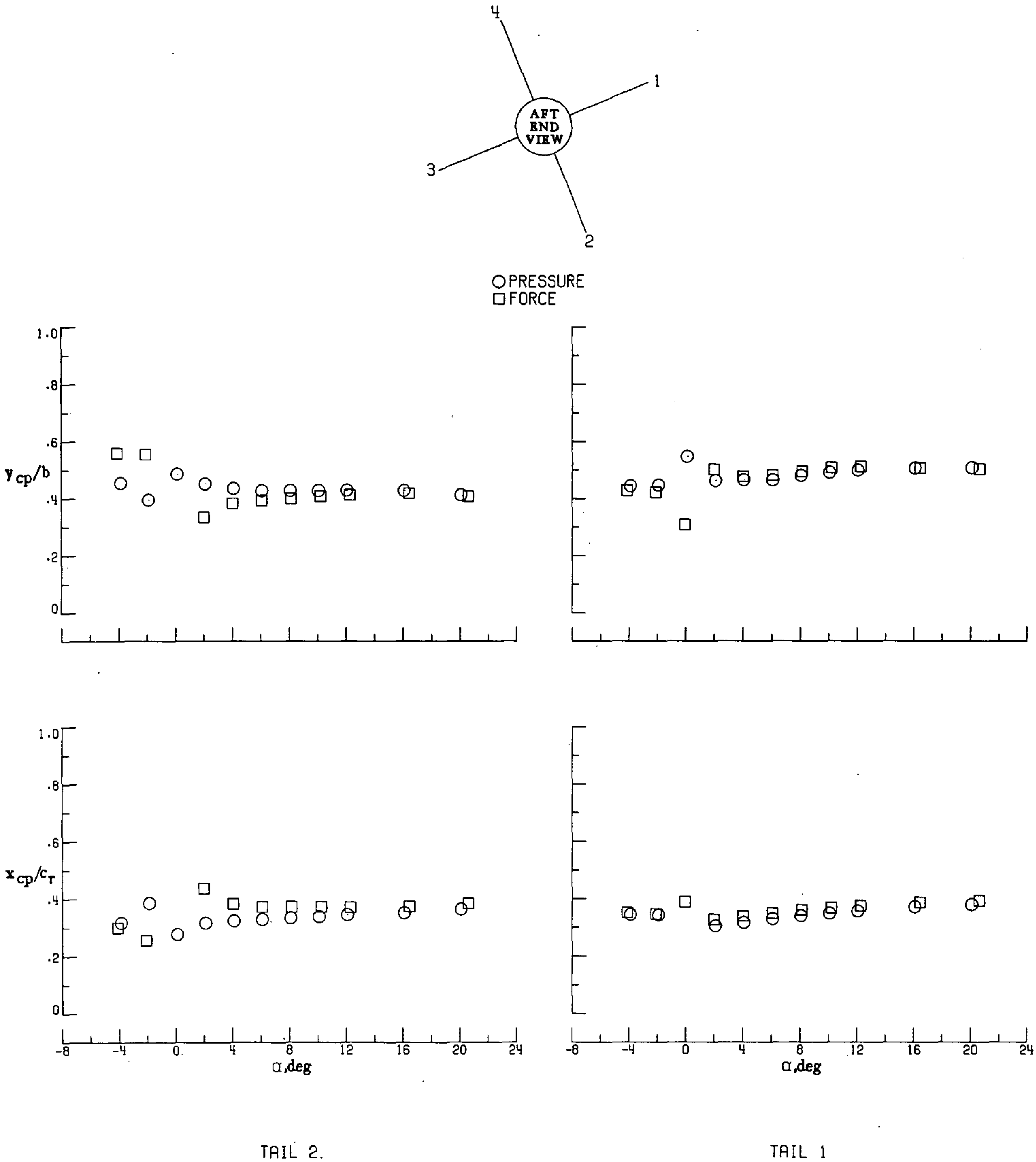

(d) $\phi = 67.5°$.

Figure 13.- Continued.

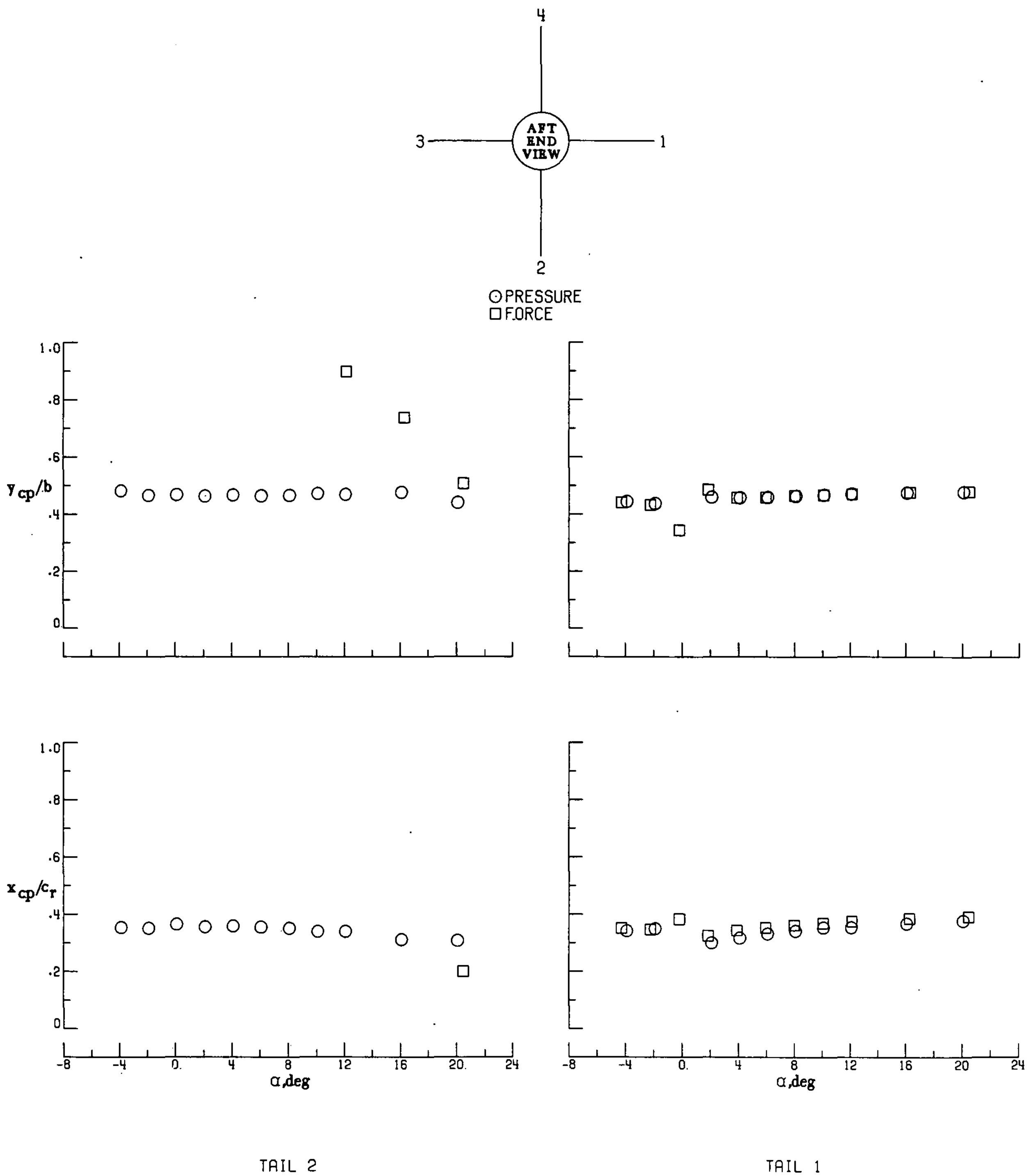

(e) $\phi = 90^{\circ}$.

Figure 13.- Concluded.

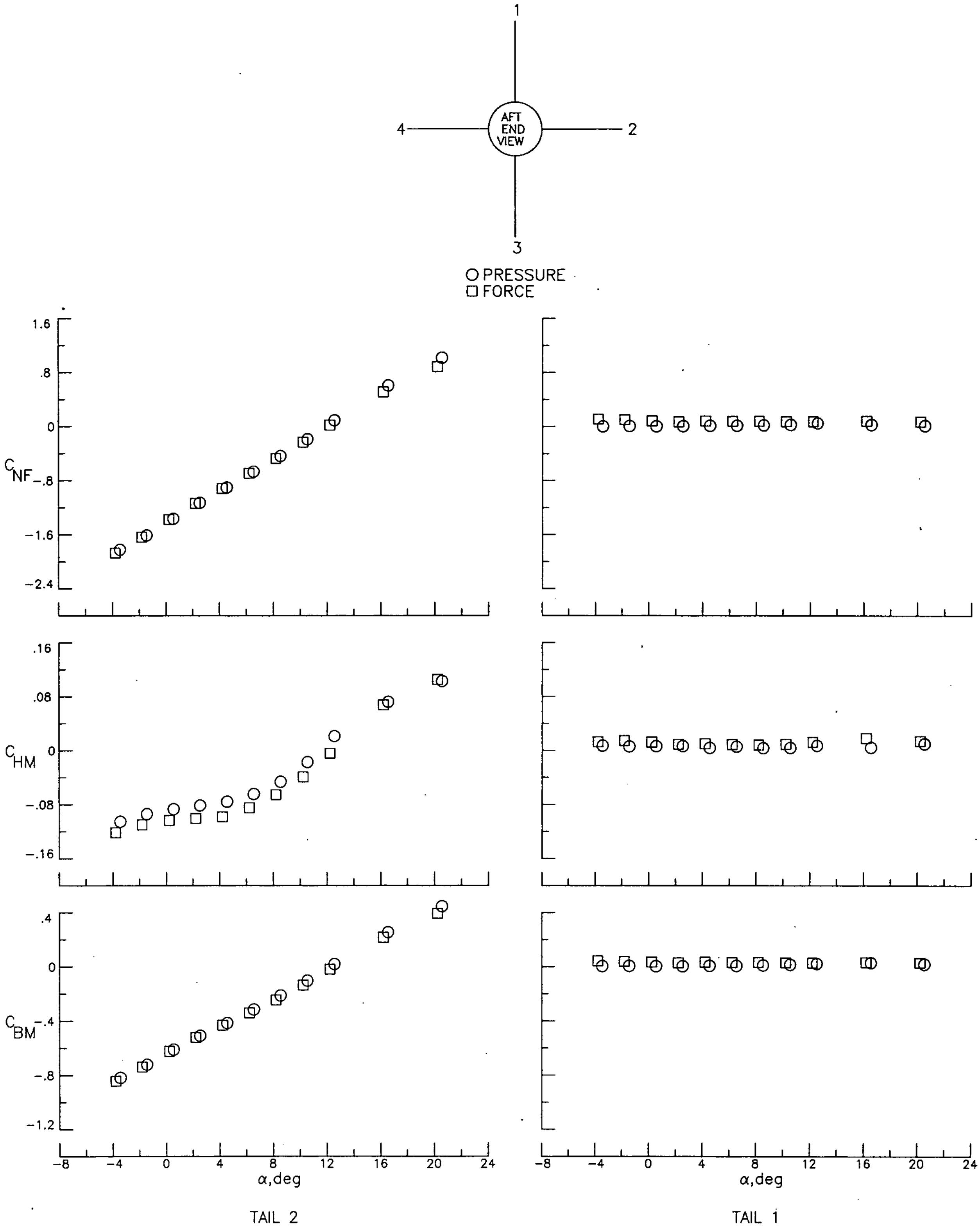

(a) $\phi = 0^{o}$.

Figure 14.- Comparison of balance-measured and pressure-integrated panel loads for T_A at $\delta = -15^{o}$ and $M = 1.60$.

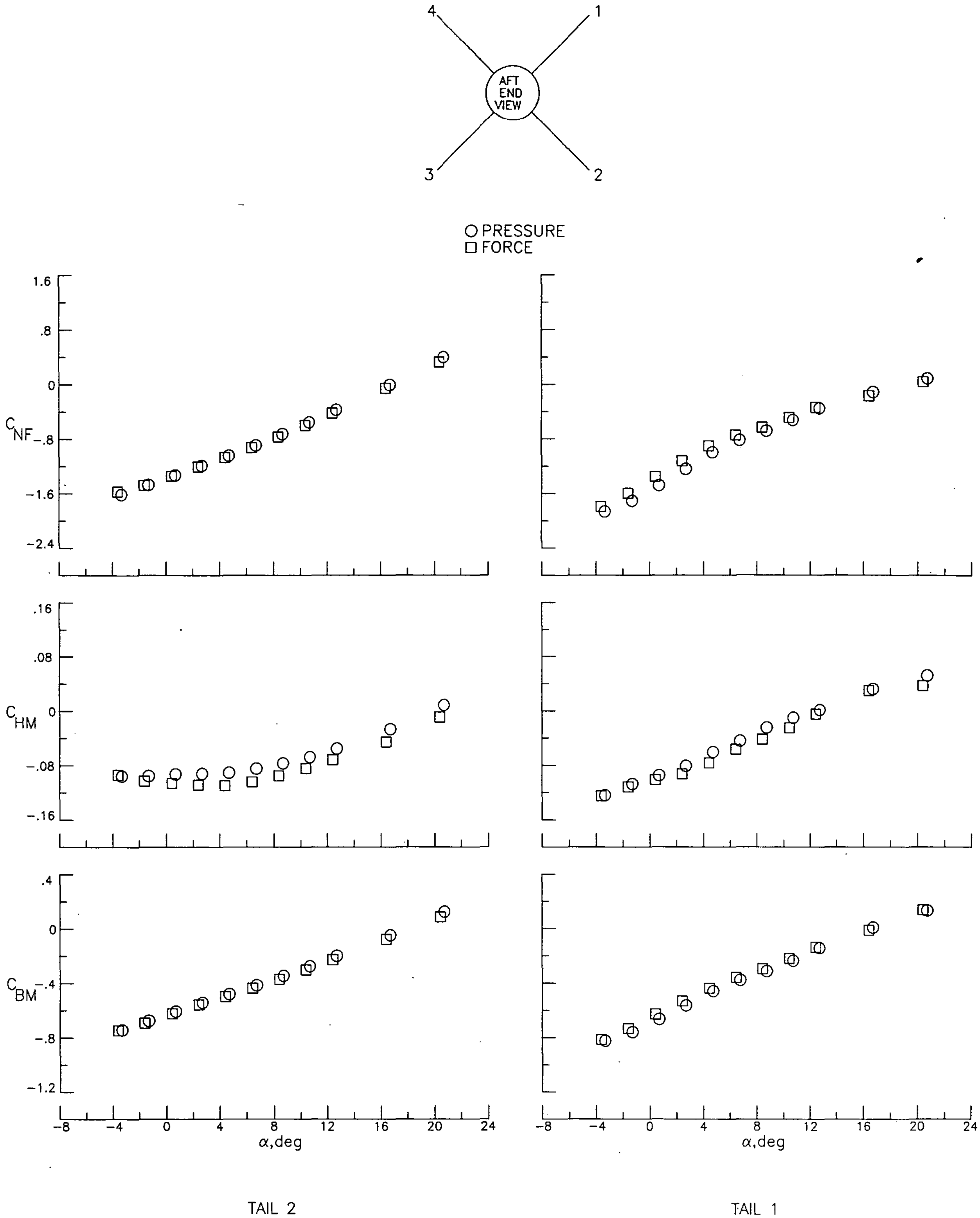

(b) $\phi = 45^{\circ}$.

Figure 14.- Concluded.

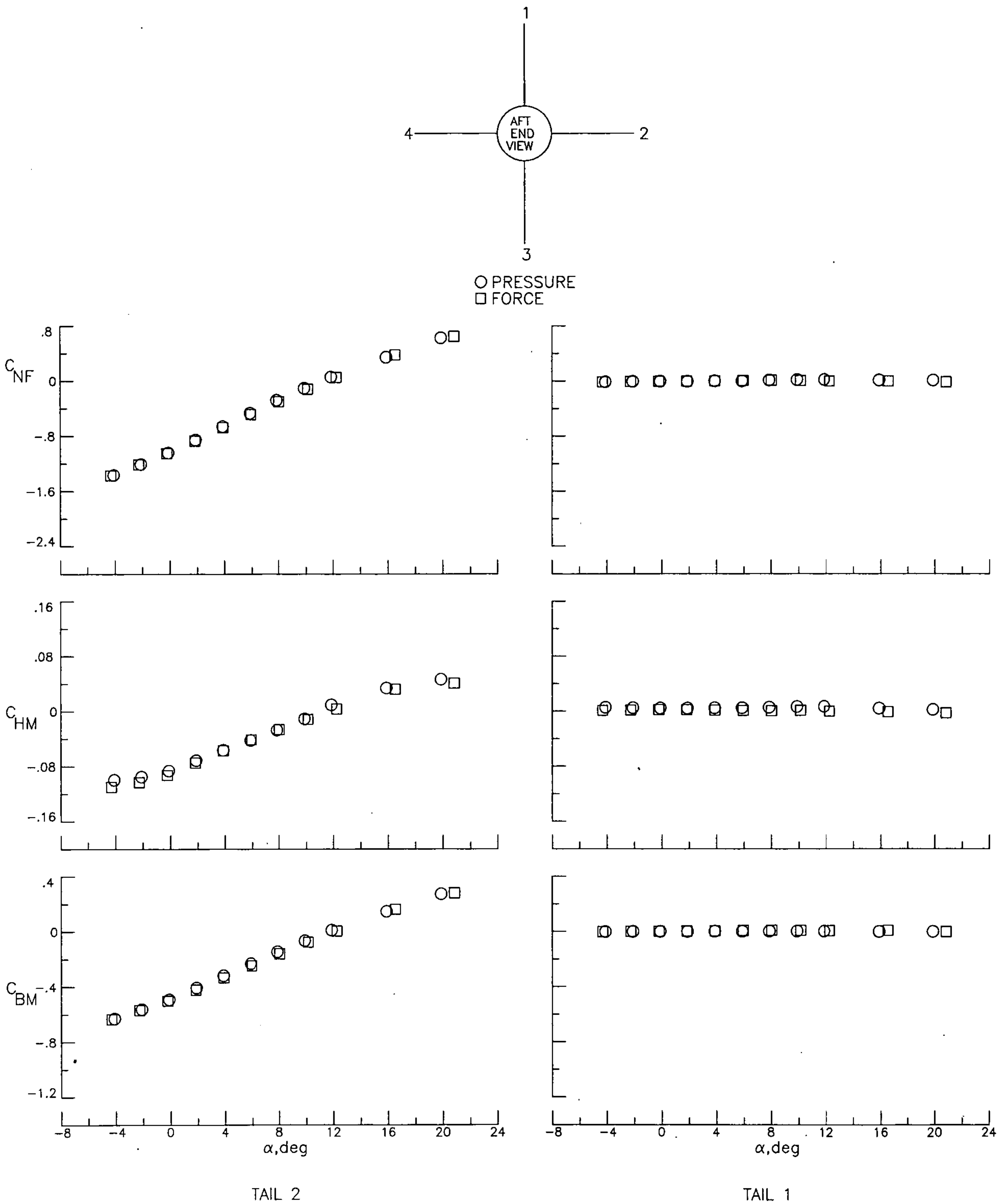

(a) $\phi = 0^{\circ}$.

Figure 15.- Comparison of balance-measured and pressure-integrated panel loads for T_A at $\delta = -15^{\circ}$ and $M = 2.36$.

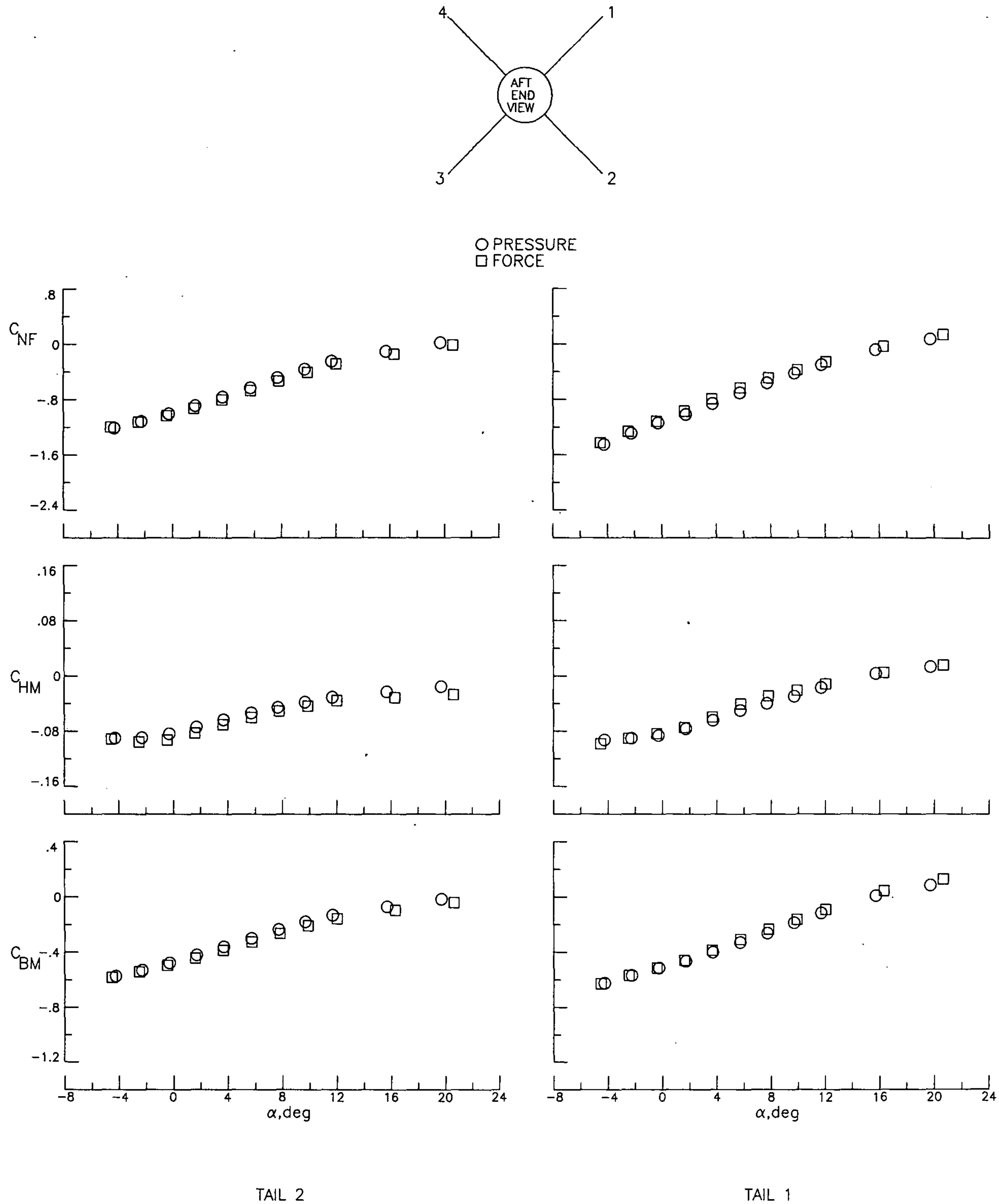

(b) $\phi = 45^{\circ}$.

Figure 15.- Concluded.

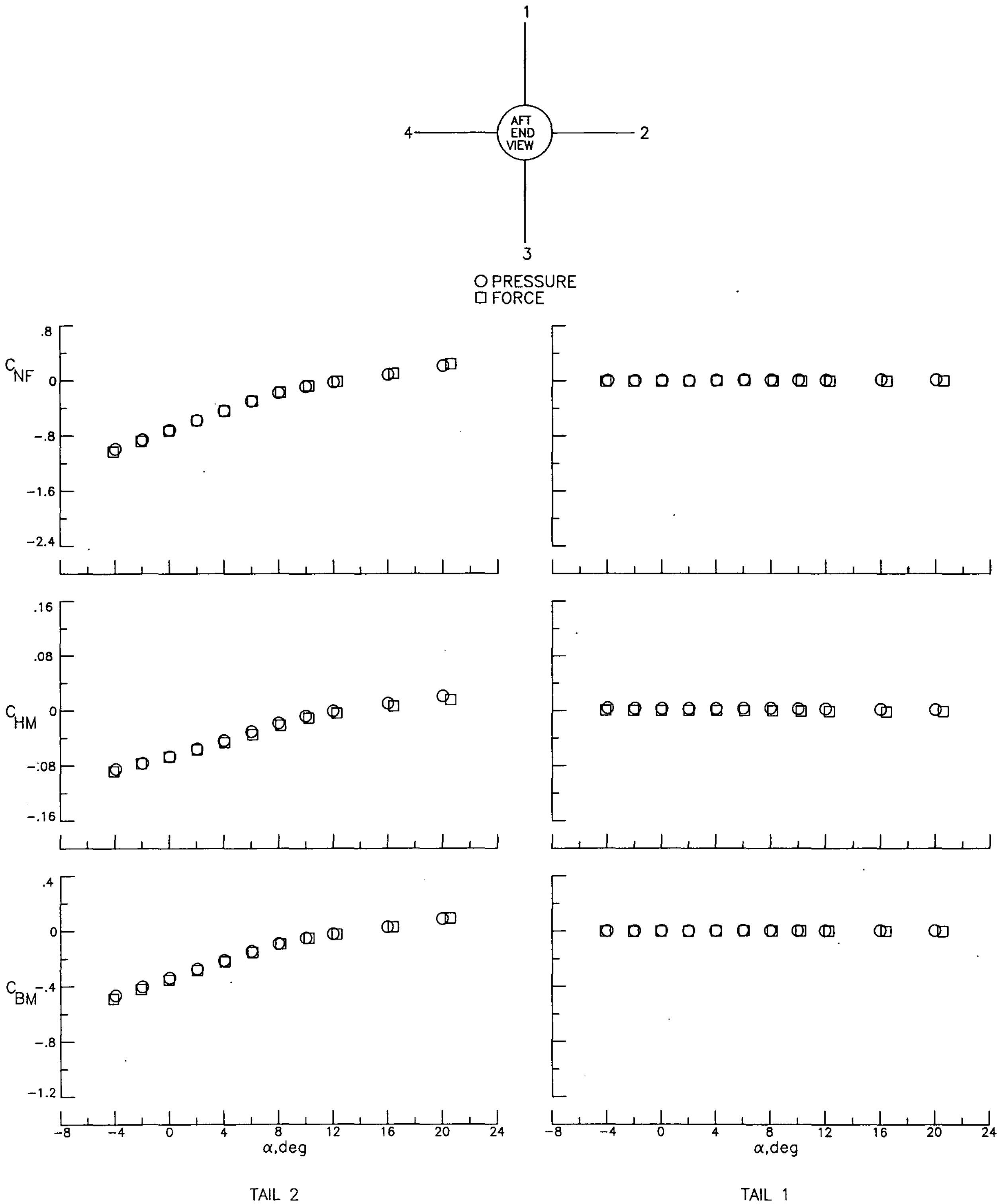

(a) $\phi = 0^{\circ}$.

Figure 16.- Comparison of balance-measured and pressure-integrated panel loads for T_A at $\delta = -15^{\circ}$ and $M = 3.70$.

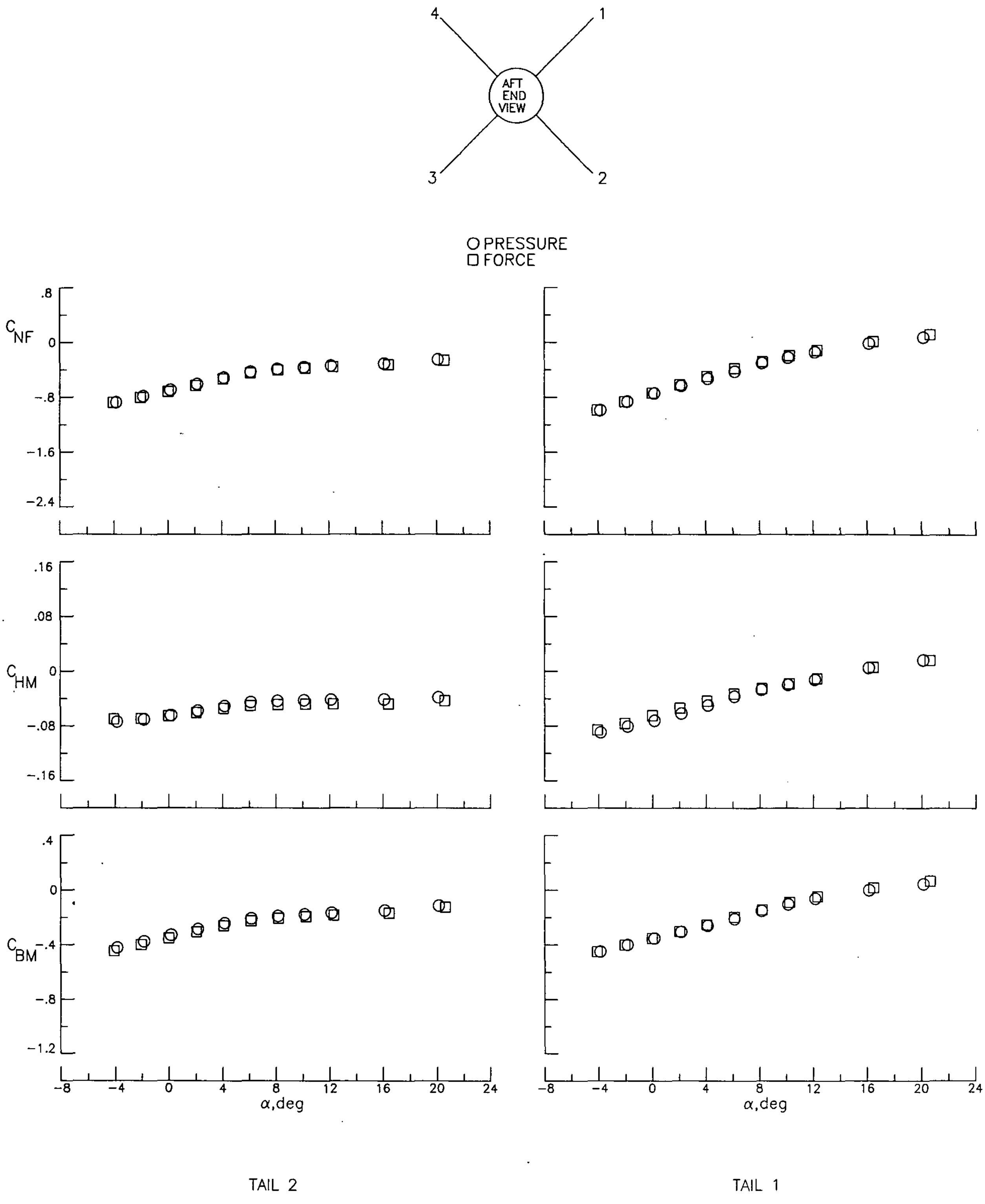

(b) $\phi = 45^{\circ}$.

Figure 16.- Concluded.

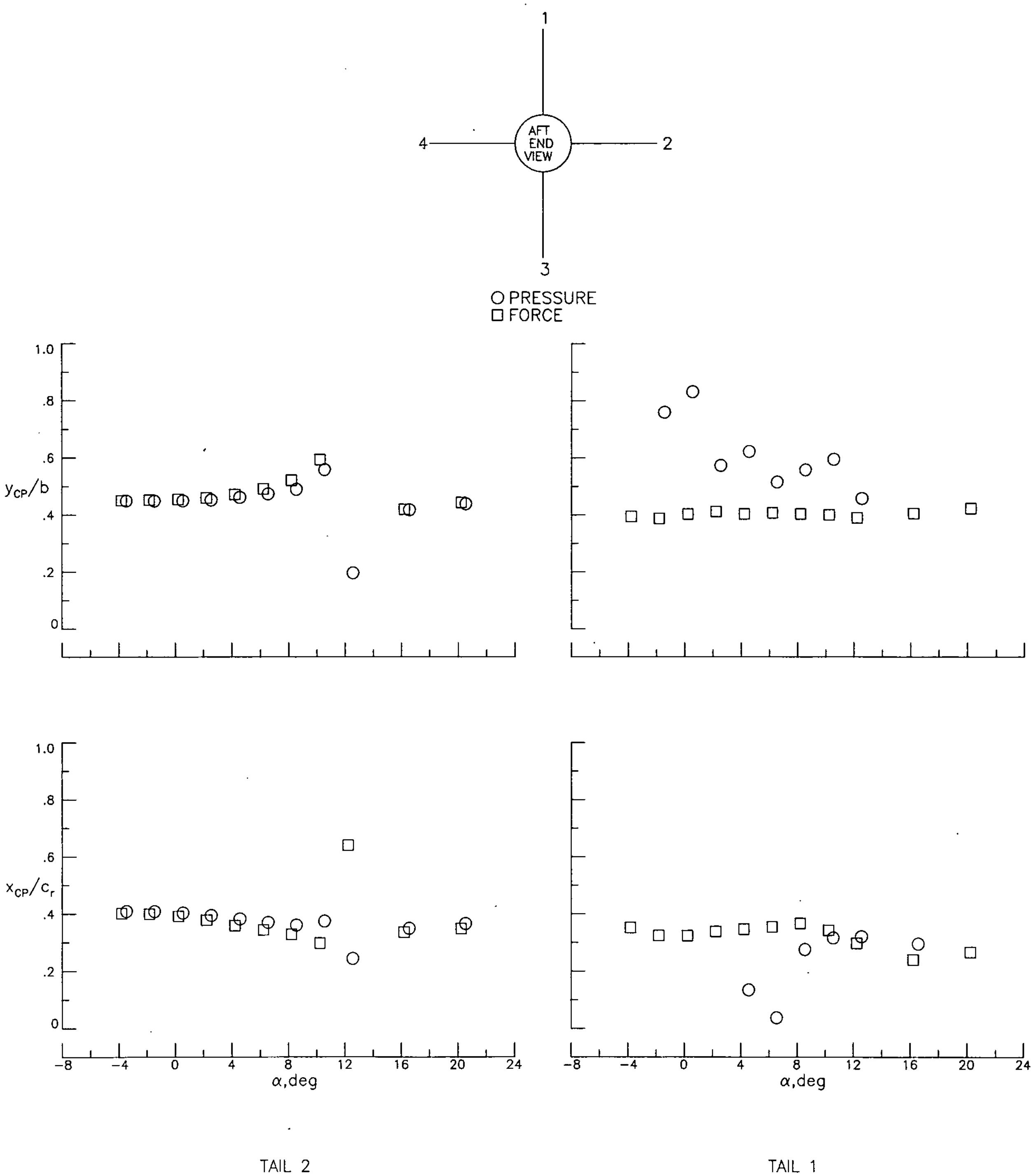

(a) $\phi = 0^{\circ}$.

Figure 17.- Comparison of balance-measured and pressure-integrated centers of pressure for T_A at $\delta = -15^{\circ}$ and $M = 1.60$.

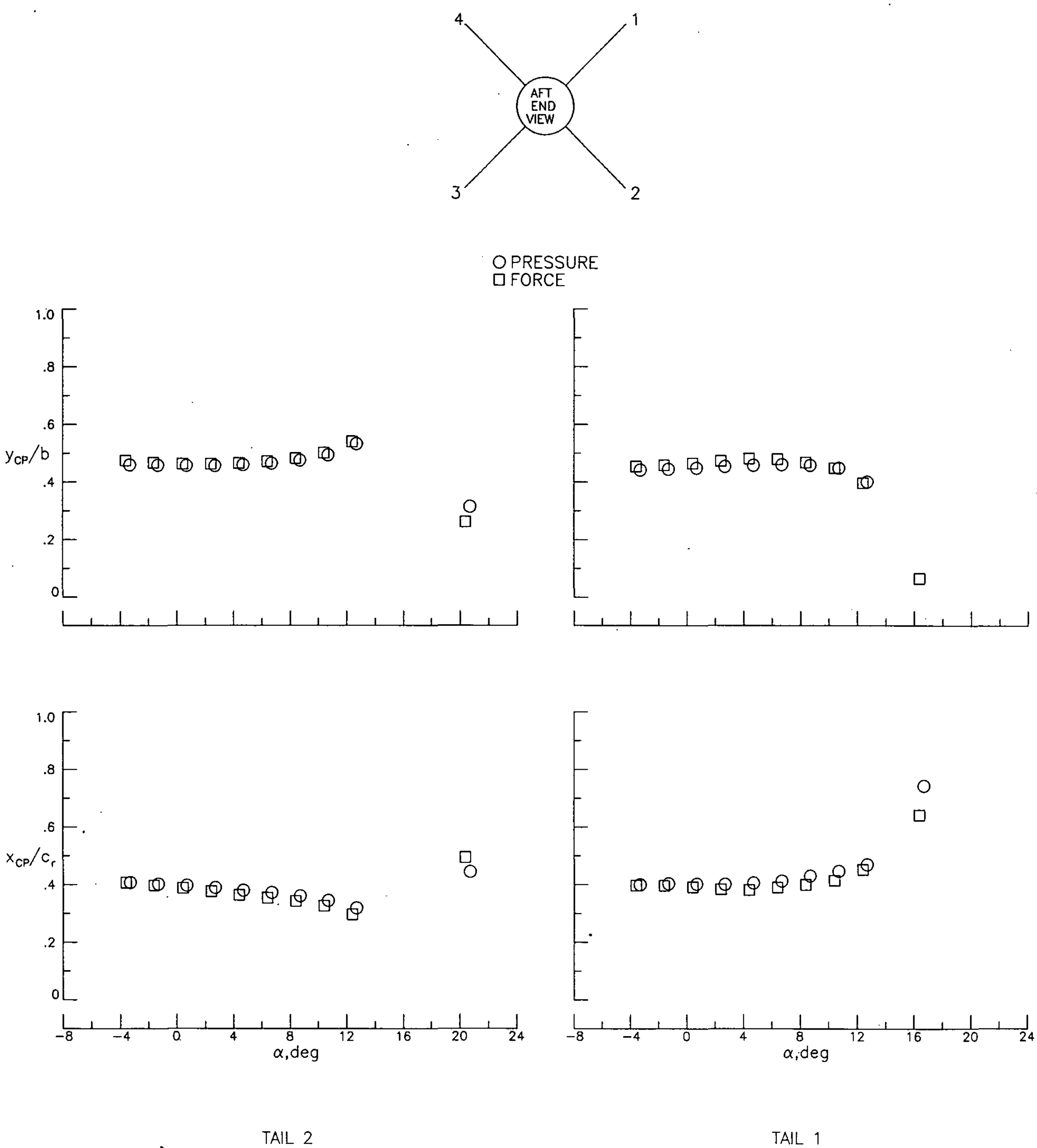

(b) $\phi = 45^{\circ}$.

Figure 17.- Concluded.

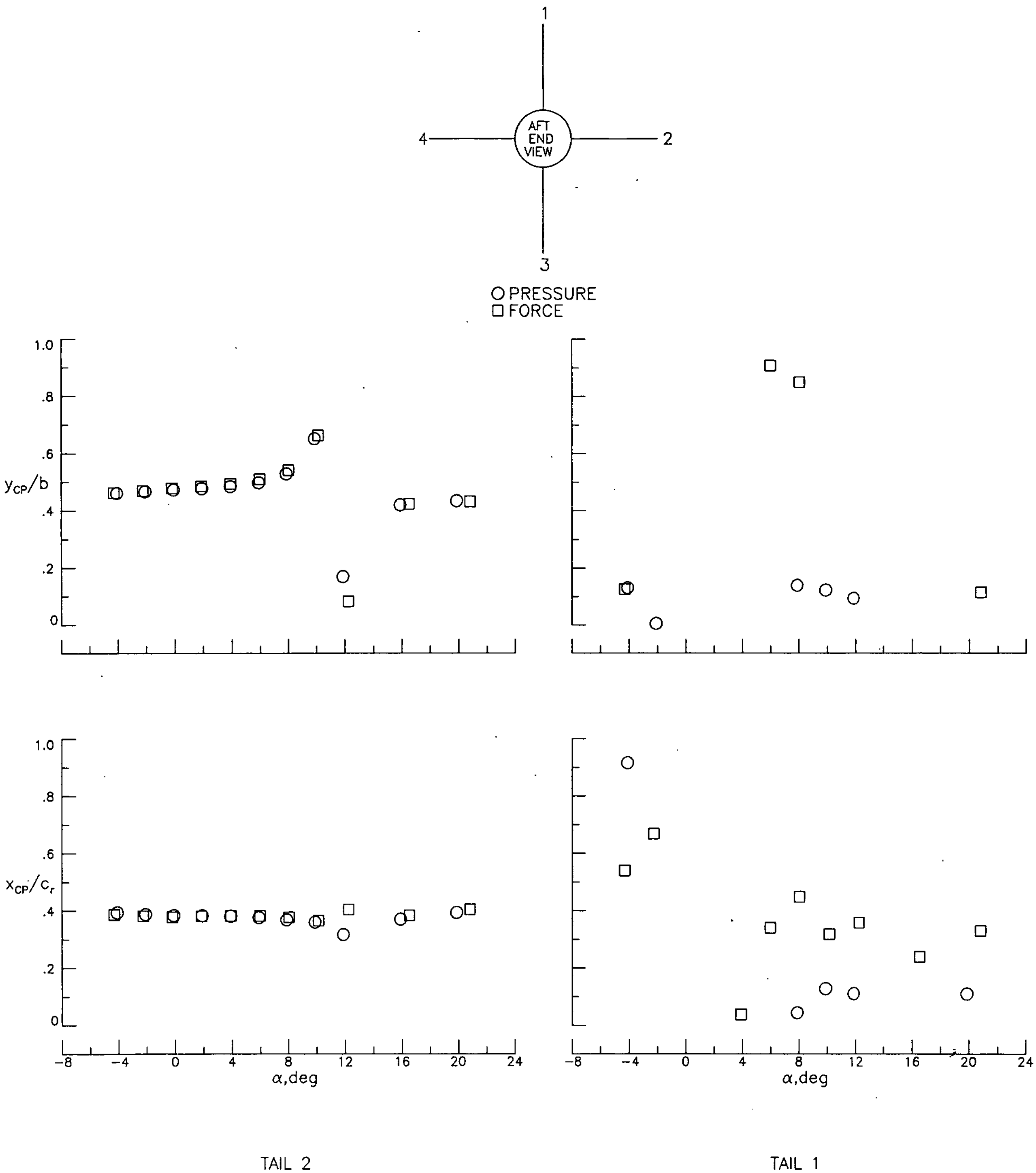

(a) $\phi = 0^{\circ}$.

Figure 18.- Comparison of balance-measured and pressure-integrated centers of pressure for T_A at $\delta = -15^{\circ}$ and $M = 2.36$.

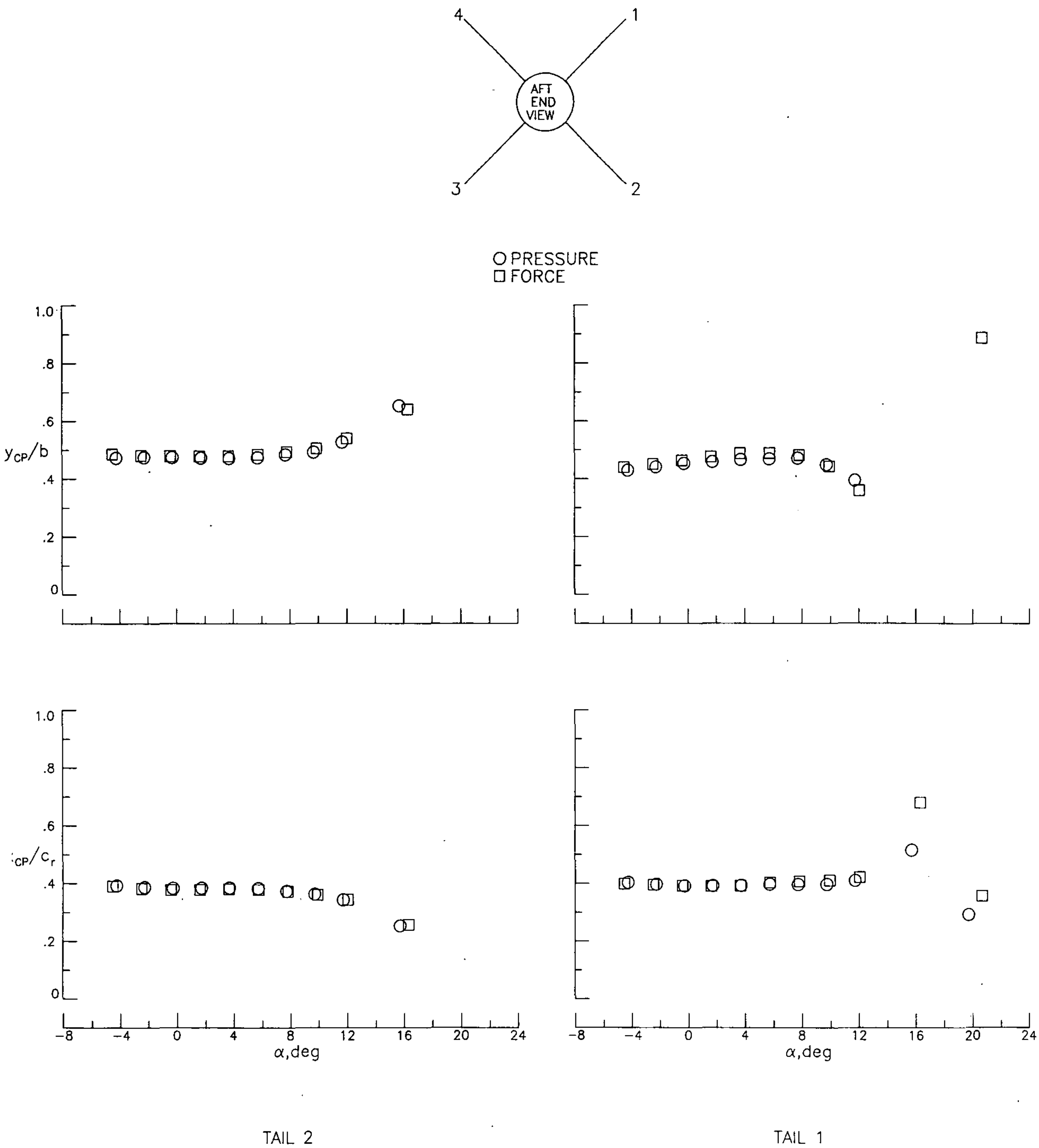

(b) $\phi = 45^\circ$.

Figure 18.- Concluded.

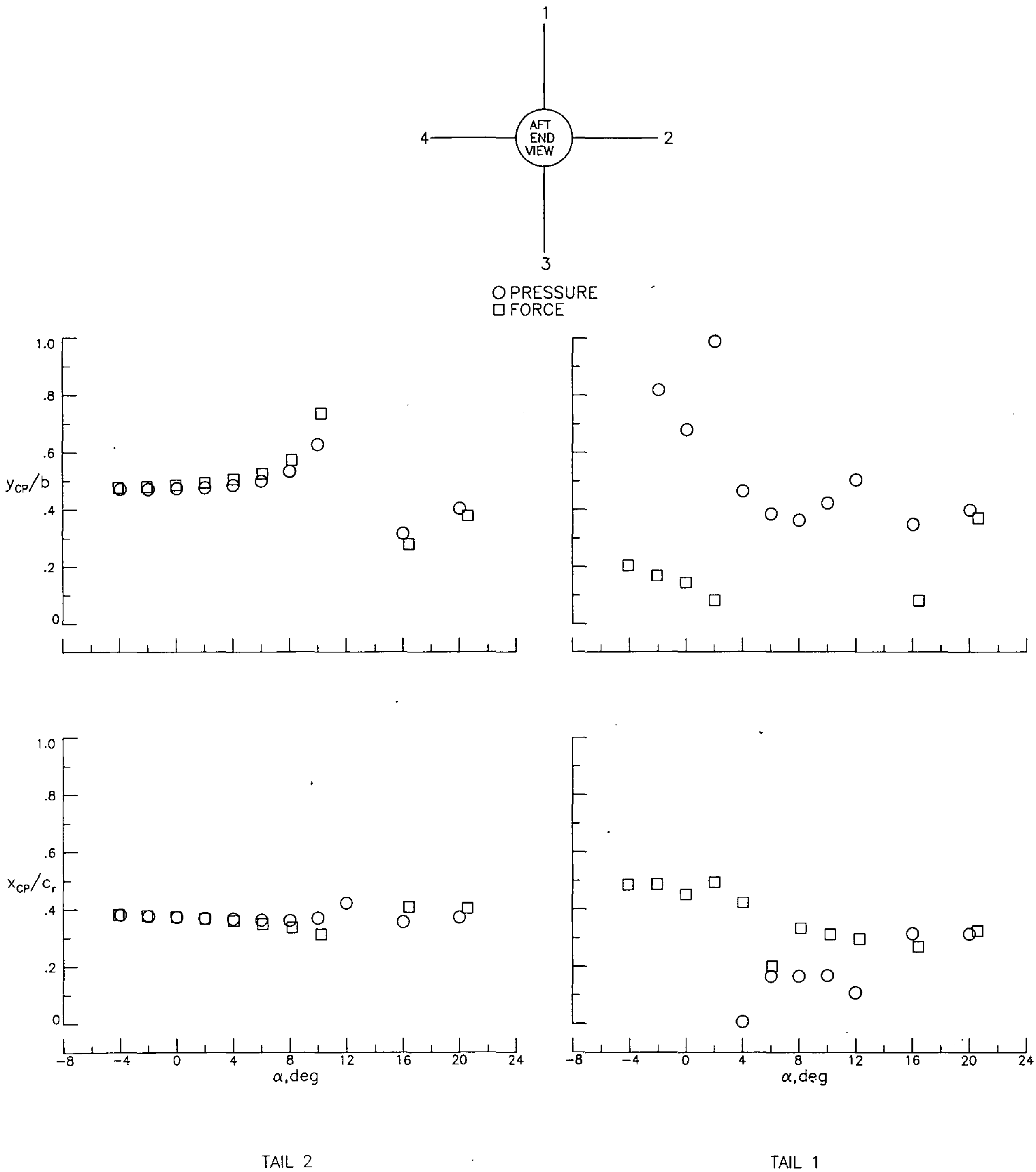

(a) $\phi = 0^{\circ}$.

Figure 19.- Comparison of balance-measured and pressure-integrated centers of pressure for T_A at $\delta = -15^{\circ}$ and $M = 3.70$.

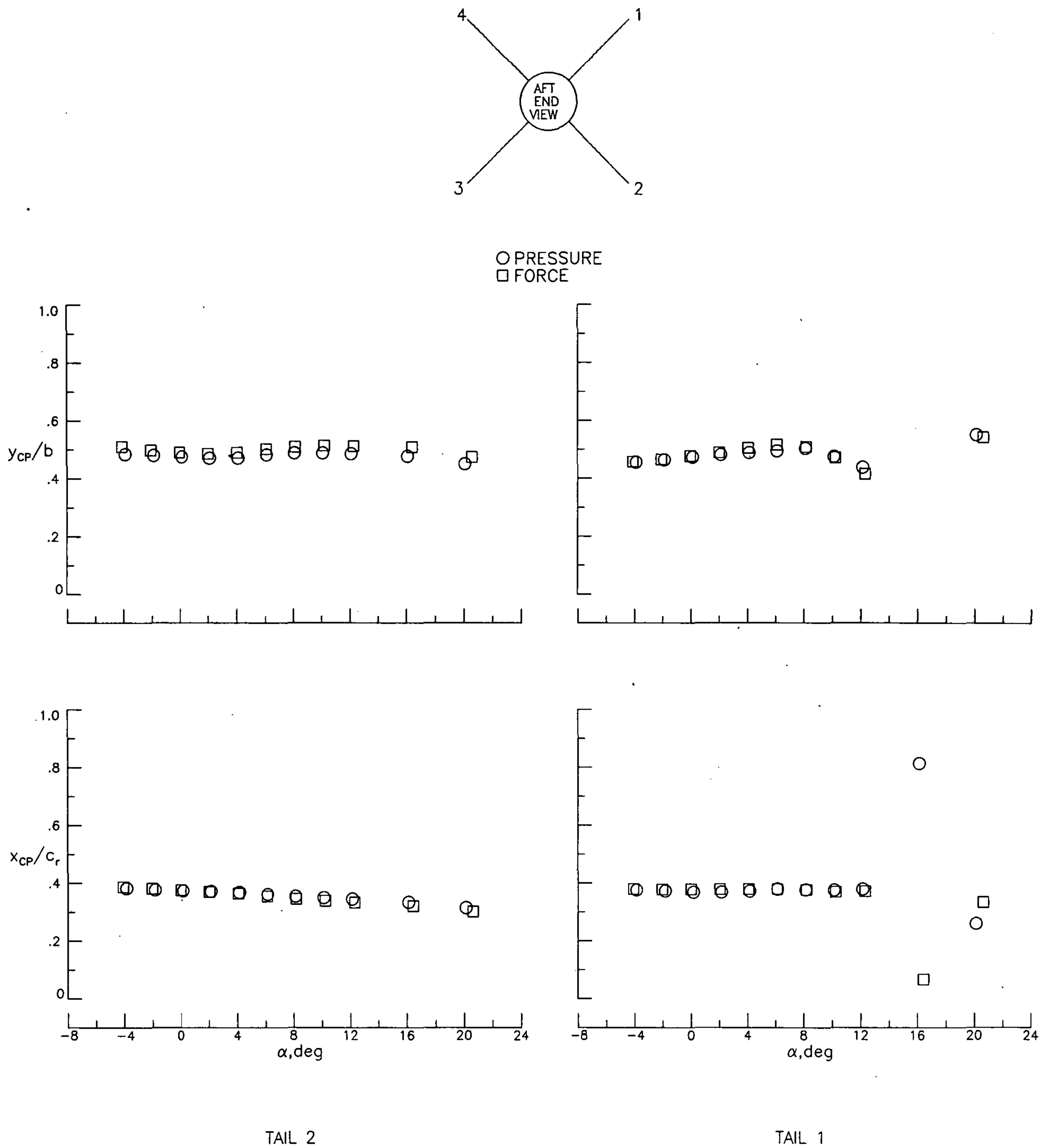

(b) $\phi = 45^{\circ}$.

Figure 19.- Concluded.

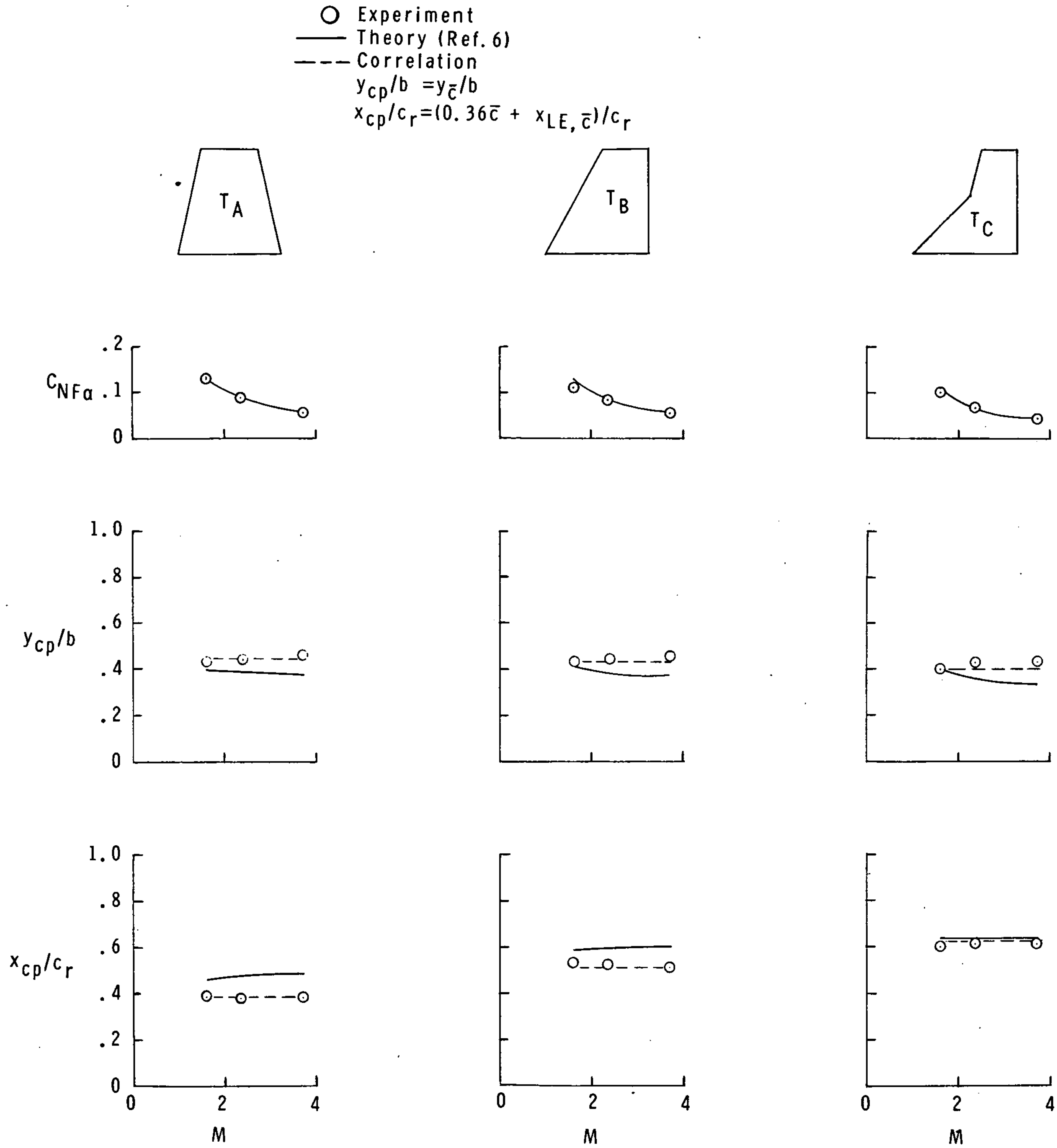

Figure 20.- Comparison of experimental and theoretical control-surface normal-force slope and centers of pressure of horizontal panel at $\phi = 0^{\circ}$ and $\delta = 0^{\circ}$.

1. Report No. NASA TM-81787	2. Government Accession No.	3. Recipient's Catalog No.
4. Title and Subtitle A STUDY OF PANEL LOADS AND CENTERS OF PRESSURE OF THREE DIFFERENT CRUCIFORM AFT-TAIL CONTROL SURFACES OF A WINGLESS MISSILE FROM MACH 1.60 TO 3.70		5. Report Date May 1980
		6. Performing Organization Code
7. Author(s) Milton Lamb and Charles D. Trescot, Jr.		8. Performing Organization Report No. L-13501
9. Performing Organization Name and Address NASA Langley Research Center Hampton, VA 23665		10. Work Unit No. 505-43-23-02
		11. Contract or Grant No.
12. Sponsoring Agency Name and Address National Aeronautics and Space Administration Washington, DC 20546		13. Type of Report and Period Covered Technical Memorandum
		14. Sponsoring Agency Code
15. Supplementary Notes		

16. Abstract

An investigation was made of the forces and moments on the cruciform aft-tail control surfaces of a wingless missile model to determine the variation of panel load and center of pressure with angle of attack, tail deflection, model roll angle, and Mach number. Also, a limited force-moment and surface-pressure investigation was made on a noncircular aft end. These investigations were made in the Langley Unitary Plan Wind Tunnel at Mach numbers of 1.60, 2.36, and 3.70 and at a Reynolds number per meter of 6.6×10^6.

17. Key Words (Suggested by Author(s))		18. Distribution Statement	
Panel loads Panel centers of pressure Supersonic Mach numbers Missile configuration		Unclassified - Unlimited Subject Category 02	
19. Security Classif. (of this report) Unclassified	20. Security Classif. (of this page) Unclassified	21. No. of Pages 109	22. Price* $6.50

*For sale by the National Technical Information Service, Springfield, Virginia 22161

NASA-Langley, 1980